

Transversality for a Class of 3D Oscillators

via Gyrostat Equations

Jinlu Kuang *and* A. Y. T. Leung

*Faculty of Science and Engineering,
City University of Hong Kong, Hong Kong SAR, P. R. China
Fax +852-27887612 or 27889643
E-mail: ejlkuang@ntu.edu.sg
E-mail: bcaleung@cityu.edu.hk*

Abstract

The class of 3D oscillators of interest includes the modified Brockett, Chua, Duffing, Ueda, modified Kapitaniak, generalized Lorenz, forced Lorenz, Rossler and YSVO oscillators whose chaotic analyses are performed in an unified manner for the first time in the paper. The homoclinic orbits of a symmetric gyrostat with wheels under torque-free motions are first exploited. The effects of the small external perturbation torques upon the rotational motions of the forced symmetric gyrostat are investigated using the equation of the Melnikov integral. The real zeros of the Melnikov integral determine the transversality of the homoclinic orbits leading to a necessary condition for the existence of chaos. The equations of the 3D oscillators are then reduced to the Euler equations of the perturbed rotational motions of symmetric gyrostats. Algorithms are established to compute the required gyrostat parameters for representing the 3D oscillators at the onset of the transversality. These parameters include the angular momenta of the wheels and the principal moments of inertia. The existence of real zeros of the Melnikov integral for the symmetric gyrostat implies the existence of transversal intersections of the perturbed

solutions of the 3D oscillators. The 4th order Runge-Kutta algorithm is utilized to simulate and crosscheck the long-term chaotic behaviors of the dynamical systems.

Key Words: **Chaos, Gyrostat, Melnikov integral, Lorenz equations,**

Chua double scroll equations, Ueda equations

Section 1. Introduction

By a digital computer, Lorenz [1] found in 1963 that most solutions of the Lorenz equations tended to a certain attracting set and produced an important example of chaos. Almost concurrently, Melnikov [2] established the Melnikov integral dealing with the transversal homoclinic/heteroclinic intersections associated with the saddle point of a one-degree-of-freedom system with a time period perturbation. No previous attempt has been made to study the transversal homoclinic intersections of the Lorenz oscillator by means of the Melnikov integral for the rotational motion of the gyrostat. The problem is studied in this paper by using a generalised Melnikov integral and by extending the Lorenz oscillator to symmetrical gyrostat in forced attitude motion whose solutions are homoclinic under torque-free motions. The proposed method is further generalized to a class of 3D oscillators including the modified Brockett [3,4], Chua [5], Duffing [5], Ueda [6], modified Kapitaniak [7], generalized Lorenz [8], forced Lorenz, Rossler [9, 10], and YSVO [11] oscillators. Algorithms required to determine the gyrostat parameters are formulated when the Melnikov integral vanishes at real zeros. The existence of real zeros of the extended Melnikov integral for the symmetric gyrostat implies the existence of transversal intersections in the interested 3D oscillators.

In what follows, progress on chaos in dynamical systems and the Melnikov integral are reviewed in Subsection 1.1. Achievements on classical attitude dynamics of gyrostats are examined in Subsection 1.2. The Deprit canonical variables transforming the attitude dynamics ready for the Melnikov analysis are introduced in Subsection 1.3. Improvements of the Melnikov integral due to Holmes and Marsden [12] as well as Wiggins and Shaw [13] are given in Subsections 1.4 and 1.5 respectively. Other works relevant to the attitude dynamics of gyrostats with or without moving parts or appendages are discussed in Subsection 1.6. Reviews on the essential works relevant to this paper are given in Subsection 1.7.

1.1 Nonlinear oscillators and Melnikov's integral

Theory of chaos was pioneered by Poincare in the nineteenth century. Birkhoff, Cartwright and Littlewood, and Levison contributed to the earlier establishment of chaos theory as mentioned in Guckenheimer and Holmes [14] and Chen and Leung [15]. Around 1960, Smale [16] discovered the horseshoe map that played an important role in the explanation of chaos occurrences. Ueda [6] constructed the chaotic regions of Duffing's equation using an analogue computer in the 1960s which was verified analytically using harmonic balance via period doubling by Leung and Fung [17]. By a digital computer, Lorenz [1] found that most solutions of the Lorenz equations tended to a certain attracting set producing an important example of chaos. Almost concurrently, Melnikov [2] established the Melnikov integral dealing with the transversal homoclinic /heteroclinic intersections associated with the saddle point of a one-degree-of-freedom system with a time period perturbation.

Feigenbaum [18] discovered a universal constant for functions approaching chaos via periodic doubling. The Feigenbaum constant characterized the geometric series of a bifurcation parameter approaching to its limiting values. He found a route to chaos for certain functions both quantitatively and qualitatively. The discovery of the Feigenbaum constant marked a milestone in chaos research. Smale [16] stated that chaos was a new science that established the omnipresence of unpredictability as a fundamental feature of common experience. He claimed that the essence of chaos lies in the unpredictability of the long-term behaviours of a deterministic system. Recently, many applications of chaos have been made across a broad spectrum of scientific disciplines – physics [19], ecology [20], socio-politics [21], engineering [22], economics [23], chemistry, fluid mechanics and more[23, 24]. Among the classic icons of modern nonlinear dynamics, the Lorenz equation is still one of the most well known. A huge literature [14, 15, 25, 26] has grown on the subject of Lorenz equations since 1970. The Feigenbaum constant [27] was also found in the Lorenz equation.

Tucker [28, 29] proved that the Lorenz equations supported a strange attractor using a method combining the normal form theory with an extensive numerical search. That method was rigorous on one hand but very far from physical intuition because of the numerical search endeavours involved on the other hand. Festa *et al* [26] reformulated the Lorenz dynamical system in the phase space in terms of a first-exit-time problem. He found that the onset of chaos due to discontinuous solutions of a transcendental problem was initiated by the time when a particle crosses a potential wall. The dynamical issue on the Lorenz attractor was listed as the 14th problem in mathematics for the 21st century by Smale [30]. Smale [30] asked: “Can one decide if a given dynamical system is chaotic? Is

there an algorithm which uses the coefficients of a dynamical system as input to determine if the dynamics is chaotic and no otherwise?" This paper addresses the challenge by presenting a necessary condition for the existence of chaos by detecting analytically the transversal intersections of stable and unstable manifolds of the symmetric gyrostat equivalent to the 3D oscillators which have not been successfully investigated previously.

The scientific research of chaos is of both theoretical and practical significance. Chaotic oscillations have been observed in a large number of mechanical, electrical, elastic and biochemical systems as also outlined in Chen and Leung [15], and Moon [20]. However, bifurcations and chaos have only been studied recently for the rotational gyrostat whose stability issues are of significance to the design of the gyrostat satellite [31], spinning projectiles [32] and elastica dynamics [20].

1.2 Classical Attitude Dynamics of Gyrostats

A gyrostat consists of a carrier with wheels as shown in Figure 1. It is a mechanical model of a three-axis stabilized satellite [31] or for spinning projectiles [32]. Hughes [31] collected many theoretical and engineering models of gyrostats under torque-free or gravity-gradient torque conditions. An extensive background is found in Wittenburg [33]. The rotational motion of the gyrostats was first investigated by Wangerin [34] and Volterra [35]. The classical attitude dynamics issues of the gyrostats have attracted the attention of many scientists since the 1950's [32, 36 - 39]. Rumyantsev [32] reviewed the stability and instability issues of the liquid-filled solid body and presented some sufficient criteria for the stability of the permanent rotation of gyrostats

via Lyapunov's direct method. The Lyapunov-Rumyantsev potential theory provided a theoretical foundation for the attitude stability design for the liquid-filled artificial satellite and the spinning liquid-filled projectiles. Wittenburg [33] acquired the polhode curves on the inertia ellipsoid of the base body for different wheel speeds using Wangerin method [34] and Volterra method [35], respectively. The chaotic attitude dynamics of the gyrostat is a new topic investigated recently.

The applications of the Deprit canonical variables [40] with the Melnikov integral for detecting the chaotic dynamics of the gyrostats are reviewed in the following subsections.

1.3 The Deprit Canonical Variables and the Melnikov Integral

Deprit [40] invented a homogeneous canonical transformation reducing the free rotation of a rigid body to a conservative Hamiltonian system with one degree of freedom. The Melnikov integral based on the Hamiltonian equations of the rotational motions of the gyrostat in terms of Deprit canonical variables is the main analytical tool for treating the bifurcation and chaos issues of the nonlinear attitude dynamics. Based upon the Deprit variables, Kuang *et al* [39, 41] established a new version of the Melnikov integral for a damped gyrostat under the influence of small periodic disturbance torques. The Melnikov integral is originated from the paper of Melnikov [2]. The Melnikov integral is an effective method for proving the occurrences of the transversal heteroclinic /homoclinic orbits in the Poincare map of the perturbed system by measuring the “distance” between the stable and unstable manifolds associated with the saddle points.

The detailed materials on the Melnikov integral may be found in Melnikov [2], Guckenheimer and Holmes [14], Chen and Leung [15], Moon [20], and Chow *et al* [42].

The application of the Melnikov integral in the chaotic attitude motions of the satellite models with complex configurations may be found in references [43 – 49]. Gray *et al* [43] utilized the Melnikov integral to study the chaotic dynamics of an attitude transition maneuver of a torque-free rigid body in going from minor axis spin to major axis spin under the influence of small damping. Gray *et al* [44] established an analytical criterion for chaotic attitude dynamics of flexible satellites with nonlinearly damped controller by means of the Melnikov integral. They [45] also investigated the heteroclinic bifurcations of rigid bodies containing internally moving parts with viscous dampers. They [43 – 45] transformed the Euler equations of the rigid-body attitude motion to a set of two dimensional ordinary differential equations by using spherical coordinates to map the momentum sphere surface to a plane. Based upon the reduced two dimensional ordinary differential equations that are suitable for the application of the Melnikov integral, they derived a necessary inequality condition for chaos in terms of the system parameters. Or [46] studied the chaotic attitude dynamics of a dual-spinner subject to the action of an internal oscillatory torque and Coulomb friction. By using the Melnikov integral, he developed a necessary condition for the existence of transversal homoclinic points and homoclinic tangencies of chaotic motions. Cooper and Bishop [47] applied the Melnikov integral to the rotational motion of a damped rigid body subjected to a small time-varying perturbation. Miller *et al* [48] studied the nonlinear attitude dynamics of a satellite with a flexible appendage, a damper, and moving internal sub-masses by means of the Melnikov integral. Chen and Liu [49] dealt with the chaotic attitude motion of a

magnetic rigid satellite with internal damping in circular orbit near the equatorial plane of the Earth by means of the Melnikov integral.

1.4 Improvement of the Melnikov Integral Due to Holmes and Marsden [12]

The original Melnikov method [2] is applicable to a one-degree-of-freedom system with a time period perturbation only. Holmes and Marsden [12, 50, 51] generalized the Melnikov integral to high-dimensional conservative Hamiltonian systems. The Hamiltonian and non-Hamiltonian perturbations of integrable two-degree-of-freedom Hamiltonian systems containing homoclinic and periodic orbits were investigated. They [50] showed that small coupling perturbations with the addition of positive and negative damping broke the integrability by introducing Smale's horseshoes. They [12, 50] derived theorems that established the existence of horseshoes and Arnold diffusion for nearly integrable Hamiltonian systems with three or more degrees of freedom via Lie groups. They showed that: (1) a simplified model of the rigid body with one attachment had horseshoes and with two or more attachments had Arnold diffusion; and (2) a rigid body under gravity close to a symmetric integrable Lagrangian top had horseshoes. Using a reduction strategy, they [12] analyzed the perturbation of a homoclinic orbit in an integrable Hamiltonian system. They [51] addressed the general question of perturbations of integrable multidimensional Hamiltonian systems. With an unperturbed system containing a homoclinic orbit and at least two families of periodic orbits associated with action angle coordinates, they used the Kolmogorov-Arnold-Moser (KAM) theory to show that some of the resulting tori persisted under small perturbations and used a vector of Melnikov integrals to show with hypotheses that the stable and

unstable manifolds intersected transversely. They [51] concluded that this transversal intersection was ultimately responsible for the Arnold diffusion on each energy surface. They established the existence of Arnold diffusion in Hamiltonian systems with at least three degrees of freedom. This in turn implied that the system was nonintegrable in the classical sense.

The application of the Melnikov integral developed by Holmes and Marsden [12] to the attitude chaos detection of the gyrostat may be found in Tong *et al* [52] and Kuang *et al* [53]. Tong *et al* [52] investigated the chaotic attitude motions of a gyrostat consisting of an asymmetric carrier with an axisymmetric rotor rotating about a fixed point under the influence of the gravitational force by using the Melnikov integral of Holmes and Marsden [12]. The Deprit canonical variables were used to describe the Hamiltonian equations of the rotational motion of the gyrostat in Tong *et al* [52]. Kuang *et al* [53] studied the chaotic attitude tumbling of an asymmetric gyrostat in a gravitational field using the Deprit variables together with the Melnikov integral of Holmes and Marsden [12].

1.5 Improvement of the Melnikov Integral Due to Wiggins and Shaw [13]

The generalization of the Melnikov method to a three-dimensional system of a slowly varying oscillator with “one and half” degrees of freedom was due to Wiggins and Shaw [13]. The slowly varying oscillator consisted of a weakly perturbed single-degree-of-freedom system with an additional equation of slow motion. In that paper, they established an analytical criterion for detecting transversal intersections of stable and unstable manifolds of such dissipative systems. Transversal intersections implied the

existence of Smale's horseshoes via the Smale-Birkhoff homoclinic theorem. They also described a simplified visual model of three-dimensional Smale's horseshoes whenever a map possessed a transverse homoclinic point. The utilization of the Melnikov integral due to Wiggins and Shaw [13] for detecting the transversal intersections between the stable and unstable manifolds of a disturbed gyrostat under the action of small periodic torques can be found in Tong *et al* [54], Tong and Tabarrok [55], Kuang *et al* [38, 39, 41, 56]. Tong *et al* [54] introduced the Deprit variables to transform the Euler equations to the Hamiltonian form for the application of the Melnikov integral developed either for the dissipative attitude motions of the rigid bodies under the action of small periodic perturbation torques from Wiggins and Shaw [13] or for the conservative attitude motions of rigid bodies under the influence of small gravitational perturbation torques from Holmes and Marsden [12]. By the Melnikov integral, the transversal interactions of stable and unstable manifolds for the perturbed rigid-body attitude motions were detected. Based on the Hamiltonian equations derived in terms of Deprit's variables, Tong and Tabarrok [55] investigated the chaotic attitude motion of self-excited rigid bodies under the action of small periodic perturbation torques by using the Melnikov integral developed by Wiggins and Shaw [13]. Kuang *et al* [41] investigated the chaotic attitude motions of dissipative satellites that were modelled as gyrostats or gyrostat satellites subjected to small perturbation torques using Deprit's variables. Applying the Melnikov integral of Wiggins and Shaw [13], Kuang *et al* [39, 41] established a general version of the Melnikov integral for a dissipative gyrostat subjected to small applied torques. Based on that general version of the Melnikov integral for the forced angular motion of a gyrostat, Kuang *et al* [38, 39, 56] studied the chaotic attitude dynamics of dissipative

satellites, either asymmetrical or symmetrical. The other new contribution in Kuang *et al* [38, 39, 56] was the acquisition of the homoclinic orbits for the angular motions of the torque-free gyrostat with different configurations. With the help of the Melnikov integral of Holmes and Marsden [12], Kuang *et al* [53] investigated the chaotic attitude tumbling of an asymmetric gyrostat under the action of gravity-gradient torques. According to Rumenantsev [32], when the motions of the contained liquid were irrotational, the attitude dynamic equations of a rotational liquid-filled body would be identical with those of a solid body to which a rotating gyroscope was joined. Consequently, the conclusions of Kuang *et al* [36 – 39, 41, 53, 56] would also hold for the rotational motions of a solid body containing irrotational liquid under certain appropriate assumptions.

1.6 Gyrostats with /without Moving Parts

Recent research on the dynamics and control of the chaotic instabilities in a spinning spacecraft or gyrostat may be found in Meehan and Asokanthan [57 – 61] and Beletskii *et al* [62, 63]. Meehan and Asokanthan [57, 58] showed numerically the existence of chaotic instabilities in a rotating body with internal dissipation disturbed by an external periodically varying torque. They found that the onset of chaotic motion was characterized primarily by period doubling for increasing torque amplitudes. They [59] investigated the control of the chaotic vibrations in a simplified model of a spinning satellite with a circumferential nutational damper. They used two techniques: recursive proportional feedback and continuous delayed feedback. Their numerical simulation results showed the effectiveness of the two control techniques in eliminating chaotic instabilities in a spinning satellite with internal energy dissipation when it was perturbed

by external periodically varying torques. They [60] achieved the control of chaotic instabilities in a simplified model of a spinning satellite with dissipation by using an algorithm derived from Lyapunov's second method. They [60] extended their methodology proposed in 1999 to the control of chaotic motion in a dual-spin satellite with nutational damping. Beletskii *et al* [62, 63] investigated the orientation problems of the artificial and natural celestial bodies by means of a numerical implementation of the Poincare map. Regular and chaotic motions were identified and their evolution was traced in parametric space. Distinctions were made between regular (or resonance), quasi-regular (or conditionally periodic), and chaotic trajectories. Some closely relevant research work was limited to chaos in the nonlinear attitude dynamics of the rigid body model when the perturbations were Hamiltonian by Dovbysh [64] and Koiller [65]. Some research work of non-Hamiltonian perturbations to the rigid body attitude dynamics has dealt almost exclusively with stable equilibriums by Rubanovskii [66]. It is impossible to discuss other references cited due to limited space.

Briefly, it is noted that the Euler dynamical equations describing the rotational motions of the gyrostat with/without moving parts (i.e., control equipments) have rich nonlinear dynamics. It includes bifurcations and chaos that may be detected by using the Melnikov integral associated with numerical simulations. The Melnikov integral and the homoclinic orbits of the torque-free symmetrical gyrostat developed previously by the authors [39] paved theoretical foundation for the research and development of the Melnikov integral for the investigated dynamical systems such as Lorenz, and Chua double scroll equations, *etc.*

1.7 Essential Work of This Paper

The objective of this paper is to construct effective algorithms to show that transversal homoclinic intersections of certain 3D oscillators can be determined in a unified approach from the rotational motion of the perturbed symmetric gyrostat by means of the Melnikov analysis. The Melnikov integral proposed by Kuang *et al* [39] is used to establish a theoretic framework for determining the existence of the transversal intersections between the stable and unstable manifolds of the symmetric gyrostat which is equivalent to the class of 3D oscillators of Lorenz [1], modified Brockett [3, 4], Chua [5], Duffing [5], Ueda [6], forced Lorenz, Kapitaniak [7], generalized Lorenz [8], Rossler [9, 10] and Yalcin *et al* [11].

Because the Melnikov integral is a function of the angular momenta and the moments of the principal inertia of the equivalent symmetric gyrostat, the angular momenta and the moments of the principal inertia can be determined numerically when the Melnikov integral vanishes with real roots. The existence of the real roots of the Melnikov integral implies the existence of transversal homoclinic intersections in chaotic dynamics in the sense of Smale's horseshoes. Using the homoclinic orbits of rotational motions of the torque-free symmetric gyrostat, one can find the Melnikov integral for the above-mentioned dynamical systems with details listed in Examples (1 - 9) in Section 6. The relationships between the 3D oscillators and the Euler equations of the symmetrical gyrostat are established through the Melnikov integral.

The paper is organized as follows. A review on the methodology used in the later part of the introduction is given in Section 1. The transversality of the rotational motions of perturbed gyrostats will be investigated extensively in Section 2 to prepare for the

study of the class of the interested 3D oscillators in Section 3. The Melnikov integral will then be derived explicitly for each of the oscillators in Section 4 and the parameters of the gyrostats will be determined in Section 5 for the transversal intersections of each of the 3D oscillators. Analytical results are cross-checked using the long-term behaviours of the dynamical systems simulated by the 4th Runge-Kutta integration in Section 6.

Section 2. The Melnikov integral for the perturbed gyrostat

In this section, the topics discussed include the governing equations of the rotational motion of the perturbed gyrostat in Subsection 2.1, the homoclinic orbits of the torque-free symmetric gyrostat in Subsection 2.2, the Melnikov integral for the perturbed gyrostat in Subsection 2.3, the conditions of hyperbolic fixed points of the torque-free symmetric gyrostat in Subsection 2.4, the construction of homoclinic orbits for the torque-free symmetric gyrostat in Subsection 2.5, the property of the associating functions in Subsection 2.6 and the equation of the Melnikov integral in Subsection 2.7.

These topics are important for the later investigation of the 3D oscillators in question.

2.1 Governing equations of the rotational motion of the perturbed gyrostat

The gyrostat is composed of a carrier with rotating elements inside it. In Figure 1, $OXYZ$ is the inertial coordinate system and $Oxyz$ is the body-fixed coordinate system. The rotating elements are called the momentum exchange devices or wheels. The system is assumed to be rotating about the centre of the mass under the action of external

disturbance torques. From theorem of moment of momentum, the differential equations of the rotational motion of the gyrostat system are given by [31, 33, 35]

$$I_{xx} \frac{d\omega_x}{dt} = (I_{yy} - I_{zz})\omega_y\omega_z + \omega_z h_y - \omega_y h_z + T_x, \quad (x \ y \ z) \quad (1)$$

where the notation $(x \ y \ z)$ denotes that only one of the three equations is written down and the other two can be obtained by cyclic permutation of the indices $(x \rightarrow y \rightarrow z)$. The parameters I_{xx} , I_{yy} , and I_{zz} are the principal moments of inertia of the gyrostat including the wheels in $Oxyz$. Constants h_x , h_y , and h_z are the components of the vector sum of the relative angular momentum of all the wheels with respect to $Oxyz$. The state variables ω_x , ω_y , and ω_z are the components of the angular velocities of the gyrostat in $Oxyz$. The external disturbed torques T_x , T_y , and T_z are assumed to be of the following form

$$\begin{aligned} T_k &= \varepsilon(\mu_{kx}\omega_x + \mu_{ky}\omega_y + \mu_{kz}\omega_z + \Pi_{xy}^k\omega_x\omega_y + \Pi_{yz}^k\omega_y\omega_z + \Pi_{zx}^k\omega_z\omega_x + T_{k0}) \\ &= \varepsilon M_k(\omega_x, \omega_y, \omega_z, t) \end{aligned} \quad (2)$$

where the subscript/superscript $k = x, y, z$. The coefficients μ_{ij} for $i, j = x, y, z$ and Π_{ij}^k for $i, j, k = x, y, z$ are constants to be determined according to the algorithms established in the next section for various oscillators. $T_{k0}(\omega_x, \omega_y, \omega_z)$ for $k = x, y$, and z are also to be specified in the next section. ε is a small parameter ($0 < \varepsilon \ll 1$).

Introducing the Deprit variables [40], one can transform the Euler equations (1) into the Hamiltonian equations for the application of the Melnikov integral proposed by Wiggins and Shaw [13]. The Hamiltonian equations of the rotational motions of the gyrostat in terms of Deprit variables can be found in Kuang *et al* [39, 41]. The existence

of the transversal intersections of the stable and unstable manifolds associated with the saddle point of the system may be determined by the Melnikov integral which represents the first order measurement in the perturbation parameter ε for the separation distance of the stable and unstable manifolds of a dynamical system. The Melnikov integral is computed along the homoclinic orbits of the torque-free gyrostat. Thus, it is necessary to study the homoclinic orbits of the torque-free gyrostat. In this paper, one restricts to the homoclinic orbits of the symmetric gyrostat under torque-free motion.

2.2 The homoclinic orbits of the torque-free symmetric gyrostat

Euler's dynamical differential equations (1) of the symmetric gyrostat under torque-free motion take the form

$$I_{xx} \frac{d\bar{\omega}_x}{dt} - (I_{yy} - I_{zz})\bar{\omega}_y\bar{\omega}_z + \bar{\omega}_y h_z - \bar{\omega}_z h_y = 0, \quad (x \ y \ z) \quad (3)$$

where the over-bar stands for homoclinic orbits. The relation $I_{xx} = I_{yy}$ holds for a symmetrical gyrostat. The first integrals of the rotational motions of the gyrostat under a torque-free condition are given by

$$\sum_{k=x,y,z} I_{kk} \bar{\omega}_k^2 = 2T = \text{const}, \quad \sum_{k=x,y,z} (I_{kk} \bar{\omega}_k + h_k)^2 = G_p^2 = \text{const} \quad (4)$$

where the first integral in the first of equations (4) denotes the conservation of energy and the first integral in the second of equations (4) denotes the conservation of angular momentum of the torque-free gyrostat.

The complete solutions to equations (3, 4) can be given in closed form in terms of the kinetic energy T and the total angular momentum G_p of the torque-free gyrostat [31, 33, 34]. From Euler's equations (3) associated with the first integrals (4), the homoclinic

orbits of Euler's dynamical differential equations of the rotational motion of the symmetric gyrostat under torque-free motion are expressed as

$$\bar{\omega}_k(t) = \frac{\omega_{k0} + \omega_{k1} \tanh u + \omega_{k2} \tanh^2 u + \omega_{k3} \tanh^3 u + \omega_{k4} \tanh^4 u}{(D_3 + D_4 \tanh^2 u)^2} \quad (5)$$

where $k = x, y, z$ and

$$u = \beta(t - t_a) \quad (6)$$

and the parameter t_a stands for the initial time. The coefficients ω_{ij} for $i = x, y, z$,

$j = 0, 1, 2, 3, 4$, and D_3, D_4 , and β , are given as below.

$$\left. \begin{aligned} \omega_{x0} &= \frac{h_x f_0}{h_x^2 + h_y^2}, & \omega_{x1} &= \frac{-2\beta h_y (D_2 D_3 - D_1 D_4) I_{zz}}{h_x^2 + h_y^2}, & \omega_{x2} &= \frac{h_x f_1}{h_x^2 + h_y^2} \\ \omega_{x3} &= \frac{2\beta h_y (D_2 D_3 - D_1 D_4) I_{zz}}{h_x^2 + h_y^2}, & \omega_{x4} &= \frac{h_x f_2}{h_x^2 + h_y^2} \end{aligned} \right\} \quad (7)$$

$$\left. \begin{aligned} \omega_{y0} &= \frac{h_y f_0}{h_x^2 + h_y^2}, & \omega_{y1} &= \frac{2\beta h_x (D_2 D_3 - D_1 D_4) I_{zz}}{h_x^2 + h_y^2}, & \omega_{y2} &= \frac{h_y f_1}{h_x^2 + h_y^2} \\ \omega_{y3} &= \frac{-2\beta h_x (D_2 D_3 - D_1 D_4) I_{zz}}{h_x^2 + h_y^2}, & \omega_{y4} &= \frac{h_y f_2}{h_x^2 + h_y^2} \end{aligned} \right\} \quad (8)$$

$$\omega_{z0} = D_1 D_3, \quad \omega_{z1} = 0, \quad \omega_{z2} = D_1 D_4 + D_2 D_3, \quad \omega_{z3} = 0, \quad \omega_{z4} = D_2 D_4 \quad (9)$$

$$\left. \begin{aligned} f_0 &= \frac{[I_{zz}(I_{xx} - I_{zz})D_1^2 - 2I_{zz}h_z D_1 D_3 + (G_p^2 - 2I_{xx}T - h_x^2 - h_y^2 - h_z^2)D_3^2]}{2I_{xx}} \\ f_1 &= \frac{1}{I_{xx}} [I_{zz}(I_{xx} - I_{zz})D_1 D_2 - I_{zz}h_z(D_2 D_3 + D_1 D_4) + (G_p^2 - 2I_{xx}T - h_x^2 - h_y^2 - h_z^2)D_3 D_4] \\ f_2 &= \frac{[I_{zz}(I_{xx} - I_{zz})D_2^2 - 2I_{zz}h_z D_2 D_4 + (G_p^2 - 2I_{xx}T - h_x^2 - h_y^2 - h_z^2)D_4^2]}{2I_{xx}} \end{aligned} \right\} \quad (10)$$

where

$$\begin{aligned} D_1 &= \Omega_{z4}(\Omega_{z1} - \Omega_{z3}), & D_2 &= \Omega_{z1}(\Omega_{z3} - \Omega_{z4}), \\ D_3 &= \Omega_{z1} - \Omega_{z3}, & D_4 &= \Omega_{z3} - \Omega_{z4} \quad \text{if} \quad \Omega_{z4} \leq \bar{\omega}_z \leq \Omega_{z3} \end{aligned} \quad (11)$$

or

$$\begin{aligned} D_1 &= \Omega_{z1}(\Omega_{z3} - \Omega_{z4}), & D_2 &= \Omega_{z4}(\Omega_{z1} - \Omega_{z3}), \\ D_3 &= \Omega_{z3} - \Omega_{z4}, & D_4 &= \Omega_{z1} - \Omega_{z3} \quad \text{if} \quad \Omega_{z3} \leq \bar{\omega}_z \leq \Omega_{z1} \end{aligned} \quad (12)$$

and Ω_{zk} ($k = 1, 2, 3, 4$) are the real roots of the polynomial equation

$$a_4 \bar{\omega}_z^4 + a_3 \bar{\omega}_z^3 + a_2 \bar{\omega}_z^2 + a_1 \bar{\omega}_z + a_0 = 0 \quad (13)$$

where

$$a_4 = -\frac{1}{4I_{xx}^2}(I_{xx} - I_{zz})^2, \quad a_3 = \frac{1}{I_{xx}^2}(I_{xx} - I_{zz})h_z \quad (14), (15)$$

$$a_2 = -\frac{1}{I_{xx}^2 I_{zz}} \left[I_{zz} h_z^2 + I_{xx} (h_x^2 + h_y^2) + \frac{1}{2} (I_{xx} - I_{zz}) (G_p^2 - 2I_{xx}T - h_x^2 - h_y^2 - h_z^2) \right] \quad (16)$$

$$a_1 = \frac{h_z}{I_{xx}^2 I_{zz}} (G_p^2 - 2I_{xx}T - h_x^2 - h_y^2 - h_z^2) \quad (17)$$

$$a_0 = \frac{1}{4I_{xx}^2 I_{zz}^2} [8I_{xx}(h_x^2 + h_y^2)T - (G_p^2 - 2I_{xx}T - h_x^2 - h_y^2 - h_z^2)^2] \quad (18)$$

In addition, the parameter β in equation (6) is given by

$$\beta = \frac{1}{2} \sqrt{|a_4|(\Omega_{z1} - \Omega_{z3})(\Omega_{z2} - \Omega_{z4})} \quad (19)$$

The four real roots $\Omega_{z1}, \Omega_{z2}, \Omega_{z3}$, and Ω_{z4} of the polynomial equation (13) satisfy the following relations

$$\Omega_{z1} > \Omega_{z2} = \Omega_{z3} > \Omega_{z4} \quad (20)$$

so that the component of the angular velocity $\bar{\omega}_z(t)$ will actually be the homoclinic orbit of the following equation [39]

$$\left(\frac{d\bar{\omega}_z}{dt} \right)^2 = a_4\bar{\omega}_z^4 + a_3\bar{\omega}_z^3 + a_2\bar{\omega}_z^2 + a_1\bar{\omega}_z + a_0 \quad (21)$$

The detailed formulation procedure for the homoclinic orbits (5) can be found in Kuang *et al* [39]. The homoclinic orbits play a key role in the application of the Melnikov integral to the investigation of the transversal homoclinic intersections of the disturbed symmetric gyrostat.

2.3 The Melnikov integral for the perturbed gyrostat

Applying the Melnikov integral established by Wiggins and Shaw [13], originally for slowly varying oscillators, to the disturbed attitude motions of the gyrostat, the authors [39, 41] obtained a version of Melnikov integral for the gyrostat as follows, with the brief exposition in Appendix,

$$M(t_0) = \int_{-\infty}^{+\infty} \sum_{k=x,y,z} M_k(\bar{\omega}_x(t), \bar{\omega}_y(t), \bar{\omega}_z(t), t + t_0) \bar{W}_k(t) dt \quad (22)$$

where $\bar{\omega}_x(t), \bar{\omega}_y(t)$ and $\bar{\omega}_z(t)$ are the homoclinic orbits of the symmetric gyrostat under torque-free motion, defined in equations (5). The associating functions, $\bar{W}_k(t)$ for $k = x, y, z$ appearing in equation (22), are defined by

$$\begin{aligned} \bar{W}_k(t) &= \bar{\omega}_k(t) - \alpha(I_{kk}\bar{\omega}_k(t) + h_k) \\ &= \frac{W_{k0} + W_{k1} \tanh u + W_{k2} \tanh^2 u + W_{k3} \tanh^3 u + W_{k4} \tanh^4 u}{(D_3 + D_4 \tanh^2 u)^2} \end{aligned} \quad (23)$$

where the coefficients W_{kj} for $k = x, y, z$ and $j = 0, 1, 2, 3, 4$ may be expressed as

$$\left. \begin{array}{l} W_{x0} = (1 - \alpha I_{xx}) \omega_{x0} - \alpha h_x D_3^2 \\ W_{x1} = (1 - \alpha I_{xx}) \omega_{x1} \\ W_{x2} = (1 - \alpha I_{xx}) \omega_{x2} - 2\alpha h_x D_3 D_4 \\ W_{x3} = (1 - \alpha I_{xx}) \omega_{x3} \\ W_{x4} = (1 - \alpha I_{xx}) \omega_{x4} - \alpha h_x D_4^2 \end{array} \right\}, \quad \left. \begin{array}{l} W_{y0} = (1 - \alpha I_{yy}) \omega_{y0} - \alpha h_y D_3^2 \\ W_{y1} = (1 - \alpha I_{yy}) \omega_{y1} \\ W_{y2} = (1 - \alpha I_{yy}) \omega_{y2} - 2\alpha h_y D_3 D_4 \\ W_{y3} = (1 - \alpha I_{yy}) \omega_{y3} \\ W_{y4} = (1 - \alpha I_{yy}) \omega_{y4} - \alpha h_y D_4^2 \end{array} \right\} \quad (24), (25)$$

$$\left. \begin{array}{l} W_{z0} = (1 - \alpha I_{zz}) \omega_{z0} - \alpha h_z D_3^2 \\ W_{z1} = (1 - \alpha I_{zz}) \omega_{z1} \\ W_{z2} = (1 - \alpha I_{zz}) \omega_{z2} - 2\alpha h_z D_3 D_4 \\ W_{z3} = (1 - \alpha I_{zz}) \omega_{z3} \\ W_{z4} = (1 - \alpha I_{zz}) \omega_{z4} - \alpha h_z D_4^2 \end{array} \right\} \quad (26)$$

with

$$\alpha = \frac{\omega_{xp}(I_{xx}\omega_{xp} + h_x) + \omega_{yp}(I_{yy}\omega_{yp} + h_y)}{(I_{xx}\omega_{xp} + h_x)^2 + (I_{yy}\omega_{yp} + h_y)^2} \quad (27)$$

where ω_{xp} and ω_{yp} are the first two coordinates of a hyperbolic fixed point of the symmetric gyrostat under torque-free motion. The hyperbolic fixed points, ω_{xp} , ω_{yp} , and ω_{zp} , are governed by the following equations

$$(I_{yy} - I_{zz})\omega_{yp}\omega_{zp} + \omega_{zp}h_y - \omega_{yp}h_z = 0, \quad (x \ y \ z) \quad (28)$$

which are directly derived from equations (1) or (3) when setting $\omega_k = \omega_{kp} = \text{const}$ and $T_k = 0$ for $k = x, y, z$.

It is required in the Melnikov integral (22) that the fixed points ω_{xp} , ω_{yp} , and ω_{zp} of the symmetric gyrostat under torque-free motion be hyperbolic. The conditions for the fixed points to be hyperbolic are presented at the following subsection.

2.4 The hyperbolic fixed points of the torque-free symmetric gyrostat

The conditions for the fixed point to be hyperbolic are that the eigenvalues of the vector field linearized at the fixed point must have non-zero real parts. Therefore, the following inequality

$$\left(\frac{\partial^2 H_a}{\partial l \partial L} \right)^2 - \frac{\partial^2 H_a}{\partial l^2} \frac{\partial^2 H_a}{\partial L^2} > 0 \quad (29)$$

is true at the hyperbolic fixed point $(\omega_{xp}, \omega_{yp}, \omega_{zp})$, where H_a is the Hamiltonian of the gyrostat as given in Kuang *et al* [39] and the pair of variables (l, L) is two of the six Deprit variables of the gyrostat. Also

$$\left. \begin{aligned} \frac{\partial^2 H_a}{\partial l \partial L} &= 0 \\ \frac{\partial^2 H_a}{\partial l^2} &= \frac{h_x(I_{xx}\omega_{xp} + h_x)}{I_{xx}} + \frac{h_y(I_{yy}\omega_{yp} + h_y)}{I_{yy}} \end{aligned} \right\} \quad (30)$$

$$\frac{\partial^2 H_a}{\partial L^2} = \left(\frac{1}{I_{zz}} - \frac{1}{I_{xx}} \right) + \left[\frac{h_x(I_{xx}\omega_{xp} + h_x)}{I_{xx}} + \frac{h_y(I_{yy}\omega_{yp} + h_y)}{I_{yy}} \right] \frac{G_p^2}{[G_p^2 - (I_{zz}\omega_{zp} + h_z)^2]^2} \quad (31)$$

$$\omega_{xp} = \frac{h_x F_0}{h_x^2 + h_y^2}, \quad \omega_{yp} = \frac{h_y F_0}{h_x^2 + h_y^2} \quad (32)$$

$$\left. \begin{aligned} F_0 &= \frac{1}{2I_{xx}} \left[I_{zz}(I_{xx} - I_{zz})\omega_{zp}^2 - 2I_{zz}h_z\omega_{zp} + G_p^2 - 2I_{xx}T - h_x^2 - h_y^2 - h_z^2 \right] \\ \omega_{zp} &= \Omega_{z2} \quad \text{or} \quad \omega_{zp} = \Omega_{z3} \end{aligned} \right\} \quad (33)$$

Thus, the fixed points in equations (32) and (33) are hyperbolic points of the associated Hamiltonian equations satisfying inequality (29). General methods for solving the fixed points of the rotational motion of the symmetric gyrostat under torque-free motion from equations (28) may be found in Wittenburg [33] and Kuang *et al* [38]. From formulas (32) and (33), one deduces that the fixed points depend on the physical parameters

$I_{xx}, I_{yy}, I_{zz}, h_x, h_y, h_z$ and two first integrals T, G_p of the symmetric gyrostat under torque-free motion. Different sets of parameters $I_{xx}, I_{yy}, I_{zz}, h_x, h_y, h_z, T, G_p$ will result in different fixed points whether hyperbolic or not. The hyperbolic fixed points correspond to the homoclinic orbits of the symmetric gyrostat under torque-free motion. Thus, the following subsection will study the construction of the homoclinic orbits for the torque-free symmetric gyrostat.

2.5 Construction of the homoclinic orbits for the torque-free symmetric gyrostat

The conditions $\Omega_{z1} > \Omega_{z2} = \Omega_{z3} > \Omega_{z4}$ in equation (20) ensure that the polynomial equation (13) has real roots. The well-known relations between the coefficients of the polynomial equation and its roots are

$$\left. \begin{array}{l} a_3 = -a_4(\Omega_{z1} + \Omega_{z2} + \Omega_{z3} + \Omega_{z4}) \\ a_2 = a_4(\Omega_{z1}\Omega_{z2} + \Omega_{z2}\Omega_{z3} + \Omega_{z3}\Omega_{z4} + \Omega_{z4}\Omega_{z1} + \Omega_{z4}\Omega_{z2} + \Omega_{z1}\Omega_{z3}) \\ a_1 = -a_4(\Omega_{z1}\Omega_{z2}\Omega_{z3} + \Omega_{z2}\Omega_{z3}\Omega_{z4} + \Omega_{z3}\Omega_{z4}\Omega_{z1} + \Omega_{z1}\Omega_{z2}\Omega_{z4}) \\ a_0 = a_4(\Omega_{z1}\Omega_{z2}\Omega_{z3}\Omega_{z4}) \end{array} \right\} \quad (34)$$

One assumes that $\Omega_{z1}, \Omega_{z2} = \Omega_{z3}, \Omega_{z4}$ are given and

$$R_r = G_p^2 - 2I_{xx}T - h_x^2 - h_y^2 - h_z^2 \quad (35)$$

From equations (14) – (18), one may obtain

$$h_z = \frac{a_3 I_{xx}^2}{(I_{xx} - I_{zz})}, \quad R_r = \frac{a_1 I_{xx}^2 I_{zz}}{h_z}, \quad h_x^2 + h_y^2 = \frac{-(I_{zz} h_z^2 + 0.5(I_{xx} - I_{zz})R_r + I_{xx}^2 I_{zz} a_2)}{I_{xx}} \quad (36)$$

$$T = \frac{4I_{xx}^2 I_{zz}^2 a_0 + R_r^2}{8I_{xx}(h_x^2 + h_y^2)}, \quad G_p^2 = 2I_{xx}T + (h_x^2 + h_y^2) + h_z^2 + \frac{a_1 I_{xx}^2 I_{zz}}{h_z} \quad (37)$$

The relationships between the physical parameters $I_{xx}, I_{yy}, I_{zz}, h_x^2 + h_y^2, h_z, G_p$ and T and the four real roots $\Omega_{z1} > \Omega_{z2} = \Omega_{z3} > \Omega_{z4}$ of the polynomial equation (13) can be constructed as follows. Given the four real roots $\Omega_{z1} > \Omega_{z2} = \Omega_{z3} > \Omega_{z4}$ of polynomial equation (13) and the principal moments of inertia of the gyrostat I_{xx}, I_{yy}, I_{zz} , one may compute the physical parameters $h_x^2 + h_y^2, h_z, G_p$ and T corresponding to the homoclinic orbits of the symmetric gyrostat under torque-free motion from equations (36) and (37). The construction of the homoclinic orbits of the torque-free attitude motions of the symmetric gyrostat is a prerequisite for applying the Melnikov integral (22) to investigate the transversal homoclinic intersections between the stable and unstable manifolds of the disturbed symmetric gyrostat subject to the small forced torques.

The Melnikov integral (22) is an infinite integral from $-\infty$ to $+\infty$ and convergence is an issue. Therefore, one has to study the limit properties of the homoclinic orbits of the symmetric gyrostat under torque-free motion when t approaches $\pm\infty$.

2.6 The property of the associating functions $\bar{W}_k(t)$ for $k = x, y, z$

In this subsection we shall analyse the property of the associating functions $\bar{W}_k(t)$ for $k = x, y, z$ in equations (23). Substituting equations (24) – (26) and equations (7) – (12) into equations (23), one obtains

$$\lim_{t \rightarrow \pm\infty} \bar{W}_k(t) = \omega_{kp} - \alpha(I_{kk}\omega_{kp} + h_k) = W_{k0} + W_{k1} + W_{k2} + W_{k3} + W_{k4} \equiv 0 \quad (38)$$

where $k = x, y, z$.

In the derivation of the third of equations (38), the property that the root Ω_{z2} is a double root of equation (13) is applied. The third of equations (38) is equivalent to the following equation

$$4a_4\omega_{zp}^3 + 3a_3\omega_{zp}^2 + 2a_2\omega_{zp} + a_1 = 0 \quad (39)$$

which is obtained from the polynomial equation (13) after substitution of the double root ω_{zp} by onefold differentiation with respect to ω_{zp} . One can deduce from equations (38) that when the torques in equations (2) are continuous and bounded functions of the variables $\omega_x, \omega_y, \omega_z$ and t , the Melnikov integral (22) is always convergent. Thus, the properties described in equations (38) ensure the convergence of the Melnikov integral for the rotational motions of the symmetrical gyrostat subject to the small forced torques.

2.7 The equation of the Melnikov integral

We shall investigate the real zeros of the Melnikov integral (22). The real zeros of the Melnikov integral satisfy

$$\begin{aligned} 0 &= M(I_{xx}, I_{yy}, I_{zz}; h_x, h_y, h_z; T, G_p; M_x, M_y, M_z; t_0) \\ &= \int_{-\infty}^{+\infty} \sum_{x=x,y,z} M_k(\bar{\omega}_x(t), \bar{\omega}_y(t), \bar{\omega}_z(t), t + t_0) \bar{W}_k(t) dt \equiv M(t_0) \end{aligned} \quad (40)$$

We use $M(t_0)$ for simplicity but emphasize that the Melnikov integral depends on all of the parameters $I_{xx}, I_{yy}, I_{zz}, h_x, h_y, h_z, T, G_p$ and the external disturbance torque functions $M_k(\omega_x, \omega_y, \omega_z, t)$ for $k = x, y, z$ along the homoclinic orbits $\bar{\omega}_x(t), \bar{\omega}_y(t), \bar{\omega}_z(t)$ of the symmetric gyrostat under torque-free motion. From the Melnikov integral (40), one observes that the homoclinic orbits of the torque-free attitude motions play a key part in the study of the chaotic dynamics via transversal homoclinic intersections of

the perturbed gyrostat by small perturbation torques. The Melnikov integral (40) describes the complicated relationships among the physical parameters $I_{xx}, I_{yy}, I_{zz}, h_x^2 + h_y^2, h_z$ and the coefficients of external torques defined in equations (2). These relationships will be shown explicitly in the next section. The angular momenta h_x, h_y , and h_z of the wheels and the two first integrals G_p and T corresponding to the homoclinic orbits of the rotational motions of the symmetric gyrostat under torque-free motion can be determined from the equations (36) and (37).

Using the algorithms established in Kuang *et al* [38, 39, 41], when the parameters $I_{xx}, I_{yy}, I_{zz}, h_x, h_y, h_z, T, G_p$ and the external disturbance torque functions M_x, M_y, M_z are given and if there is a t_0 that makes the Melnikov integral (40) valid, one can conclude in the Appendix that there exist transversal intersections of the stable and unstable manifolds for the perturbed attitude motions of the symmetric gyrostat. The transversal intersections of the stable and unstable manifolds of the disturbed symmetric gyrostat imply that chaos may exist in the sense of Smale's horse-shoes. Lots of literature [12, 13, 37 -39, 41 – 56] focused on the application of different versions of the Melnikov integral to show the existence of chaos in the sense of Smale's horse-shoes. In this paper, similarly, we shall use just one version of the Melnikov integral (40) to show the possible existence of chaos in the sense of Smale's horse-shoes for the class of 3D oscillators of modified Brockett, Chua, Duffing, Ueda, modified Kapitaniak, generalized Lorenz, forced Lorenz, Rossler and YSVO, defined in Examples (1 - 9) in Section 6. The fundamental approach is to find the set of the appropriate physical parameters $I_{xx}, I_{yy}, I_{zz}; h_x, h_y, h_z; T, G_p$ and torque functions $M_k(\omega_x, \omega_y, \omega_z, t)$ for $k = x, y, z$ so that the Melnikov integral equation (40) have real zeros with respect to the specified variables.

Alternatively speaking, the class of the 3D oscillators is equivalent to a symmetric gyrostat disturbed by appropriate torques. Mathematically, these oscillators can be represented by the integrable system of a torque-free symmetric gyrostat with appropriate disturbing torques and system parameters to be determined by the Melnikov integral equation (40).

Section 3. A unified form of the class of the 3D oscillators

In this section, the class of 3D oscillators of the modified Brockett, Chua, Duffing, Ueda, modified Kapitaniak, forced Lorenz, generalized Lorenz, Rossler and YSVO equations will be represented in a unified form of the equivalent symmetric gyrostat and the appropriate disturbance torque functions. The extended Melnikov integral for the class of oscillators will be derived in the next section.

Usually, for a dissipative or conservative dynamical system governed by a finite set of linear ordinary differential equations, a constant excitation leads to a constant response, while a periodic excitation leads to a periodic response. Non-periodic solutions have sometimes been regarded as the result of non-periodic or random excitations. Lorenz [1] found in nonlinear differential equations that non-periodic solutions exist under periodic excitations. Since then, many other chaotic dynamical systems corresponding to nonlinear differential equations have been discovered by numerical means. However, no convincing analytical methods are found to demonstrate the possible existence of chaos in the class of the 3D oscillators mentioned above. A necessary condition for determining analytically the onset of transversal intersections in the sense of Smale's horseshoes for the 3D oscillators will be derived using the Melnikov integral (40).

Consider the class of oscillators described by three state variables ω_x, ω_y , and ω_z

$$\frac{d\omega_k}{dt} = \theta_{kx}\omega_x + \theta_{ky}\omega_y + \theta_{kz}\omega_z + \Theta_{xy}^k\omega_x\omega_y + \Theta_{yz}^k\omega_y\omega_z + \Theta_{zx}^k\omega_z\omega_x + \beta_k(\omega_x, \omega_y, \omega_z, \beta_{x0}, t) \quad (41)$$

where $k = x, y, z$, and the time t is the only independent variable. $\theta_{ij}, \Theta_{ij}^k, \beta_k$ for $i, j, k = x, y, z$ are known constants. In addition, assume β_k to be of the following form

$$\beta_k(\omega_x, \omega_y, \omega_z, \beta_{x0}, t) = \Gamma_{kx}\omega_x^3 + \Gamma_{ky}\omega_y^3 + \Gamma_{kz}\omega_z^3 + N_k(\omega_x, \omega_y, \omega_z, t) + \beta_{k0} \left. \right\} + d_{kx}\sin(\Omega_x t) + d_{ky}\sin(\Omega_y t) + d_{kz}\sin(\Omega_z t) \quad (42)$$

where $k = x, y, z$ and $\Gamma_{ij}, d_{ij}, \beta_{i0}$ for $i, j = x, y, z$ are known constants. $N_k(\omega_x, \omega_y, \omega_z, t)$ for $k = x, y, z$ stand for the other nonlinear terms that are accounted for on the right sides of equations (41). Denote the matrices whose entries are θ_{ij} , Θ_{ij} , Γ_{ij} and d_{ij} for $i, j = x, y, z$ as θ _matrix, Θ _matrix, Γ _matrix and d _matrix respectively. Denote also the columns whose entries are β_{i0} , Ω_i and N_i for $i = x, y, z$ as β _column, Ω _column and N _column respectively. Then the class of the 3D oscillators can be united in one form using these matrices and columns as given in equations (147) – (148).

Comparing the forced symmetric gyrostat (1) under the disturbed torques (2) in the dynamical systems (41), one obtains the following matrix identities

$$\varepsilon \begin{bmatrix} \mu_{xx} & \mu_{xy} & \mu_{xz} \\ \mu_{yx} & \mu_{yy} & \mu_{yz} \\ \mu_{zx} & \mu_{zy} & \mu_{zz} \end{bmatrix} = \begin{bmatrix} I_{xx} & 0 & 0 \\ 0 & I_{yy} & 0 \\ 0 & 0 & I_{zz} \end{bmatrix} \begin{bmatrix} \theta_{xx} & \theta_{xy} & \theta_{xz} \\ \theta_{yx} & \theta_{yy} & \theta_{yz} \\ \theta_{zx} & \theta_{zy} & \theta_{zz} \end{bmatrix} + \begin{bmatrix} 0 & h_z & -h_y \\ -h_z & 0 & h_x \\ h_y & -h_x & 0 \end{bmatrix} \quad (43)$$

$$\varepsilon \begin{bmatrix} \Pi_{xx} & \Pi_{xy} & \Pi_{xz} \\ \Pi_{yx} & \Pi_{yy} & \Pi_{yz} \\ \Pi_{zx} & \Pi_{zy} & \Pi_{zz} \end{bmatrix} = \begin{bmatrix} I_{xx} & 0 & 0 \\ 0 & I_{yy} & 0 \\ 0 & 0 & I_{zz} \end{bmatrix} \begin{bmatrix} \Theta_{xy}^x & \Theta_{yz}^x & \Theta_{zx}^x \\ \Theta_{xy}^y & \Theta_{yz}^y & \Theta_{zx}^y \\ \Theta_{xy}^z & \Theta_{yz}^z & \Theta_{xy}^z \end{bmatrix} + \begin{bmatrix} 0 & I_{zz} - I_{yy} & 0 \\ 0 & 0 & I_{xx} - I_{zz} \\ I_{yy} - I_{xx} & 0 & 0 \end{bmatrix} \quad (44)$$

$$\varepsilon \begin{bmatrix} T_{x0}(\omega_x, \omega_y, \omega_z, \beta_{x0}, t) \\ T_{y0}(\omega_x, \omega_y, \omega_z, \beta_{x0}, t) \\ T_{z0}(\omega_x, \omega_y, \omega_z, \beta_{x0}, t) \end{bmatrix} = \begin{bmatrix} I_{xx}\beta_x(\omega_x, \omega_y, \omega_z, \beta_{x0}, t) \\ I_{yy}\beta_y(\omega_x, \omega_y, \omega_z, \beta_{y0}, t) \\ I_{zz}\beta_z(\omega_x, \omega_y, \omega_z, \beta_{z0}, t) \end{bmatrix} \quad (45)$$

where the left-hand terms of equations (43) – (45) are called the μ _matrix, Π _matrix and T _column, respectively, for further references in Section 5.

Equations (43) – (45) relate the symmetrical gyrostat (1) to the unified class of the oscillators (41). Given the dynamical system (41), one can obtain the corresponding dynamical system (1) of the disturbed gyrostat. Therefore, the Melnikov integral equation (40) can be used to determine whether or not the stable and unstable manifolds intersect transversally and thus detect the possible chaotic dynamics of the class of the 3D oscillators.

Section 4. The explicit Melnikov integral

The explicit Melnikov integral of the gyrostat will be given in this section for the application to the class of the 3D oscillators in the next two sections. The extended Melnikov integral is first partitioned into smaller manageable forms in equation (46) in Subsection 4.1. The integrals I_{const} , I_{linear} , I_{cross} , I_{cube} , I_{forced} , $I_{N_{\text{chua}}}(t_0)$ and $I_{N_{\text{m}}\text{Rossler}}(t_0)$ are computed in Subsections 4.2 to 4.9 respectively. In what follows, the essential formulas for linking the Melnikov integral and the Lorenz dynamical systems, Chua double scroll systems, and similar systems are presented in detail.

4.1 Partitions of the Melnikov integral

In this section, we shall derive the explicit version of the Melnikov integral (40).

Substitution of equations (2) of the torque functions $M_k(\omega_x, \omega_y, \omega_z, t)$ for $k = x, y, z$ into the Melnikov integral (22) yields

$$\varepsilon M(t_0) = I_{\text{const}} + I_{\text{linear}} + I_{\text{cross}} + I_{\text{cube}} + I_N(t_0) + I_{\text{forced}}(t_0) \quad (46)$$

where

$$I_{\text{const}} = \int_{-\infty}^{+\infty} (I_{xx}\beta_{x0}\bar{W}_x(t) + I_{yy}\beta_{y0}\bar{W}_y(t) + I_{zz}\beta_{z0}\bar{W}_z(t)) dt \quad (47)$$

$$I_{\text{linear}} = \int_{-\infty}^{+\infty} \left[\sum_{k=x,y,z} \varepsilon (\mu_{kx}\bar{\omega}_x(t) + \mu_{ky}\bar{\omega}_y(t) + \mu_{kz}\bar{\omega}_z(t)) \bar{W}_k(t) \right] dt \quad (48)$$

$$I_{\text{cross}} = \int_{-\infty}^{+\infty} \left[\sum_{k=x,y,z} \varepsilon (\Pi_{xy}^k \bar{\omega}_x(t) \bar{\omega}_y(t) + \Pi_{yz}^k \bar{\omega}_y(t) \bar{\omega}_z(t) + \Pi_{zx}^k \bar{\omega}_z(t) \bar{\omega}_x(t)) \bar{W}_k(t) \right] dt \quad (49)$$

$$I_{\text{cube}} = \int_{-\infty}^{+\infty} \left[\sum_{k=x,y,z} I_{kk} (\Gamma_{kx}\bar{\omega}_x(t)^3 + \Gamma_{ky}\bar{\omega}_y(t)^3 + \Gamma_{kz}\bar{\omega}_z(t)^3) \bar{W}_k(t) dt \right] \quad (50)$$

$$I_{\text{forced}}(t_0) = \int_{-\infty}^{+\infty} \sum_{k=x,y,z} \left\{ I_{kk} \left[d_{kx} \sin(\Omega_x(t+t_0)) + d_{ky} \sin(\Omega_y(t+t_0)) + d_{kz} \sin(\Omega_z(t+t_0)) \right] \bar{W}_k(t) \right\} dt \quad (51)$$

$$I_N(t_0) = \int_{-\infty}^{+\infty} \left[\sum_{k=x,y,z} I_{kk} N_k(\bar{\omega}_x(t), \bar{\omega}_y(t), \bar{\omega}_z(t), t+t_0) \bar{W}_k(t) \right] dt \quad (52)$$

The last integral (52) denotes the contribution of the terms $N_k(\omega_x, \omega_y, \omega_z, t)$ for $k = x, y, z$ and will converge if the functions $N_k(\omega_x, \omega_y, \omega_z, t)$ for $k = x, y, z$ are assumed to be continuous, bounded functions with respect to the time t . The computations of the last integral will be intensively studied in Subsections 4.8 and 4.9.

4.2 Computation of the Integral I_{const} in equation (47)

Substituting equations (23) into equation (47), one obtains

$$I_{\text{const}} = \int_{-\infty}^{+\infty} \frac{\sum_{k=0}^4 (W_{ck} \tanh^k)}{(D_3 + D_4 \tanh^2 u)^2} dt \quad (53)$$

where u is defined in equation (6) and

$$W_{ck} = I_{xx} \beta_{x0} W_{xk} + I_{yy} \beta_{y0} W_{yk} + I_{zz} \beta_{z0} W_{zk} \quad (54)$$

for $k = 0, 1, 2, 3$, and 4 . Thus, one can further rewrite equation (53) into the form

$$I_{\text{const}} = \int_{-\infty}^{+\infty} \frac{\sum_{k=0}^{16} (W_{wk} \tanh^k u)}{(D_3 + D_4 \tanh^2 u)^8} dt \quad (55)$$

where W_{wk} for $k = 0, 1, \dots, 16$ are given by

$$\sum_{k=0}^{16} (W_{wk} \tanh^k u) = \left(\sum_{k=0}^4 (W_{ck} \tanh^k u) \right) \left(\sum_{k=0}^{12} (W_k'' \tanh^k u) \right) \quad (56)$$

W_k'' for $k = 0, 1, 2, \dots, 12$ are derived from the polynomial equation

$$(D_3 + D_4 \tanh^2 u)^6 = \sum_{k=0}^{12} (W_k'' \tanh^k u), \text{ where}$$

$$\left. \begin{array}{ll} W_0'' = (D_3)^6, & W_2'' = 6(D_3)^5 D_4 \\ W_4'' = 15(D_3)^4 (D_4)^2, & W_6'' = 20(D_3)^3 (D_4)^3 \\ W_8'' = 15(D_3)^2 (D_4)^4, & W_{10}'' = 6D_3 (D_4)^5 \\ W_{12}'' = 6(D_4)^6, & W_1'' = W_3'' = W_5'' = W_7'' = W_9'' = W_{11}'' = 0 \end{array} \right\}$$

One observes that the coefficients W_{wk} for $k = 0, 1, \dots, 16$ are the functions of the parameters $I_{xx}, I_{yy}, I_{zz}; h_x, h_y, h_z; T, G_p$ when the $\beta_{x0}, \beta_{y0}, \beta_{z0}$ are given.

4.3 Computation of the integral I_{linear} in equation (48)

Substituting equations (5) and equations (23) into equation (48), one obtains

$$I_{\text{linear}} = \int_{-\infty}^{+\infty} \frac{\sum_{k=0}^8 (T_k \tanh^k u)}{\left(D_3 + D_4 \tanh^2 u \right)^4} dt \quad (57)$$

where u is defined in equation (6) and

$$T_k = \sum_{i,j=x,y,z} (\varepsilon \mu_{ij} b_{ijk}) \quad (58)$$

with $k = 0, 1, \dots, 8$ in which b_{ijk} may be formulated from the equation

$$\sum_{k=0}^8 (b_{ijk} \tanh^k u) = \left(\sum_{k=0}^4 (\omega_{jk} \tanh^k u) \right) \left(\sum_{k=0}^4 (W_{ik} \tanh^k u) \right) \quad (59)$$

where $i, j = x, y, z$. One can further rewrite equation (57) into the form

$$I_{\text{linear}} = \int_{-\infty}^{+\infty} \frac{\sum_{k=0}^{16} (T_{ik} \tanh^k u)}{\left(D_3 + D_4 \tanh^2 u \right)^8} dt \quad (60)$$

where T_{ik} for $k = 0, 1, 2, \dots, 16$ may be obtained from the equation such as

$$\sum_{k=0}^{16} (T_{ik} \tanh^k u) = \left(\sum_{k=0}^8 (T_k \tanh^k u) \right) \left(\sum_{k=0}^8 (t_k'' \tanh^k u) \right) \quad (61)$$

where t_k'' ($k = 0, 1, 2, \dots, 8$) are derived from the following polynomial identity

$$(D_3 + D_4 \tanh^2 u)^4 = \sum_{k=0}^8 (t_k'' \tanh^k u)$$

with

$$\left. \begin{array}{ll} t_0'' = (D_3)^4, & t_2'' = 4(D_3)^3 D_4 \\ t_4'' = 6(D_3)^2 (D_4)^2, & t_6'' = 4D_3 (D_4)^3 \\ t_8'' = (D_4)^4, & t_1'' = t_3'' = t_5'' = t_7'' = 0 \end{array} \right\}$$

The coefficients T_{ik} ($k = 0, 1, \dots, 16$) defined in equation (61) are the functions of the parameters $I_{xx}, I_{yy}, I_{zz}; h_x, h_y, h_z; T, G_p$ when the μ _matrix is given.

4.4 Computation of the integral I_{cross} in equation (49)

Substituting equations (5) and equations (23) into equation (49), one obtains

$$I_{\text{cross}} = \int_{-\infty}^{+\infty} \frac{\sum_{k=0}^{12} (E_k \tanh^k u)}{(D_3 + D_4 \tanh^2 u)^6} dt \quad (62)$$

where u is defined in equation (6) and

$$E_p = \sum_{k=x,y,z} (\varepsilon \Pi_{xy}^k d_{xyp}^k + \varepsilon \Pi_{yz}^k d_{yzp}^k + \varepsilon \Pi_{zx}^k d_{zxp}^k) \quad (63)$$

with $p = 0, 1, \dots, 12$ in which d_{ijp}^k may be derived from the polynomial equation

$$\sum_{p=0}^{12} (d_{ijp}^k \tanh^p u) = \left(\sum_{p=0}^4 (W_{kp} \tanh^p u) \right) \left(\sum_{p=0}^8 (c_{ijp} \tanh^p u) \right) \quad (64)$$

where $i, j, k = x, y, z$ and the coefficients c_{ijk} may be derived from the equation

$$\sum_{p=0}^8 (c_{ijp} \tanh^p u) = \left(\sum_{p=0}^4 (\omega_{jp} \tanh^p u) \right) \left(\sum_{p=0}^4 (c_{ip} \tanh^p u) \right) \quad (65)$$

where $i, j = x, y, z$. One can further rewrite equation (62) into the form

$$I_{\text{cross}} = \int_{-\infty}^{+\infty} \frac{\sum_{k=0}^{16} (E_{ek} \tanh^k u)}{(D_3 + D_4 \tanh^2 u)^8} dt \quad (66)$$

where E_{ek} for $k = 0, 1, 2, \dots, 16$ may be derived from the equation

$$\sum_{k=0}^{16} (E_{ek} \tanh^k u) = \left(\sum_{k=0}^4 (E_{ek} \tanh^k u) \right) \left(\sum_{k=0}^4 (e_k \tanh^k u) \right) \quad (67)$$

in which e_k for $k = 0,1,2,3,4$ are derived from the polynomial equation

$$(D_3 + D_4 \tanh^2 u)^2 = \sum_{k=0}^4 (e_k \tanh^k u)$$

with $e_0 = (D_3)^2$, $e_2 = 2D_3D_4$, $e_4 = (D_4)^2$, $e_1 = e_3 = 0$. From equations (67), one deduces that the coefficients E_{ek} for $k = 0,1,\dots,16$ in equation (66) are also functions of the parameters $I_{xx}, I_{yy}, I_{zz}; h_x, h_y, h_z; T, G_p$ when the Π -matrix is given.

4.5 Computation of the integral I_{cube} in equation (50)

Substituting equations (5) and equations (23) into equation (50), one obtains

$$I_{\text{cube}} = \int_{-\infty}^{+\infty} \frac{\sum_{k=0}^{16} (F_{fk} \tanh^k u)}{(D_3 + D_4 \tanh^2 u)^8} dt \quad (68)$$

where u is defined in equation (6) and

$$F_{fj} = \sum_{k=x,y,z} \left[I_{kk} (\varepsilon \Gamma_{kx} f_{xkj} + \varepsilon \Gamma_{ky} f_{ykj} + \varepsilon \Gamma_{kz} f_{z kj}) \right] \quad (69)$$

with $j = 0,1,\dots,16$ in which

$$\sum_{j=0}^{16} (f_{ikj} \tanh^j u) = \left(\sum_{j=0}^4 (W_{kj} \tanh^j u) \right) \left(\sum_{j=0}^{12} (d_{ij} \tanh^j u) \right) \quad (70)$$

where $i,k = x,y,z$ with coefficients f_{ij} satisfying the polynomial equation

$$\sum_{j=0}^{12} f_{ij} \tanh^j u = \left(\sum_{j=0}^4 \omega_{ij} \tanh^j u \right) \left(\sum_{j=0}^8 c_{ij} \tanh^j u \right) \quad (71)$$

where $i = x,y,z$ in which coefficients c_{ij} satisfying the polynomial equation

$$\sum_{j=0}^8 c_{ij} \tanh^j u = \left(\sum_{j=0}^4 \omega_{ij} \tanh^j u \right) \left(\sum_{j=0}^4 \omega_{ij} \tanh^j u \right) \quad (72)$$

with $i = x, y, z$.

From the equation (69) one may conclude that the coefficients F_{jk} for $k = 0, 1, \dots, 16$ are also functions of the parameters $I_{xx}, I_{yy}, I_{zz}; h_x, h_y, h_z; T, G_p$ when the Γ -matrix is given.

4.6 Computation of the integral I_{forced} in equation (51)

Using trigonometric function formulas, one obtains from equation (51) that

$$I_{\text{forced}}(t_0) = \sum_{k=x,y,z} [B_k \cos(\Omega_k t_0) + S_k \sin(\Omega_k t_0)] \quad (73)$$

where

$$\left. \begin{aligned} B_k &= \int_{-\infty}^{+\infty} [I_{xx} d_{xk} \bar{W}_x(t) + I_{yy} d_{yk} \bar{W}_y(t) + I_{zz} d_{zk} \bar{W}_z(t)] \sin(\Omega_k t) dt \\ S_k &= \int_{-\infty}^{+\infty} [I_{xx} d_{xk} \bar{W}_x(t) + I_{yy} d_{yk} \bar{W}_y(t) + I_{zz} d_{zk} \bar{W}_z(t)] \cos(\Omega_k t) dt \end{aligned} \right\} \quad (74)$$

with $k = x, y, z$.

Substituting equations (23) into equations (74), one obtains

$$B_k = \int_{-\infty}^{+\infty} \frac{\sum_{m=0}^4 (B_{km} \tanh^m u)}{\left(D_3 + D_4 \tanh^2 u \right)^2} \sin(\Omega_k t) dt, \quad S_k = \int_{-\infty}^{+\infty} \frac{\sum_{m=0}^4 (B_{km} \tanh^m u)}{\left(D_3 + D_4 \tanh^2 u \right)^2} \cos(\Omega_k t) dt \quad (75)$$

where

$$B_{km} = I_{xx} d_{xk} W_{xm} + I_{yy} d_{yk} W_{ym} + I_{zz} d_{zk} W_{zm} \quad (76)$$

with $k = x, y, z$ and $m = 0, 1, 2, 3, 4$.

The following conditions ensure the convergence of the integrals in equations

(75),

$$B_{k1} + B_{k3} = 0, \quad B_{k0} + B_{k2} + B_{k4} = 0 \quad (77)$$

with $k = x, y, z$. From equations (38), one can deduce that equations (77) hold always.

Using the residue theory, one may obtain from equation (75) that

$$\left. \begin{aligned} B_k &= \int_{-\infty}^{+\infty} \frac{(-B_{k3}) \sinh(2u) \sin(\Omega_k t)}{2D_4^2 (\sinh^2 u + G \cosh^2 u)^2} dt = B_{k3} J_k \\ S_k &= \int_{-\infty}^{+\infty} \frac{[(-B_{k2} - 2B_{k4}) \cosh(2u) - B_{k2}] \cos(\Omega_k t)}{2D_4^2 (\sinh^2 u + G \cosh^2 u)^2} dt = \beta_{k1} (B_{k2} + B_{k4}) + \beta_{k2} B_{k2} \end{aligned} \right\} \quad (78)$$

with $k = x, y, z$, and $G = D_3/D_4$ and

$$J_k = \frac{(-\pi)}{4\beta D_4^2 (G+1)^2 \left[1 - \cosh\left(\frac{\pi\Omega_k}{\beta}\right) \right]} \times \left[\frac{\frac{\Omega_k}{\beta} \sin(2\theta_a) \cosh\left(\frac{\Omega_k \theta_a}{\beta}\right)}{\sin^2 \theta_a \cos^2 \theta_a} + \frac{\frac{\Omega_k}{\beta} \sin(2\theta_b) \cosh\left(\frac{\Omega_k \theta_b}{\beta}\right)}{\sin^2 \theta_b \cos^2 \theta_b} \right] \quad (79)$$

with $i\theta_a + i\theta_b = i\pi$, $0 < \theta_a < \pi$ and $0 < \theta_b < \pi$, where i is the imaginary unit.

$i\theta_a$ and $i\theta_b$ are the imaginary roots of the following equations as shown by Kuang *et al* [41] and Or [46]

$$\sinh(i\theta_a) - i\sqrt{G} \cosh(i\theta_a) = 0, \quad \sinh(i\theta_b) + i\sqrt{G} \cosh(i\theta_b) = 0 \quad (80)$$

$$\beta_{k1} = \frac{(-\pi)}{4\beta D_4^2 (G+1)^2 \left[1 - \cosh\left(\frac{\pi\Omega_k}{\beta}\right) \right]} \times$$

$$\left[\frac{2\sin(2\theta_a)\cosh\left(\frac{\Omega_k\theta_a}{\beta}\right) - \frac{\Omega_k}{\beta} \cos(2\theta_a)\sinh\left(\frac{\Omega_k\theta_a}{\beta}\right)}{\sin^2\theta_a \cos^2\theta_a} + \right.$$

$$\frac{2\sin(2\theta_b)\cosh\left(\frac{\Omega_k\theta_b}{\beta}\right) - \frac{\Omega_k}{\beta} \cos(2\theta_b)\sinh\left(\frac{\Omega_k\theta_b}{\beta}\right)}{\sin^2\theta_b \cos^2\theta_b} +$$

$$\left. \frac{\cos^2(2\theta_a)\cosh\left(\frac{\Omega_k\theta_a}{\beta}\right) + \cos^2(2\theta_b)\cosh\left(\frac{\Omega_k\theta_b}{\beta}\right)}{\sin^3\theta_a \cos^3\theta_a + \sin^3\theta_b \cos^3\theta_b} \right] \quad (81)$$

$$\beta_{k2} = \frac{(-\pi)}{2\beta D_4^2 (G+1)^2 \left[1 - \cosh\left(\frac{\pi\Omega_k}{\beta}\right) \right]} \times$$

$$\left[\frac{\left(-\frac{\Omega_k}{\beta}\right) \sinh\left(\frac{\Omega_k\theta_a}{\beta}\right) + \left(-\frac{\Omega_k}{\beta}\right) \sinh\left(\frac{\Omega_k\theta_b}{\beta}\right)}{\sin^2\theta_a \cos^2\theta_a + \sin^2\theta_b \cos^2\theta_b} + \right.$$

$$\left. \frac{\cos(2\theta_a)\cosh\left(\frac{\Omega_k\theta_a}{\beta}\right) + \cos(2\theta_b)\cosh\left(\frac{\Omega_k\theta_b}{\beta}\right)}{\sin^3\theta_a \cos^3\theta_a + \sin^3\theta_b \cos^3\theta_b} \right] \quad (82)$$

with $k = x, y, z$.

Substituting equations (78) into equation (73), one obtains

$$I_{\text{forced}}(t_0) = \sum_{k=x,y,z} \sum_{m=x,y,z} d_{km} I_{kk} \left[(\beta_{m1} + \beta_{m2}) \sin(\Omega_m t_0) W_{k2} + J_m \cos(\Omega_m t_0) W_{k3} + 2\beta_{m1} \sin(\Omega_m t_0) W_{k4} \right] \quad (83)$$

when the following equations

$$\begin{bmatrix} d_{xx} & d_{yx} & d_{zx} \\ d_{xy} & d_{yy} & d_{zy} \\ d_{xz} & d_{yz} & d_{zz} \end{bmatrix} \begin{bmatrix} I_{xx}(W_{x0} + W_{x2} + W_{x4}) \\ I_{yy}(W_{y0} + W_{y2} + W_{y4}) \\ I_{zz}(W_{z0} + W_{z2} + W_{z4}) \end{bmatrix} = 0 \quad (84)$$

hold. Equations (84) are derived from the second of equations (77). From equations (38), equations (84) hold always. Moreover, one may also deduce that the coefficients β_{km} and J_k for $k = x, y, z; m = 1, 2$ are also functions of the parameters $I_{xx}, I_{yy}, I_{zz}; h_x, h_y, h_z; T, G_p$ when the Ω _column is given.

4.7 Computation of the $I_{\text{const}} + I_{\text{linear}} + I_{\text{cross}} + I_{\text{cube}}$ in equation (46)

Adding equations (55), (60), (66) and (68), one obtains

$$I_{\text{const}} + I_{\text{linear}} + I_{\text{cross}} + I_{\text{cube}} = \int_{-\infty}^{+\infty} \frac{\sum_{k=0}^{16} (g_k \tanh^k u)}{(D_3 + D_4 \tanh^2 u)^8} dt \quad (85)$$

where u is defined in equation (6) and

$$g_k = W_{wk} + T_{tk} + E_{ek} + F_{fk} \quad (86)$$

with $k = 0, 1, \dots, 16$. W_{wk} are defined in equation (56), T_{tk} in equation (61), E_{ek} in equation (67) and F_{fk} in equation (69).

One further obtains from equation (46) that the Melnikov integral takes the form

$$\varepsilon M(t_0) = \int_{-\infty}^{+\infty} \frac{\sum_{k=0}^{16} (g_k \tanh^k u)}{(D_3 + D_4 \tanh^2 u)^8} dt + I_N(t_0) + I_{\text{forced}}(t_0) \quad (87)$$

Setting the transformation $x = \tanh u$ from the last equation, one gets

$$\varepsilon M(t_0) = \int_{-1}^{+1} \frac{\sum_{k=0}^8 (g_{2 \times k} x^{2k})}{(D_3 + D_4 x^2)^8 (1-x^2)} dx + I_N(t_0) + I_{\text{forced}}(t_0) \quad (88)$$

Thus, in order to ensure the convergence of the integral (88), it is required that the following equations hold simultaneously

$$\left. \begin{array}{l} g_0 + g_2 + g_4 + g_6 + g_8 + g_{10} + g_{12} + g_{14} + g_{16} = 0 \\ \lim_{t \rightarrow \pm\infty} [I_{xx} d_{xk} \bar{W}_x(t) + I_{yy} d_{yk} \bar{W}_y(t) + I_{zz} d_{zk} \bar{W}_z(t)] = 0 \\ \lim_{t \rightarrow \pm\infty} [N_k(\bar{\omega}_x(t), \bar{\omega}_y(t), \bar{\omega}_z(t), t + t_0) \bar{W}_k(t)] = 0 \end{array} \right\} \quad (89)$$

where $k = x, y, z$ and the last equations (89) are derived from equation (87) with equations (74) together with equation (52).

Assume that $N_k(\bar{\omega}_x(t), \bar{\omega}_y(t), \bar{\omega}_z(t), t + t_0)$ for $k = x, y$, and z are continuous, real, and bounded functions of the variables $\bar{\omega}_x, \bar{\omega}_y, \bar{\omega}_z$, and t . Then, from the properties of the homoclinic orbits (38) of the torque-free symmetric gyrostat, one can deduce that all of equations (89) hold simultaneously. The convergence issue of the integral $I_N(t_0)$ in equation (52) will be discussed further in the subsections 4.8 and 4.9 in detail when $N_k(\bar{\omega}_x(t), \bar{\omega}_y(t), \bar{\omega}_z(t), t + t_0)$ for $k = x, y, z$ are bounded and real functions of time t as in the Chua double scroll equations and the modified Rossler model of turbulence.

Therefore, the Melnikov integral equation (88) may be expressed as

$$\varepsilon M(t_0) = \frac{1}{\beta} \sum_{k=1}^8 \beta_k I_k + I_N(t_0) + I_{\text{forced}}(t_0) \quad (90)$$

by integration. The parameters β_k, I_k for $k = 1, 2, \dots, 8$ are the functions of the parameters

$I_{xx}, I_{yy}, I_{zz}; h_x, h_y, h_z; T, G_p$ when given the θ _matrix, Θ _matrix, β _column,

Ω _column, N _column, Γ _matrix, and d _matrix, μ _matrix, Π _matrix and T _column. The parameters β_k, I_k for $k = 1, 2, \dots, 8$ can be computed in the following way. Using the method of partial fractions, one finds from equation (85)

$$I_{\text{const}} + I_{\text{linear}} + I_{\text{cross}} + I_{\text{cube}} = \frac{1}{\beta} \int_{-1}^{+1} \left[\sum_{k=0}^8 \frac{\beta_k}{(D_3 + D_4 x^2)^k} + \frac{\beta_9}{(1-x)} + \frac{\beta_{10}}{(1+x)} \right] dx \quad (91)$$

where

$$\left. \begin{aligned} \beta_k &= \frac{1}{[8-(k+1)]!(D_4)^{8-k}} \lim_{x^2 \rightarrow \left(\frac{-D_3}{D_4}\right)} \frac{d^{8-k}}{d(x^2)^{8-k}} \left[\frac{\sum_{j=0}^8 g_{2 \times j} x^{2j}}{(1-x^2)} \right] \\ \beta_9 &= \beta_{10} = \frac{g_0 + g_2 + g_4 + g_6 + g_8 + g_{10} + g_{12} + g_{14} + g_{16}}{2(D_3 + D_4)^8} = 0 \end{aligned} \right\} \quad (92)$$

with $k = 1, 2, \dots, 8$. From equations (92), one gets

$$\beta_k = \sum_{j=1}^9 C_{(9-k),j} g_{2 \times (j-1)} \quad (93)$$

with $k = 8, 7, \dots, 2, 1, 0$ and

$$C_{1,k} = \frac{(-D_3)^{k-1}}{(D_4)^{k-2}(D_3 + D_4)}, \quad C_{2,k} = \frac{(-D_3)^{k-2} [(k-1)D_4 + (k-2)D_3]}{(D_4)^{k-2}(D_3 + D_4)^2} \quad (94)$$

$$C_{3,k} = \frac{2(-D_3)^{k-3} \left[\frac{(k-1)(k-2)}{2!} (D_4)^2 + \frac{(k-1)(k-3)}{1! \times 1!} D_3 D_4 + \frac{(k-2)(k-3)}{2!} (D_3)^2 \right]}{(D_4)^{k-2}(D_3 + D_4)^3} \quad (95)$$

$$\begin{aligned} C_{4,k} &= \frac{3(-D_3)^{k-4}}{(D_4)^{k-2}(D_3 + D_4)^4} \left[\frac{(k-1)(k-2)(k-3)}{3!} (D_4)^3 + \frac{(k-1)(k-2)(k-4)}{2!} D_3 (D_4)^2 \right. \\ &\quad \left. + \frac{(k-1)(k-3)(k-4)}{2!} (D_3)^2 D_4 + \frac{(k-2)(k-3)(k-4)}{3!} (D_3)^3 \right] \end{aligned} \quad (96)$$

$$\begin{aligned}
C_{5,k} = & \frac{4(-D_3)^{k-5}}{(D_4)^{k-2}(D_3+D_4)^5} \left[\frac{(k-1)(k-2)(k-3)(k-4)}{4!} (D_4)^4 \right. \\
& + \frac{(k-1)(k-2)(k-3)(k-5)}{3!} D_3 (D_4)^3 + \frac{(k-1)(k-2)(k-4)(k-5)}{2! \times 2!} (D_3)^2 (D_4)^2 \\
& \left. + \frac{(k-1)(k-3)(k-4)(k-5)}{3!} (D_3)^3 D_4 + \frac{(k-2)(k-3)(k-4)(k-5)}{4!} (D_3)^4 \right] \quad (97)
\end{aligned}$$

$$\begin{aligned}
C_{6,k} = & \frac{5(-D_3)^{k-6}}{(D_4)^{k-2}(D_3+D_4)^6} \left[\frac{(k-1)(k-2)(k-3)(k-4)(k-5)}{5!} (D_4)^5 \right. \\
& + \frac{(k-1)(k-2)(k-3)(k-4)(k-6)}{4!} D_3 (D_4)^4 + \frac{(k-1)(k-2)(k-3)(k-5)(k-6)}{3! \times 2!} (D_3)^2 (D_4)^3 \\
& + \frac{(k-1)(k-2)(k-4)(k-5)(k-6)}{3! \times 2!} (D_3)^3 (D_4)^2 + \frac{(k-1)(k-3)(k-4)(k-5)(k-6)}{4!} (D_3)^4 D_4 \\
& \left. + \frac{(k-2)(k-3)(k-4)(k-5)(k-6)}{5!} (D_3)^5 \right] \quad (98)
\end{aligned}$$

$$\begin{aligned}
C_{7,k} = & \frac{6(-D_3)^{k-7}}{(D_4)^{k-2}(D_3+D_4)^7} \left[\frac{\prod_{j=1}^6 (k-j)}{6!} (D_4)^6 + \frac{\prod_{j=1(j \neq 6)}^7 (k-j)}{5!} (D_4)^5 D_3 + \frac{\prod_{j=2}^7 (k-j)}{6!} (D_3)^6 \right. \\
& + \frac{\prod_{j=1(j \neq 5)}^7 (k-j)}{4! \times 2!} (D_4)^4 (D_3)^2 + \frac{\prod_{j=1(j \neq 4)}^7 (k-j)}{3! \times 3!} (D_4)^3 (D_3)^3 \\
& \left. + \frac{\prod_{j=1(j \neq 3)}^7 (k-j)}{4! \times 2!} (D_4)^2 (D_3)^4 + \frac{\prod_{j=1(j \neq 2)}^7 (k-j)}{5!} D_4 (D_3)^5 \right] \quad (99)
\end{aligned}$$

$$C_{8,k} = \frac{7(-D_3)^{k-8}}{(D_4)^{k-2}(D_3+D_4)^8} \left[\frac{\prod_{j=1}^7 (k-j)}{7!} (D_4)^7 + \frac{\prod_{j=1(j \neq 7)}^8 (k-j)}{6!} (D_4)^6 D_3 \right. \\ \left. + \frac{\prod_{j=1(j \neq 6)}^8 (k-j)}{5! \times 2!} (D_4)^5 (D_3)^2 + \frac{\prod_{j=1(j \neq 5)}^8 (k-j)}{4! \times 3!} (D_4)^4 (D_3)^3 + \frac{\prod_{j=1(j \neq 4)}^8 (k-j)}{4! \times 3!} (D_4)^3 (D_3)^4 \right] \quad (100)$$

$$+ \frac{\prod_{j=1(j \neq 3)}^8 (k-j)}{2! \times 5!} (D_4)^2 (D_3)^5 + \frac{\prod_{j=1(j \neq 2)}^8 (k-j)}{6!} D_4 (D_3)^6 + \frac{\prod_{j=2}^8 (k-j)}{7!} (D_3)^7 \right]$$

$$C_{9,k} = \frac{(-D_3)^{k-9}}{2(D_4)^{k-1}(D_3+D_4)^8} \left[\frac{\prod_{j=1}^8 (k-j)}{8!} (D_4)^8 + \frac{\prod_{j=1(j \neq 8)}^9 (k-j)}{7!} (D_4)^7 D_3 \right. \\ \left. + \frac{\prod_{j=1(j \neq 7)}^9 (k-j)}{6! \times 2!} (D_4)^6 (D_3)^2 + \frac{\prod_{j=1(j \neq 6)}^9 (k-j)}{5! \times 3!} (D_4)^5 (D_3)^3 \right. \\ \left. + \frac{\prod_{j=1(j \neq 5)}^9 (k-j)}{4! \times 4!} (D_4)^4 (D_3)^4 + \frac{\prod_{j=1(j \neq 4)}^9 (k-j)}{3! \times 5!} (D_4)^3 (D_3)^5 \right. \\ \left. + \frac{\prod_{j=1(j \neq 3)}^9 (k-j)}{6! \times 2!} (D_4)^2 (D_3)^6 + \frac{\prod_{j=1(j \neq 2)}^9 (k-j)}{7!} D_4 (D_3)^7 + \frac{\prod_{j=2}^9 (k-j)}{8!} (D_3)^8 \right] \quad (101)$$

with $k = 1, 2, \dots, 9$ in equations (94) – (101).

Equation (101) can be simplified as $C_{9,k} = 1/ \left[2(D_2 + D_4)^8 \right]$ for $k = 1, 2, \dots, 9$.

When equations (89) hold, one may obtain from equation (91) that

$$I_{\text{const}} + I_{\text{linear}} + I_{\text{cross}} + I_{\text{cube}} = \frac{1}{\beta} \sum_{k=0}^8 \left[\beta_k \int_{-1}^{+1} \frac{1}{(D_3 + D_4 x^2)^k} dx \right] = \frac{1}{\beta} \sum_{k=0}^8 \beta_k I_k \quad (102)$$

where

$$I_k = \int_{-1}^{+1} \frac{1}{(D_3 + D_4 x^2)^k} dx \quad (103)$$

with

$$\left. \begin{aligned} I_k &= \frac{1}{D_3(k-1)(D_3 + D_4)^{k-1}} + \frac{2k-3}{2(k-1)D_3} I_{k-1} \\ I_1 &= \int_{-1}^{+1} \frac{1}{(D_3 + D_4 x^2)} dx = \frac{2}{\sqrt{D_3 D_4}} \tan^{-1} \left(\sqrt{\frac{D_4}{D_3}} \right) \end{aligned} \right\}, \text{ where } k = 2, 3, \dots$$

By means of equations (93) and (103), $I_{\text{const}} + I_{\text{linear}} + I_{\text{cross}} + I_{\text{cube}}$ defined in equation (85) can be computed analytically by the use of equation (102). Therefore, the Melnikov integral can be computed according to the algorithms described by equation (90) when the integral $I_N(t_0)$ can also be integrated, either numerically or analytically. See the next subsection for detailed discussions.

When one assumes that the physical parameters $h_x, h_y, h_z, I_{xx}, I_{yy}, I_{zz}$, and t_0 are given in order that the Melnikov integral (40) hold where the Melnikov integral is defined in equation (90), then, by Corollary 1 in the Appendix, there exist transversal intersections between the stable and unstable manifolds of the disturbed symmetric gyrostat. When the Melnikov integral is independent of t_0 , an alternative Corollary 2 in the Appendix states that, if the homoclinic orbit of equations (5) depends on a vector of parameters μ_0 in the Melnikov integral (40) where the Melnikov integral of the disturbed symmetric gyrostat is defined in equation (90), then there exists a bifurcation value μ near μ_0 at which non-transversal homoclinic orbits occur.

The computational algorithms in this section are presented for the addition $I_{\text{const}} + I_{\text{linear}} + I_{\text{cross}} + I_{\text{cube}} + I_{\text{forced}}$ of the Melnikov integral for the disturbed symmetric

gyrostat. Similar to the computation of $I_N(t_0)$, one needs to deal with the integrals according to the individual integrand of the $I_N(t_0)$ of the dynamical systems. Because of the extraordinary complicated nonlinear terms of N -column in the dynamical systems such as the Chua and modified Rossler turbulence models, the integral $I_N(t_0)$ in equation (52) will be treated with an additional effort as shown in the next subsections.

4.8 The computation of the integral $I_{N_{\text{chua}}}(t_0)$ for the Chua double scroll system

In this subsection, we will discuss the computation of the integral $I_{N_{\text{chua}}}(t_0)$ for the Chua double scroll equations. The Chua double scroll system is a set of three piecewise linear equations [5], given by

$$\frac{d\omega_x}{dt} = \alpha'' [\omega_y - f(\omega_x)], \quad \frac{d\omega_y}{dt} = \omega_x - \omega_y + \omega_z, \quad \frac{d\omega_z}{dt} = -\beta'' \omega_y \quad (104)$$

with $\alpha'' = 9$, $\beta'' = \frac{100}{7}$ and

$$f(\omega_x) = \begin{cases} m_1 \omega_x + (m_0 - m_1), & \text{if } \omega_x \geq 1 \\ m_0 \omega_x & \text{if } |\omega_x| \leq 1 \\ m_1 \omega_x - (m_0 - m_1), & \text{if } \omega_x < -1 \end{cases} \quad (105)$$

where $m_0 = \frac{-1}{7}$, $m_1 = \frac{2}{7}$.

Comparing the Chua double scroll equations (104) and (105) with the generic dynamical system equations (41) and (42), one obtains easily the parameters $\theta_{ij}, \Theta_{ij}, \beta_i, \Omega_i, N_i, \Gamma_{ij}$, and d_i for $i = x, y, z; j = x, y, z$ for the Chua double scroll equations, respectively, for example

$$N_x(\omega_x, \omega_y, \omega_z, t) = -\alpha'' f(\omega_x), \quad N_y(\omega_x, \omega_y, \omega_z, t) = 0, \quad N_z(\omega_x, \omega_y, \omega_z, t) = 0 \quad (106)$$

It is noted that the complexity of the Chua double scroll equations lies in the piecewise properties of the $N_x(\omega_x, \omega_y, \omega_z, t)$ in equations (105, 106). Substituting equations (106) into equation (52), one further obtains

$$I_{N_{\text{chua}}} = \int_{-\infty}^{+\infty} \left[-I_{xx} \alpha'' f(\bar{\omega}_x(t) \bar{W}_x(t)) \right] dt = I_{N1} + I_{N2} + I_{N3} \quad (107)$$

Substituting the piecewise function (105) into the first of equations (107), one gets

$$I_{Ni} = \alpha_{Ni} \int_{-\infty}^{t_r} \bar{\omega}_x(t) \bar{W}_x(t) dt + \beta_{Ni} \int_{-\infty}^{t_r} \bar{W}_x(t) dt \quad (108)$$

where $i = 1, 2, 3$ and

$$\left. \begin{array}{l} \alpha_{N1} = -\alpha'' I_{xx} m_1, \quad \beta_{N1} = -\alpha'' I_{xx} (m_0 - m_1) \\ \alpha_{N2} = -\alpha'' I_{xx} m_0, \quad \beta_{N2} = 0 \\ \alpha_{N3} = -\alpha'' I_{xx} m_1, \quad \beta_{N3} = \alpha'' I_{xx} (m_0 - m_1) \end{array} \right\} \quad (109)$$

and the parameters t_r and t_R are real, positive roots of the following equations respectively

$$\left. \begin{array}{l} \frac{\omega_{x0} + \omega_{x1} \tanh(\beta t_r) + \omega_{x2} \tanh^2(\beta t_r) + \omega_{x3} \tanh^3(\beta t_r) + \omega_{x4} \tanh^4(\beta t_r)}{(D_3 + D_4 \tanh^2(\beta t_r))^2} = 1 \\ \frac{\omega_{x0} + \omega_{x1} \tanh(\beta t_R) + \omega_{x2} \tanh^2(\beta t_R) + \omega_{x3} \tanh^3(\beta t_R) + \omega_{x4} \tanh^4(\beta t_R)}{(D_3 + D_4 \tanh^2(\beta t_R))^2} = -1 \end{array} \right\} \quad (110)$$

In order to analytically integrate the integrals in equations (108) in a unified formula for programming purpose, one assumes the transformation $x = \tanh(\beta t)$. Then from equations (108), one obtains

$$I_{Nk} = \int_{T_{rk}}^{T_{Rk}} \frac{\sum_{j=0}^8 X_{kj} x^j}{\beta(D_3 + D_4 x^2)^4 (1-x^2)} dx \quad (111)$$

for $k = 1, 2, 3$ and the coefficient X_{kj} for $j = 0, 1, 2, \dots, 8$ are defined by

$$\begin{bmatrix} X_{k0} \\ X_{k1} \\ X_{k2} \\ X_{k3} \\ X_{k4} \\ X_{k5} \\ X_{k6} \\ X_{k7} \\ X_{k8} \end{bmatrix} = \alpha_{Nk} \begin{bmatrix} \omega_{j0} & 0 & 0 & 0 & 0 \\ \omega_{j1} & \omega_{j0} & 0 & 0 & 0 \\ \omega_{j2} & \omega_{j1} & \omega_{j0} & 0 & 0 \\ \omega_{j3} & \omega_{j2} & \omega_{j1} & \omega_{j0} & 0 \\ \omega_{j4} & \omega_{j3} & \omega_{j2} & \omega_{j1} & \omega_{j0} \\ 0 & \omega_{j4} & \omega_{j3} & \omega_{j2} & \omega_{j1} \\ 0 & 0 & \omega_{j4} & \omega_{j3} & \omega_{j2} \\ 0 & 0 & 0 & \omega_{j4} & \omega_{j3} \\ 0 & 0 & 0 & 0 & \omega_{j4} \end{bmatrix} \begin{bmatrix} W_{x0} \\ W_{x1} \\ W_{x2} \\ W_{x3} \\ W_{x4} \\ 0 \\ 0 \\ 0 \\ 0 \end{bmatrix} + \beta_{Nk} \begin{bmatrix} W_{i0} \\ W_{i1} \\ W_{i2} \\ W_{i3} \\ W_{i4} \end{bmatrix} \quad (112)$$

where the upper limit and lower limit of the interval in the integral (111) are defined by

$$\begin{aligned} T_{Rk} &= \begin{cases} \tanh(t_r) & \text{when } k=1 \\ \tanh(t_R) & \text{when } k=2 \\ 1 & \text{when } k=3 \end{cases} \\ T_{rk} &= \begin{cases} -1 & \text{when } k=1 \\ \tanh(t_r) & \text{when } k=2 \\ \tanh(t_R) & \text{when } k=3 \end{cases} \end{aligned} \quad (113)$$

From the first of equations (38) it is shown that $x = \pm 1$ are the roots of the following polynomial equations

$$\sum_{j=0}^8 X_{kj} x^j = 0 \quad (114)$$

where $k = 1, 2, 3$. Therefore, from the equations (111), one obtains

$$I_{Nk} = \int_{T_{rk}}^{T_{Rk}} \frac{\sum_{j=0}^6 Y_{kj} x^j}{\beta(D_3 + D_4 x^2)^4} dx \quad (115)$$

where

$$\left. \begin{aligned} Y_{k0} &= X_{k0}, \quad Y_{k1} = X_{k1}, \quad Y_{k2} = X_{k0} + X_{k2}, \quad Y_{k3} = X_{k1} + X_{k3} \\ Y_{k4} &= X_{k0} + X_{k2} + X_{k4}, \quad Y_{k5} = X_{k1} + X_{k3} + X_{k5}, \quad Y_{k6} = X_{k0} + X_{k2} + X_{k4} + X_{k6} \end{aligned} \right\} \quad (116)$$

or $Y_{k5} = -X_{k7}$, $Y_{k6} = -X_{k8}$ for $k = 1, 2, 3$.

By setting

$$R_{js} = \int_{T_{rk}}^{T_{Rk}} \frac{x^j}{(D_3 + D_4 x^2)^s} dx \quad (117)$$

for $j = 0, 1, 2, \dots, 6$, and $s = 1, 2, 3, 4$, one further obtains

$$\left. \begin{aligned} R_{01} &= \frac{1}{\sqrt{D_3 D_4}} \left[\tan^{-1} \left(T_{Rk} \sqrt{\frac{D_4}{D_3}} \right) - \tan^{-1} \left(T_{rk} \sqrt{\frac{D_4}{D_3}} \right) \right] \\ R_{0,s} &= \frac{1}{2(s-1)D_3} \left[\frac{T_{Rk}}{\left(D_3 + D_4 T_{Rk}^2 \right)^{s-1}} - \frac{T_{rk}}{\left(D_3 + D_4 T_{rk}^2 \right)^{s-1}} \right] + \frac{(2s-3)}{2(s-1)D_3} R_{0,s-1} \\ R_{1,s} &= \frac{1}{2(s-1)D_4} \left[\frac{T_{Rk}}{\left(D_3 + D_4 T_{Rk}^2 \right)^{s-1}} - \frac{T_{rk}}{\left(D_3 + D_4 T_{rk}^2 \right)^{s-1}} \right] \end{aligned} \right\} \quad (118)$$

for $s = 2, 3, 4$.

$$\left. \begin{aligned} R_{24} &= \frac{R_{03} - D_3 R_{04}}{D_4}, \quad R_{34} = \frac{R_{13} - D_3 R_{14}}{D_4}, \quad R_{44} = \frac{R_{02} - 2D_3 R_{03} + (D_3)^2 R_{04}}{(D_4)^2} \\ R_{54} &= \frac{R_{12} - 2D_3 R_{13} + (D_3)^2 R_{14}}{(D_4)^2}, \quad R_{64} = \frac{R_{01} - 3D_3 R_{02} + 3(D_3)^2 R_{03} - (D_3)^3 R_{04}}{(D_4)^3} \end{aligned} \right\} \quad (119)$$

Substituting the equation (117) with equations (118) and (119), one obtains from equation (115)

$$I_{Nk} = \frac{1}{\beta} \sum_{j=0}^6 (Y_{kj} \times R_{j4}) \quad \text{for } k = 1, 2, 3.$$

Thus, upon substitution of the last equations into the equation (107), the integral

$I_{N_chua}(t_0)$ for the Chua double scroll system takes the form

$$I_{N_chua} = \frac{1}{\beta} \sum_{k=1}^3 \sum_{j=0}^6 (Y_{kj} \times R_{j4}) \quad (120)$$

The analytical evaluation of the integral (107) is an important step for the computation of the Melnikov integral (40). The integral formulas (107) will also apply to the modified Brocket, modified Kapitaniak, YSVO equations with Chua functions (105). The integral I_{N_chua} in equation (107) is a function of the parameters I_{xx}, I_{yy}, I_{zz} ; $h_x, h_y, h_z; T, G_p$ in the same way as the terms $I_{\text{const}}, I_{\text{linear}}, I_{\text{cross}}, I_{\text{cube}}$ and $I_{\text{forced}}(t_0)$.

4.9 The computation of the integral $I_{N_m_Rossler}(t_0)$ for the modified Rossler model

of turbulence

In 1979, Rossler [10] proposed a set of six-variable non-linear differential equations arisen from chaos and turbulence of relaxation oscillators. Here, the modified Rossler model of turbulence will be discussed. The modified system in terms of the variables $\omega_x, \omega_y, \omega_z, u_x, u_y$, and u_z are given by

$$\frac{d\omega_x}{dt} = 20 - \omega_y - \omega_z - u_x, \quad (x y z) \quad (121)$$

$$\frac{du_x}{dt} = a(\omega_x - 10)^m + b(\omega_x - 10)^{m+1} + (\omega_x - 10)u_x, \quad (x y z) \quad (122)$$

where $a = 0.1, m = 2, b = 0.01$. Equations (121) and (122) represent the Rossler model of turbulence [10] when $a = 0.01, m = 0, b = 0$.

Assume

$$\varphi_k(t) = \exp \left\{ \int_0^t [\omega_k(s) - \omega_{kp}] \right\}, \quad \omega_{kp} = 10 \quad (123)$$

for $k = x, y$, and z .

From equations (122), one obtains the solutions with respect to the variables u_x ,

u_y , and u_z given by

$$u_k(t) = u_k(0)\varphi_k(t) + \int_0^t \left\{ a[\omega_k(s) - \omega_{kp}]^m + b[\omega_k(s) - \omega_{kp}]^{m+1} \right\} \frac{\varphi_k(t)}{\varphi_k(s)} ds \quad (124)$$

for $k = x, y$, and z . The $u_k(0)$ are the initial values of the variables u_k for $k = x, y$, and z . Therefore, equations (121) may be rewritten as

$$\frac{d\omega_x}{dt} = 20 - \omega_y - \omega_z - u_x(t), \quad (x, y, z) \quad (125)$$

where $u_k(t)$ for $k = x, y$, and z are defined in equations (124).

Comparing the modified Rossler dynamical system (125) with the generic equations (41) and (42), one finds that the Θ _matrix, Ω _column, Γ _matrix, and d _matrix are all zero. The θ _matrix, β _column, and N _column for the modified Rossler dynamical system of turbulence respectively are defined by

$$\theta_matrix = \begin{bmatrix} 0 & -1 & -1 \\ -1 & 0 & -1 \\ -1 & -1 & 0 \end{bmatrix}, \quad \beta_column = \begin{bmatrix} 20 \\ 20 \\ 20 \end{bmatrix}, \quad N_column = \begin{bmatrix} -u_x(t) \\ -u_y(t) \\ -u_z(t) \end{bmatrix} \quad (126)$$

Because $u_k(t)$ for $k = x, y$, and z are the integral functions defined in equations (125), it is required to analyse the contribution of the N _column defined in the third group of equations (126) to the Melnikov integral for the modified Rossler model of turbulence in detail. Substitution of the third group of equations (126) into equation (52) yields

$$I_{N_m_Rossler}(t_0) = - \int_{-\infty}^{+\infty} \left\{ \sum_{k=x,y,z} \left[I_{kk} \bar{W}_k(t) \bar{u}_k(t+t_0) \right] \right\} dt \quad (127)$$

where the function $\bar{u}_k(t)$ may be computed along the homoclinic orbits of the rotational motion of the torque-free symmetric gyrostat

$$\left. \begin{aligned} \bar{u}_k(t) &= u_k(0)\bar{\varphi}_k(t+t_0) + \int_0^{t+t_0} \left\{ a[\bar{\omega}_k(s) - \omega_{kp}]^m + b[\bar{\omega}_k(s) - \omega_{kp}]^{m+1} \right\} \frac{\bar{\varphi}_k(t+t_0)}{\bar{\varphi}_k(s)} ds \\ \bar{\varphi}_k(t) &= \exp \left\{ \int_0^t [\bar{\omega}_k(s) - \omega_{kp}] dt \right\} \end{aligned} \right\} \quad (128)$$

for $k = x, y, z$ and $\bar{\omega}_k(s)$ is the homoclinic orbit of the rotational motions of the equivalent symmetric gyrostat under torque-free motions as defined in equations (5). By using the properties of the homoclinic orbit of the torque-free symmetric gyrostat, i.e.,

$$\lim_{s \rightarrow \pm\infty} \bar{\omega}_k(s) = \omega_{kp} \quad (129)$$

for $k = x, y$, and z , one obtains

$$\bar{\varphi}_k(s) = \exp \left\{ \frac{1}{\beta} [P_{k0} K_{02}(s) + P_{k1} K_{12}(s) + P_{k2} K_{22}(s)] \right\} \quad (130)$$

where

$$P_{k0} = \omega_{k0} - \omega_{kp} D_3^2, \quad P_{k1} = \omega_{k1}, \quad P_{k2} = \omega_{k2} - 2\omega_{kp} D_3 D_4 + P_{k0} \quad (131)$$

$$\left. \begin{aligned} K_{01}(s) &= \frac{1}{\sqrt{D_3 D_4}} \tan^{-1} \left[\sqrt{\frac{D_4}{D_3}} \tanh(\beta s) \right] \\ K_{02}(s) &= \frac{1}{2D_3} \left[\frac{\tanh(\beta s)}{D_3 + D_4 \tanh^2(\beta s)} \right] + \frac{1}{2D_3} K_{01}(s) \end{aligned} \right\} \quad (132)$$

$$\left. \begin{aligned} K_{12}(s) &= \frac{1}{2D_4} \left[\frac{1}{D_3} - \frac{1}{[D_3 + D_4 \tanh^2(\beta s)]} \right] \\ K_{22}(s) &= \frac{K_{01}(s) - D_3 K_{02}(s)}{D_4} \end{aligned} \right\} \quad (133)$$

Further, one sets

$$f_k(t + t_0) = \int_0^{t+t_0} \left\{ a[\bar{\varphi}_k(s) - \omega_{kp}]^m + b[\bar{\varphi}_k(s) - \omega_{kp}]^{m+1} \right\} \frac{1}{\bar{\varphi}_k(s)} ds \quad (134)$$

where $k = x, y, z$. Using equations (129), one rewrites equations (134) as

$$f_k(t + t_0) = \int_0^{\tanh[\beta(t+t_0)]} \left\{ \frac{a(P_{k0} + xP_{k1} + x^2P_{k2})^m (1-x^2)^{m-1}}{\beta(D_3 + D_4x^2)^2} \right. \\ \left. + \frac{b(P_{k0} + xP_{k1} + x^2P_{k2})^{m+1} (1-x^2)^m}{\beta(D_3 + D_4x^2)^2} \right\} \frac{1}{\bar{\varphi}_k(\frac{1}{\beta} \tanh^{-1}(x))} dx \quad (135)$$

for $k = x, y, z$, and $m = 2$.

By substituting the equations (128, 134) into equations (127), one rewrites the

$I_{N_m_Rossler}(t_0)$ in equation (127) as

$$I_{N_m_Rossler}(t_0) = - \int_{-\infty}^{+\infty} \left\{ \sum_{k=x,y,z} I_{kk} \bar{W}_k(t) \bar{\varphi}_k(t+t_0) [u_k(0) + f_k(t+t_0)] \right\} dt \quad (136)$$

Because $\bar{\varphi}_k(t+t_0), f_k(t+t_0)$ are the functions of time t and $\lim_{t \rightarrow \infty} \bar{W}_k(t) = 0$ for $k = x, y, z$ as shown in equations (38), the integral in equations (136) is convergent since we have shown that the functions $f_k(t+t_0)$ for $k = x, y, z$ are bounded, continuous functions whose argument ranges between $-\infty$ and $+\infty$. The integral can be computed by numerical integration. The results of the equation (136) are attributed to the assumption described in equations (129).

The selection of the parameters I_{xx} and I_{zz} to validate equations (129) will be discussed below.

From equations (34) to (36), one obtains

$$\left. \begin{aligned} h_z &= (I_{xx} - I_{zz})h_{z\Omega}, \quad R_r = R_\Omega I_{zz}(I_{xx} - I_{zz}) \\ h_x^2 + h_y^2 &= \frac{(I_{xx} - I_{zz})^2 I_{zz}}{I_{xx}} h_{xy\Omega} \end{aligned} \right\} \quad (137)$$

where

$$\left. \begin{aligned} h_{z\Omega} &= \frac{1}{4}(\Omega_{z1} + \Omega_{z2} + \Omega_{z3} + \Omega_{z4}) \\ R_\Omega &= \frac{(\Omega_{z1}\Omega_{z2}\Omega_{z3} + \Omega_{z2}\Omega_{z3}\Omega_{z4} + \Omega_{z3}\Omega_{z4}\Omega_{z1} + \Omega_{z4}\Omega_{z1}\Omega_{z2})}{(\Omega_{z1} + \Omega_{z2} + \Omega_{z3} + \Omega_{z4})} \\ h_{xy\Omega} &= \frac{1}{4}(a_{2\Omega} - 2R_\Omega - 4h_{z\Omega}) \end{aligned} \right\} \quad (138)$$

with $a_{2\Omega} = \Omega_{z1}\Omega_{z2} + \Omega_{z2}\Omega_{z3} + \Omega_{z3}\Omega_{z4} + \Omega_{z4}\Omega_{z1} + \Omega_{z4}\Omega_{z2} + \Omega_{z1}\Omega_{z3}$.

Taking

$$\omega_{xp} = \omega_{yp} = \omega_{zp} = \Omega_{z2} = \Omega_{z3} = 10 \quad (139)$$

in equations (32) and (33), one obtains

$$\frac{I_{zz}}{I_{xx}} = \frac{(\omega_{xp}^2 + \omega_{yp}^2)h_{xy\Omega}}{F_{0\Omega}^2} \quad (140)$$

with $F_{0\Omega} = \frac{1}{2}(\Omega_{z2}^2 - 2\Omega_{z2}h_{z\Omega} + R_\Omega)$.

In order to ensure the convergence of the integrals (136), it is required to select the hyperbolic fixed point of the torque-free symmetric gyrostat as the values described by equations (139). I_{xx} and I_{zz} are constrained by equation (140). From equations (32) and (139), one obtains the following relationship between h_x and h_y

$$h_x = h_y \quad (141)$$

Therefore, according to equation (140), choosing the principal moment of inertia of the symmetric gyrostat I_{xx} and I_{zz} appropriately will make the integral of equation

(136) convergent. In addition, the integral $I_{N_m_Rossler}(t_0)$ in equation (136) will be a function of the parameters $I_{xx}, I_{yy}, I_{zz}; h_x, h_y, h_z; T, G_p$ similar to the terms I_{const} , I_{linear} , I_{cross} , I_{cube} and $I_{\text{forced}}(t_0)$.

From equations (135), if $m = 0$, there are two singularities at $x = \pm 1$ in the integrand. Therefore, if $m = 0$, the Melnikov integral function diverges due to the integral (135) and thus the Melnikov integral is not suitable for the Rossler turbulence model of six state variables. By appropriately selecting the parameters I_{xx} and I_{zz} to make the hyperbolic fixed points satisfying equations (139), one can construct a Melnikov integral suitable for the study of the modified Rossler turbulence model of six variables defined in equations (121) and (122) when $m = 2$.

In the next section, we shall focus on the issue of how to compute the moments of momentum of the wheels h_x, h_y, h_z and/ or the principal moments of inertia I_{xx}, I_{yy}, I_{zz} of the equivalent symmetric gyrostat from the real zeros of the Melnikov integral equation (40) associated with equation (90), if the real zeros exist. If there are no real zeros in the Melnikov integral (40) for a specific dynamical system, then the proposed Melnikov integral is not suitable for that particular dynamical system.

Section 5. Parameter determination for transversality

In this section, algorithms are suggested to determine the moments of momentum of the wheels or the principal moments of inertia of the equivalent symmetric gyrostat when the Melnikov integral (40) vanishes at real zeros.

Algorithm 5.1 Determination for the moments of momentum of the wheels

Given the principal moments of inertia of the symmetric gyrostat, $I_{xx} = I_{yy}$, and I_{zz} , and the four real roots of equation (13), $\Omega_{z1} > \Omega_{z2} = \Omega_{z3} > \Omega_{z4}$, one may compute the component of the moment of momentum of the wheels h_z from the first of equations (36). From the third of equations (36), one finds

$$h_x = h_x(X) = h_{xy} \sin X, \quad h_y = h_y(X) = h_{xy} \cos X \quad (142)$$

where X is to be determined within $-\pi < X < \pi$, and

$$h_{xy}^2 = \frac{-[I_{zz}h_z^2 + 0.5(I_{xx} - I_{zz})R_r + I_{xx}^2 I_{zz} a_2]}{I_{xx}} \quad (143)$$

where a_2 is defined in the second of equations (34) and R_r is defined in the second of equations (36).

Substituting equations (142) into equations (7) – (12) and (24) – (26), one finds that the Melnikov integral (22) becomes a function of X and t_0 , i.e., $M(t_0) \equiv M(X, t_0)$.

One can solve for X and t_0 from the vanishing of the Melnikov integral at real zeros

$$M(t_0) \equiv M(X, t_0) = 0 \quad (144)$$

subjected to the following constraint

$$I_N(t_0) + I_{\text{forced}}(t_0) = 0 \quad (145)$$

where the function $I_{\text{forced}}(t_0)$ is defined in equation (51) or (83), and the function $I_N(t_0)$ is defined in equation (52). If equation (144) and constraint (145) hold simultaneously, then the Melnikov integral (22) would vanish as expected.

Algorithm 5.1 is applicable for the dynamical systems of modified Brockett, Chua, Duffing, Ueda, modified Kapitaniak, generalized Lorenz, forced Lorenz, Rossler

and YSVO. The following **Procedure A** for I_N in equation (52) independent of t_0 is outlined for the purpose.

Procedure A

Step A.1 Input $I_{xx}, I_{yy}, I_{zz}, \Omega_{z1}, \Omega_{z2}, \Omega_{z3}, \Omega_{z4}$;

Step A.2 Input $N = 10000$ to divide the range of $X \in (-\pi, \pi)$ into $(N-1)$

subsections by computing the i th node, $X(i) = \frac{[2i-(N+1)]\pi}{N-1}$, for $i = 1, 2, \dots, N-1$. N

should be large enough to make the computational step $dX = \frac{2\pi}{N-1}$ small so that all the

real roots \bar{X}_k for $k = 1, 2, 3, \dots$ in the range $(-\pi, +\pi)$ of X in the Melnikov integral (144)

can be scanned.

Step A.3 Compute $h_x(i), h_y(i)$ and $h_z(i)$ for $i = 1, 2, \dots, N-1$ from equations (142)

and the first of equations (36) as follows

$$\left. \begin{aligned} h_x(i) &= h_{xy} \sin[X(i)], & h_y(i) &= h_{xy} \cos[X(i)] \\ h_z &= a_3 I_{xx}^2 / (I_{xx} - I_{zz}) \end{aligned} \right\} \quad (146)$$

where $a_3 = -a_4(\Omega_{z1} + \Omega_{z2} + \Omega_{z3} + \Omega_{z4})$, and h_{xy} is defined in equation (143), and a_4 is given in equation (14).

Step A.4 Compute the θ _matrix, Θ _matrix, β _column, Ω _column, N _column, Γ _matrix, d _matrix from a particular dynamical system by using the following expressions

$$\begin{aligned}
\theta_matrix &= \begin{bmatrix} \theta_{xx} & \theta_{xy} & \theta_{xz} \\ \theta_{yx} & \theta_{yy} & \theta_{yz} \\ \theta_{zx} & \theta_{zy} & \theta_{zz} \end{bmatrix}, & \Theta_matrix &= \begin{bmatrix} \Theta_{xy}^x & \Theta_{yz}^x & \Theta_{zx}^x \\ \Theta_{xy}^y & \Theta_{yz}^y & \Theta_{zx}^y \\ \Theta_{xy}^z & \Theta_{yz}^z & \Theta_{zx}^z \end{bmatrix} \\
\beta_column &= \begin{bmatrix} \beta_{x0} \\ \beta_{y0} \\ \beta_{z0} \end{bmatrix}, & \Omega_column &= \begin{bmatrix} \Omega_x \\ \Omega_y \\ \Omega_z \end{bmatrix}, & d_matrix &= \begin{bmatrix} d_{xx} & d_{xy} & d_{xz} \\ d_{yx} & d_{yy} & d_{yz} \\ d_{zx} & d_{zy} & d_{zz} \end{bmatrix}
\end{aligned} \tag{147}$$

$$N_column = \begin{bmatrix} N_x(\omega_x, \omega_y, \omega_z, t) \\ N_y(\omega_x, \omega_y, \omega_z, t) \\ N_z(\omega_x, \omega_y, \omega_z, t) \end{bmatrix}, \quad \Gamma_matrix = \begin{bmatrix} \Gamma_{xx} & \Gamma_{xy} & \Gamma_{xz} \\ \Gamma_{yx} & \Gamma_{yy} & \Gamma_{yz} \\ \Gamma_{zx} & \Gamma_{zy} & \Gamma_{zz} \end{bmatrix} \tag{148}$$

where the entries are derived from equations (41) and (42).

Step A.5 Compute the μ _matrix, Π _matrix and T _column of the disturbed gyrostat equivalent to the dynamical system from equations (43) – (45).

Step A.6 Compute W_{wk} for $k = 0, 1, \dots, 16$ from equation (56) with I_{const} given in equation (47) or (55);

Step A.7 Compute T_{tk} for $k = 0, 1, \dots, 16$ from equation (61) with I_{linear} given in equation (48) or (60);

Step A.8 Compute E_{ek} for $k = 0, 1, \dots, 16$ from equation (67) with I_{cross} given in equation (49) or (66);

Step A.9 Compute F_{fk} for $k = 0, 1, \dots, 16$ from equation (69) with I_{cube} given in equation (50) or (68);

Step A.10 Compute g_k for $k = 0, 1, \dots, 16$ from equations (86) associated with equation (85);

Step A.11 Compute β_k, I_k for $k = 1, 2, \dots, 8$ from equations (93) and (103) associated with equation (90);

Step A.12 Compute I_N defined in equation (52) according to the specific forms of the N -column for the dynamical systems of Chua in Example 2, the modified Brockett in Example 7, the modified Kapitaniak in Example 8, and YSVO in Example 9 in Section 6;

Step A.13 Compute $\Delta(i) = \frac{1}{\beta} \sum_{k=1}^8 \beta_k I_k + I_N$ used in equation (90); Go to *Step A.3*

until $i = N - 1$.

Step A.14 Sort out the interval $[X(j), X(j+1)]$ in which $\Delta(j)\Delta(j+1) \leq 0$ for $j = 1, 2, \dots$;

Step A.15 Use the bisection method [67] to compute the zeros \bar{X}_j in the range $[X(j), X(j+1)]$ where $j = 1, 2, \dots$, provided that

$$|\Delta| = \left| \frac{1}{\beta} \sum_{k=1}^8 \beta_k I_k + I_N \right| \leq 10^{-8} \quad (149)$$

at $X = \bar{X}_j$;

Step A.16 Compute B_k and S_k for $k = x, y, z$ from equations (78);

Step A.17 Use the bisection method [67] to find the real zeros of $I_{\text{forced}}(t_0) = 0$ associated with equation (73) or (83) in certain expected intervals to give t_{0k} for $k = 1, 2, 3, \dots, \infty$

Step A.18 Check the hyperbolicity of the fixed point from equation (29). If the computed fixed point is hyperbolic, then the zeros \bar{X}_j will be selected for determining the moments of momentum of the wheels. Otherwise, choose another set of parameters $I_{xx}, I_{yy}, I_{zz}, \Omega_{z1}, \Omega_{z2}, \Omega_{z3}, \Omega_{z4}$ in *Step A.1*, and then repeat *Steps A.1* to *A.18* until the

ideal results are acquired. For the modified Rossler turbulence model [10], we have to develop a particular algorithm to deal with the convergence issue of the Melnikov integral in a different way according to the N _column (see *Algorithm 5.2* below).

Algorithm 5.2 Determination of the principal moments of inertia of the symmetric gyrostat

For the modified Rossler model of turbulence in equations (121) and (122), choosing the fixed point $\omega_{xp} = \omega_{yp} = \omega_{zp} = \Omega_{z2} = \Omega_{z3} = 10$ in equations (139) and

$$\Omega_{z2} = \Omega_{z3} > \Omega_{z4} \text{ from equation (140), i.e., } \frac{I_{zz}}{I_{xx}} = \frac{(\omega_{xp}^2 + \omega_{yp}^2)h_{xj\Omega}}{F_{0\Omega}^2}, \text{ one may compute } I_{zz}$$

as a function of the parameter Ω_{z1} when the equations (20), i.e., $\Omega_{z1} > \Omega_{z2} = \Omega_{z3} > \Omega_{z4}$, hold. $h_{xj\Omega}$ in equations (138) and $F_{0\Omega}$ in equation (140) are functions of $\Omega_{z1}, \Omega_{z2}, \Omega_{z3}$ and Ω_{z4} . Thus, the Melnikov integral (90) is a function of Ω_{z1} and t_0 , i.e., $M(t_0) \equiv M(\Omega_{z1}, t_0)$ with the fixed $\Omega_{z1}, \Omega_{z2}, \text{ and } \Omega_{z3}$. For the given initial time t_0 , one may obtain the unknown variable Ω_{z1} from the equation $M(t_0) \equiv M(\Omega_{z1}, t_0) = 0$ readily as detailed in subsection 4.9.

The following **Procedure B** relates to Algorithm 5.2 in which $I_N(t_0)$ in equation (52) or (136) is dependent upon t_0 .

Procedure B

Step B.1 Input $t_0, I_{xx}, I_{yy}, \Omega_{z2}, \Omega_{z3}, \Omega_{z4}$ with the constraint $I_{xx} = I_{yy}$ and let

$10 = \omega_{xp} = \omega_{yp} = \omega_{zp} = \Omega_{z2} = \Omega_{z3}$ where the value 10 is extracted from the equations

(122) ;

Step B.2 Input $N = 1,000$ to compute $\Omega_{z1}(i) = \Omega_{z2} + i \frac{0.2}{N}$, where $i = 1, 2, \dots, N-1$ in accordance with the constraint equations $\Omega_{z1} > \Omega_{z2} = \Omega_{z3} > \Omega_{z4}$ (see equation (20)) for extrapolating the Ω_{z1} ; N should be large enough for a successful search.

Compute I_{zz} from equation (140)

$$I_{zz}(i) = I_{xx} \frac{(\omega_{xp}^2 + \omega_{yp}^2) h_{xy\Omega}(i)}{F_{0\Omega}^2(i)} \quad (150)$$

with the following formulas derived from equations (138) – (140)

$$\left. \begin{array}{l} F_{0\Omega}(i) = \frac{1}{2} [\Omega_{z2}^2 - 2\Omega_{z2} h_{z\Omega}(i) + R_\Omega(i)] \\ h_{xy\Omega}(i) = \frac{1}{4} [a_{2\Omega}(i) - 2R_\Omega(i) - 4h_{z\Omega}^2(i)] \\ h_{z\Omega}(i) = \frac{1}{4} [\Omega_{z1}(i) + \Omega_{z2} + \Omega_{z3} + \Omega_{z4}] \end{array} \right\} \quad (151)$$

$$\left. \begin{array}{l} R_\Omega(i) = \frac{[\Omega_{z1}(i)\Omega_{z2}\Omega_{z3} + \Omega_{z2}\Omega_{z3}\Omega_{z4} + \Omega_{z3}\Omega_{z4}\Omega_{z1}(i) + \Omega_{z4}\Omega_{z1}(i)\Omega_{z2}]}{[\Omega_{z1}(i) + \Omega_{z2} + \Omega_{z3} + \Omega_{z4}]} \\ a_{2\Omega}(i) = \Omega_{z1}(i)\Omega_{z2} + \Omega_{z2}\Omega_{z3} + \Omega_{z3}\Omega_{z4} + \Omega_{z4}\Omega_{z1}(i) + \Omega_{z4}\Omega_{z2} + \Omega_{z1}(i)\Omega_{z3} \end{array} \right\} \quad (152)$$

where $i = 1, 2, \dots, N$.

Step B.3 Compute $h_x(i), h_y(i)$ and $h_z(i)$ from equations (137), (141) such as

$$\left. \begin{array}{l} h_x(i) = h_y(i) = \pm [I_{xx} - I_{zz}(i)] \sqrt{\frac{I_{zz}(i)}{2I_{xx}} h_{xy\Omega}(i)} \\ h_z(i) = [I_{xx} - I_{zz}(i)] h_{z\Omega}(i) \end{array} \right\} \quad (153)$$

where $i = 1, 2, \dots, N$.

Step B.4 to Step B.11 are similar to *Step A.4 to Step A.11* of *Procedure A* when the dynamical system is changed for the modified Rossler model of turbulence.

Step B.12 Use the adaptive Simpson numerical integration method [67] to compute $I_N(t_0; i)$ from equation (136), i.e.

$$I_N(t_0; i) = - \int_{-\infty}^{+\infty} \left\{ \sum_{k=x,y,z} I_{kk} \bar{W}_k(t) \bar{\varphi}_k(t + t_0) [u_k(0) + f_k(t + t_0)] \right\} dt \quad (154)$$

where $u_k(0)$ are the initial value of the variable u_k for $k = x, y$, and z , and $\bar{W}_k(t)$, $\bar{\varphi}_k(t + t_0)$ and $f_k(t + t_0)$ are defined in equations (23), (130) and (135) respectively.

Step B.13 Compute the quantities $\Delta(i) = \frac{1}{\beta} \sum_{k=1}^8 \beta_k I_k + I_N(t_0; i)$ as defined in equation (90); Go to *Step B.3* until $i = N - 1$.

Step B.14 Sort out the interval $[\Omega_{z1}(j), \Omega_{z1}(j+1)]$ in which $\Delta(j)\Delta(j+1) \leq 0$ for $j = 1, 2, \dots$;

Step B.15 Use the bisection method [67] to find the zeros $\bar{\Omega}_{zj}$ between $\Omega_{z1}(j)$ and $\Omega_{z1}(j+1)$ for $j = 1, 2, \dots$, provided that

$$|\Delta(j)| = \left| \frac{1}{\beta} \sum_{k=1}^8 \beta_k I_k + I_N(t_0; j) \right| \leq 10^{-8} \quad (155)$$

at $\Omega_{z1} = \bar{\Omega}_{zj}$ for $j = 1, 2, \dots$;

Step B.16 Check the hyperbolicity of the fixed point of the torque-free gyrostat by equation (29).

If the computed fixed point is hyperbolic, then the zeros $\bar{\Omega}_{zj}$ may be selected for determining the principal moments of inertia, I_{xx}, I_{yy} , and I_{zz} , of the symmetric gyrostat.

Otherwise, choose another set of parameters $t_0, I_{xx}, I_{yy}, \Omega_{z2}, \Omega_{z3}, \Omega_{z4}$ in *Step B.1*, and then repeat *Step B.1* to *B.16* until the ideal results are acquired.

Because the Melnikov integral is a highly nonlinear function of the variables t_0 , X or Ω_{z1} , solving numerically for the real zeros by the bisection method [67] is recommended.

Section 6. Simulation of long-term behaviours

The rotational motion of the forced gyrostats equivalent to the class of the 3D oscillators is determined using the Matlab software. The simulated results are given in Examples (1 – 9). The physical parameters of the gyrostat are the principal moments of inertia I_{xx}, I_{yy} and I_{zz} ; the moments of momentum of the wheels h_x, h_y and h_z . The real roots $\Omega_{z1}, \Omega_{z2}, \Omega_{z3}, \Omega_{z4}$ of the polynomial equation (13) corresponding to the homoclinic orbits of the symmetric gyrostat must satisfy the relations (20). Thus, we can deduce that the equations (20) determine the homoclinic orbits of equations (3) for applying the explicit Melnikov integral in equation (22) to the particular dynamical systems listed in Examples (1 – 9).

Some new properties of the homoclinic orbits (5) of the torque-free gyrostat are found and described in equations (38). These new properties together with Corollary 1 and Corollary 2 in the Appendix enable one to particularise the Melnikov integral (22) to study the chaotic dynamics of the 3D oscillators in this section. The N _columns characterizing the piecewise nonlinear terms in the Chua double scroll, modified Brockett, modified Kapitaniak and YSVO 2-D grid scroll systems make the Melnikov

integral very complicated to be computed analytically. The integral issues on Chua's piecewise functions were tackled in subsection 4.8.

The Melnikov integral in *Procedure A* was separated into two parts. The first part, $I_{\text{const}} + I_{\text{linear}} + I_{\text{cross}} + I_{\text{cube}}$, in equation (85) is computed in *Step A.13* of *Procedure A*. The vanishing condition of the first part in equation (85) is used to find the right solutions for the moments of momentum of the wheels h_x, h_y and h_z for given principal moments of inertia of the gyrostat I_{xx}, I_{yy} and I_{zz} and the four real roots $\Omega_{z1} > \Omega_{z2} = \Omega_{z3} > \Omega_{z4}$ of equation (13). The second part $I_{\text{forced}}(t_0)$ in equation (73) or (83) is computed in *Step A.16* of *Procedure A*. The real zeros t_0 of equation $I_{\text{forced}}(t_0) = 0$ associated with equation (83) are found by bisection algorithms [67]. Several examples of the 3D oscillators equivalent to the rotational motions of the symmetric gyrostats are obtained below by *Procedures A* and *B*, respectively.

Example 1 The forced Lorenz dynamical system

The forced Lorenz system to be discussed here is made of three nonlinear differential equations that may be expressed in terms of the variables $\omega_x, \omega_y, \omega_z$

$$\left. \begin{array}{l} \frac{d\omega_x}{dt} = -\omega_x + \rho\omega_z - \omega_z\omega_y + d_{xx} \sin(\Omega_x t) \\ \frac{d\omega_y}{dt} = -\beta''\omega_y + \omega_z\omega_x + d_{yy} \sin(\Omega_y t) \\ \frac{d\omega_z}{dt} = -\sigma\omega_z + \sigma\omega_x + d_{zz} \sin(\Omega_z t) \end{array} \right\} \quad (156)$$

where $\sigma = 10$, $\rho = 28$, $\beta'' = \frac{8}{3}$, $d_{xx} = 13$, $d_{yy} = 7$, $d_{zz} = 17$, $\Omega_x = 2\pi$, $\Omega_y = 3\pi$, and

$\Omega_z = 4\pi$. The dynamical system (156) is called as the Lorenz equations when

$d_{xx} = 0$, $d_{yy} = 0$, and $d_{zz} = 0$. The phase curves of the forced Lorenz equations (156) are depicted in Figures 2, 3, and 4 in which the time range is between 0 and 300 seconds and the initial conditions are given as $\omega_x(0) = 5$, $\omega_y(0) = 7$, and $\omega_z(0) = 5.5$.

Figure 2. Projection $(\omega_x - \omega_y)$ of the chaotic phase portrait of the forced Lorenz equations

Figure 3. Projection $(\omega_x - \omega_z)$ of the chaotic phase portrait of the forced Lorenz equations

Figure 4. Projection $(\omega_y - \omega_z)$ of the chaotic phase portrait of the forced Lorenz equations

Comparing the forced Lorenz dynamical system (156) with the dynamical system equations (41, 42, 147, 148), one obtains the β _column = $[0]_{3 \times 1}$, N _column = $[0]_{3 \times 1}$, Γ _matrix = $[0]_{3 \times 3}$, the θ _matrix, Θ _matrix, Ω _column and d _matrix for the forced Lorenz dynamical system, respectively

$$\theta \text{ matrix} = \begin{bmatrix} -1 & 0 & \rho \\ 0 & -\beta'' & 0 \\ \sigma & 0 & -\sigma \end{bmatrix}, \quad \Theta \text{ matrix} = \begin{bmatrix} 0 & -1 & 0 \\ 0 & 0 & 1 \\ 0 & 0 & 0 \end{bmatrix} \quad (157)$$

$$\Omega \text{ column} = \begin{bmatrix} 2\pi \\ 3\pi \\ 4\pi \end{bmatrix}, \quad d \text{ matrix} = \begin{bmatrix} d_{xx} & 0 & 0 \\ 0 & d_{yy} & 0 \\ 0 & 0 & d_{zz} \end{bmatrix} \quad (158)$$

The next step is to find the μ _matrix of the equivalent symmetrical gyrostat by means of the real zeros of the Melnikov integral equation (144) associated with equation (145) when the physical parameters I_{xx}, I_{yy}, I_{zz} are given and the real roots of the polynomial equation (13) are assumed and constrained by equations (20).

Selecting

$$I_{xx} = I_{yy} = 18 \text{kg.m}^2, \quad I_{zz} = 16 \text{kg.m}^2, \quad \Omega_{z1} = 8, \quad \Omega_{z2} = 6, \quad \Omega_{z3} = 6, \quad \Omega_{z4} = -5 \quad (159)$$

according to Algorithm 5.1, one obtains the four real roots from equation (144), i.e.

$$M(X, t_0) = 0,$$

$$\begin{aligned} \bar{X}_1 &= -2.10933989293170; & \bar{X}_2 &= -1.03384165778741; \\ \bar{X}_3 &= 0.67538579691389; & \bar{X}_4 &= 2.46697636307437 \end{aligned} \quad (160)$$

subjected to the constraint equation (145), i.e., $I_{\text{forced}}(t_0) = 0$. $I_N(t_0) \equiv 0$ for the forced Lorenz equations. The moments of momentum of the wheels of the torque-free equivalent symmetric gyrostat models of the forced Lorenz equations (156) are tabulated in Table 1. Four symmetrical gyrostat models are computed corresponding to the four real roots (160) of the Melnikov integral. Because $I_N(t_0) \equiv 0$, there exist many zeros t_0 satisfying the constraint equation (145), i.e., $I_{\text{forced}}(t_0) = 0$, given by

$$\begin{aligned} 0 = I_{\text{forced}}(t_0) &= B_x \cos(\Omega_x t_0) + B_y \cos(\Omega_y t_0) + B_z \cos(\Omega_z t_0) \\ &+ S_x \sin(\Omega_x t_0) + S_y \sin(\Omega_y t_0) + S_z \sin(\Omega_z t_0) \end{aligned}$$

where the coefficients B_k and S_k for $k = x, y, z$ are defined in equations (78).

The results of the coefficients B_k and S_k for $k = x, y, z$ of the equation $I_{\text{forced}}(t_0) = 0$ are tabulated in Tables 2 and 3. The corresponding hyperbolic fixed points computed according to equations (32) and (33) are given in Table 4.

Table 1 The moments of momentum of the wheels, defined in equations (142) for the forced Lorenz equations (156)

	h_x (Nms)	h_y (Nms)	h_z (Nms)

GM_1 of Forced Lorenz M.	-4.07503227367533	-2.43463453147239	7.5000000000
GM_2 of Forced Lorenz M.	-4.07889551196554	2.42815665388391	7.5000000000
GM_3 of Forced Lorenz M.	2.96777261690464	3.70481565367082	7.5000000000
GM_4 of Forced Lorenz M.	2.96492085916681	-3.70709827657845	7.5000000000

where "M." stands for "Model", and "GM" means "Gyrostat Model".

Table 2 Coefficients defined in the second of equations (78) for the forced Lorenz equations

	$S_x \times 10^3$ (Nms)	$S_y \times 10^3$ (Nms)	$S_z \times 10^3$ (Nms)
GM_1 of Forced Lorenz M.	0.16789599934830	0.00000480484456	0.00000000116052
GM_2 of Forced Lorenz M.	0.16805516919283	-0.00000479206022	0.00000000116052
GM_3 of Forced Lorenz M.	-0.12227563265513	-0.00000731159569	0.00000000116052
GM_4 of Forced Lorenz M.	-0.12215813696843	0.00000731610053	0.00000000116052

where "M." stands for "Model", and "GM" means "Gyrostat Model".

Table 3 Coefficients defined in the first of equations (78) for the forced Lorenz equations

	$B_x \times 10^4$ (Nms)	$B_y \times 10^4$ (Nms)	$B_z \times 10^4$ (Nms)
GM_1 of Forced Lorenz M.	-0.45217295755578	0.00003676849122	0.0
GM_2 of Forced Lorenz M.	0.45096985251886	0.00003680334872	0.0
GM_3 of Forced Lorenz M.	0.68807758604581	-0.00002677782999	0.0
GM_4 of Forced Lorenz M.	-0.68850152661585	-0.00002675209894	0.0

where "M." stands for "Model", and "GM" means "Gyrostat Model".

Table 4 The hyperbolic fixed points in equations (32) and (33) for the forced Lorenz equations

	ω_{xp} (Nms)	ω_{yp} (Nms)	ω_{zp} (Nms)
GM_1of Forced Lorenz M.	5.43337636490042	3.24617937529651	6.0000000000
GM_2of Forced Lorenz M.	5.43852734928738	-3.23754220517854	6.0000000000
GM_3of Forced Lorenz M.	-3.95703015587283	-4.93975420489440	6.0000000000
GM_4of Forced Lorenz M.	-3.95322781222242	4.94279770210461	6.0000000000

where "M." stands for "Model", and "GM" means "Gyrostat Model".

In Tables 1 to 4, the torque-free Model_{_k} of the forced Lorenz dynamical system corresponds to the real zeros \bar{X}_k for $k = 1, 2, 3$, and 4 in equation (160) of the Melnikov integral equation (144). The θ _matrix, Θ _matrix, β _column, Ω _column, N _column, Γ _matrix and d _matrix in equations (157) and (158) for the forced Lorenz dynamical system and the moment of momentum of the wheels in Table 1 may be used to compute the perturbation torque of the disturbed symmetric gyrostat equivalent to the forced Lorenz dynamical system from equations (43) – (45) as established in Section 3. The numerical calculations of the perturbation torque terms are straightforward and are omitted here. Therefore, the complete set of parameters in equations (43) to (45) comprising the dynamical system of the forced attitude motions of the gyrostat equivalent to the forced Lorenz dynamical system is found.

Example 2 The Chua double scroll system

The Chua double scroll system is a set of three piecewise linear equations [5], given by

$$\frac{d\omega_x}{dt} = \alpha'' [\omega_y - f(\omega_x)], \quad \frac{d\omega_y}{dt} = \omega_x - \omega_y + \omega_z, \quad \frac{d\omega_z}{dt} = -\beta'' \omega_y \quad (161)$$

with $\alpha'' = 9$, $\beta'' = \frac{100}{7}$ and

$$f(\omega_x) = \begin{cases} m_1 \omega_x + (m_0 - m_1), & \text{if } \omega_x \geq 1 \\ m_0 \omega_x & \text{if } |\omega_x| \leq 1 \\ m_1 \omega_x - (m_0 - m_1), & \text{if } \omega_x < -1 \end{cases} \quad (162)$$

where $m_0 = \frac{-1}{7}$, $m_1 = \frac{2}{7}$. The phase curves of the Chua double scroll equations (161) are depicted in Figure 5 where the time ranges between 0 and 400 seconds and the initial conditions are given as $\omega_x(0) = 0.05$, $\omega_y(0) = 0.07$, and $\omega_z(0) = 0.5$.

Figure 5. Projection $(\omega_x - \omega_y)$ of the chaotic trajectory of the Chua double scroll dynamical system

Comparing the Chua double scroll equations (161) and (162) with the generic dynamical system equations (41) and (42) as well as equations (147) and (148), one obtains the Θ -matrix $=[0]_{3 \times 3}$, β -column $=[0]_{3 \times 1}$, Ω -column $=[0]_{3 \times 1}$, Γ -matrix $=[0]_{3 \times 3}$, d -matrix $=[0]_{3 \times 3}$, and θ -matrix, N -column for the Chua double scroll equations, respectively, as follows

$$\theta \text{-matrix} = \begin{bmatrix} 0 & \alpha'' & 0 \\ 1 & -1 & 1 \\ 0 & -\beta'' & 0 \end{bmatrix}, \quad N \text{-column} = \begin{bmatrix} -\alpha'' f(\omega_x) \\ 0 \\ 0 \end{bmatrix} \quad (163)$$

In Subsection 4.8 we investigated the contribution in equation (120) of the N -column to the Melnikov integral. The quantity I_{N_chua} in equation (120) is a function of the physical parameters $I_{xx}, I_{yy}, I_{zz}, h_x, h_y, h_z, G_p, T$ of the equivalent torque-free symmetric gyrostat.

Taking $I_{xx} = I_{yy} = 18 \text{ kg.m}^2$, $I_{zz} = 16 \text{ kg.m}^2$, $\Omega_{z1} = 8$, $\Omega_{z2} = 6$, $\Omega_{z3} = 6$, and $\Omega_{z4} = -5$, in *Algorithm 5.1*, one obtains the moments of momentum of the wheels of the torque-free gyrostat models corresponding to the Chua double scroll system (161) in Table 5.

Table 5

	h_x (Nms)	h_y (Nms)	h_z (Nms)
GM-1 of Chua	-0.66547587363094	-4.70005055238223	7.500000000000000
GM-2 of Chua	-4.73979715428966	0.26010818810828	7.500000000000000
GM-3 of Chua	-0.19808778044967	4.74279396185095	7.500000000000000
GM-4 of Chua	4.74198004434481	-0.21669931326357	7.500000000000000

where “GM” stands for “Gyrostat Model”.

The torque-free gyrostat model- k of the Chua double scroll equations corresponds to the k th real root, \bar{X}_{k_chua} for $k = 1, 2, 3, 4$ of the Melnikov integral equation (144) associated with equations (90) and (145). The k th real root of the Melnikov integral in equation (144) is presented as follows

$$\begin{aligned} \bar{X}_{1_chua} &= -3.00093851226396; & \bar{X}_{2_chua} &= -1.51597382242115; \\ \bar{X}_{2_chua} &= -0.04174179203198; & \bar{X}_{4_chua} &= 1.61646262117438 \end{aligned} \quad (164)$$

The tabulated θ _matrix, Θ _matrix, β _column, Ω _column, N _column, Γ _matrix, and d _matrix in equations (163) for the Chua double scroll system, and the moment of momentum of the wheels from Table 5 may be used to compute the perturbation torque terms of the disturbed gyrostat corresponding to the Chua double scroll systems from equations (43) – (45) established in Section 3.

Example 3 The equations of Duffing and Ueda

The equations of Duffing and Ueda [5, 6] are often used as an example of a classic chaotic dynamical system. The systems of Duffing and Ueda are represented by ordinary differential equations in terms of the variables ω_x, ω_y , and ω_z

$$\frac{d\omega_x}{dt} = \omega_y, \quad \frac{d\omega_y}{dt} = k_0\omega_x - \omega_x^3 - \varepsilon''\omega_y + \gamma \cos(\Omega_y t), \quad \frac{d\omega_z}{dt} = 0 \quad (165)$$

which is called the Duffing equation [5] when $k_0 = 1$, $\varepsilon'' = 0.25$, $\gamma = 0.3$, $\Omega_y = 1$; or the Ueda system [6] when $k_0 = 0.1$, $\varepsilon'' = 0$, $\gamma = 12$, $\Omega_y = 1$. Equations (165) describe also the behaviour of a buckling beam called “Moon beam” [20]. The phase curves of the Duffing and Ueda equations (165) are depicted in Figures 6 and 7 in which the initial conditions are given as $\omega_x(0) = 0.05$, and $\omega_y(0) = 0.07$. For the Duffing equations, the time ranges between 0 and 1000 seconds and for the Ueda equations the time ranges between 0 and 300 seconds.

Figure 6 Projection ($\omega_x - \omega_y$) of Chaotic trajectory of the Duffing equations

Figure 7 Projection ($\omega_x - \omega_y$) of Chaotic trajectory of the Ueda system

Comparing the Duffing and Ueda dynamical system (165) with the generic equations (41) and (42) as well as equations (147) and (148), one can obtain the Θ _matrix = $[0]_{3 \times 3}$, β _column = $[0]_{3 \times 1}$, N _column = $[0]_{3 \times 1}$, θ _matrix, Γ _matrix, Ω _column and d _matrix for the Duffing and Ueda equations, respectively,

$$\theta \text{matrix} = \begin{bmatrix} 0 & 1 & 0 \\ k_0 & -\varepsilon'' & 0 \\ 0 & 0 & 0 \end{bmatrix}, \quad \Omega \text{column} = \begin{bmatrix} 0 \\ \Omega_y \\ 0 \end{bmatrix} \quad (166)$$

$$\Gamma \text{matrix} = \begin{bmatrix} 0 & 0 & 0 \\ -1 & 0 & 0 \\ 0 & 0 & 0 \end{bmatrix}, \quad d \text{matrix} = \begin{bmatrix} 0 & 0 & 0 \\ 0 & \gamma & 0 \\ 0 & 0 & 0 \end{bmatrix} \quad (167)$$

Taking $I_{xx} = I_{yy} = 18 \text{ kg.m}^2$, $I_{zz} = 16 \text{ kg.m}^2$, $\Omega_{z1} = 8$, $\Omega_{z2} = 6$, $\Omega_{z3} = 6$, and $\Omega_{z4} = -5$, in *Algorithm 5.1*, one obtains the moments of momentum of the wheels of the torque-free gyrostat models corresponding to the Duffing and Ueda equations tabulated in Table 6 where the parameters B_y and S_y are defined in equations (78). The solutions listed in Table 6 are based on the constraint equation $I_{\text{forced}}(t_0) = 0$ where $I_{\text{forced}}(t_0)$ is defined in equation (83).

Table 6

	h_x (Nms)	h_y (Nms)	h_z (Nms)	S_y	B_y
GM-1 of Duffing	-4.05882	-2.46156	7.500	5.70649	3.46976
GM-2 of Duffing	-4.74134	-0.23019	7.500	0.53364	4.05323
GM-3 of Duffing	-3.98463	2.57992	7.500	-5.98088	3.40634
GM-4 of Duffing	0.090568	4.74606	7.500	-11.00250	-0.07742

GM-5 of Duffing	4.058673	2.46180	7.500	-5.707059	-3.46963
GM-6 of Duffing	4.741346	0.23014	7.500	-0.533530	-4.05323
GM-7 of Duffing	3.984505	-2.58012	7.500	5.98134	-3.40623
GM-1 of Ueda	-3.733368	-2.931773	7.500	271.8619	127.6615
GM-2 of Ueda	-4.746929	-0.000192	7.500	0.0178395	162.3200
GM-3 of Ueda	-3.733340	2.931809	7.500	-271.8651	127.6606
GM-4 of Ueda	0.000131	4.746929	7.500	-440.1803	-0.004512
GM-5 of Ueda	3.733231	2.931947	7.500	-271.8779	-127.6569
GM-6 of Ueda	4.746929	0.000192	7.500	-0.017836	-162.3200
GM-7 of Ueda	3.733204	-2.931981	7.500	271.88122	-127.6559

where “G” stands for “Gyrostat” and “M” for “Model”.

Under the constraint equation $I_{\text{forced}}(t_0) = 0$, one can resort to the Melnikov integral equation (90) to find the moments of momentum of the wheels of the torque-free gyrostat models from *Algorithm 5.1*. Substitution of equations (166) and (167) into equations (83) yields

$$B_y \cos(\Omega_y t_0) + S_y \sin(\Omega_y t_0) = 0 \quad (168)$$

Obviously, there exist many real roots of t_0 in this equation.

The torque-free gyrostat model- k of the Duffing and Ueda systems corresponds to the k th real root $\bar{X}_{k_Duffing}$ or \bar{X}_{k_Ueda} of the Melnikov integral equation (144) for $k = 1, 2, \dots, 7$. The 7 real roots are

$$\begin{aligned}
\bar{X}_{1_Duffing} &= -2.11596099050910; & \bar{X}_{2_Duffing} &= -1.61930865728683 \\
\bar{X}_{3_Duffing} &= -0.99620240780661; & \bar{X}_{4_Duffing} &= 0.01908057350686 \\
\bar{X}_{5_Duffing} &= 1.02557072561452; & \bar{X}_{6_Duffing} &= 1.52229441450466 \\
\bar{X}_{7_Duffing} &= 2.14544005079811
\end{aligned} \tag{169}$$

for the Duffing system and

$$\begin{aligned}
\bar{X}_{1_Ueda} &= -2.23650277708840; & \bar{X}_{2_Ueda} &= -1.57083685456858 \\
\bar{X}_{3_Ueda} &= -0.90508047393755; & \bar{X}_{4_Ueda} &= 0.00002779577706 \\
\bar{X}_{5_Ueda} &= 0.90504354902830; & \bar{X}_{6_Ueda} &= 1.57075580536992 \\
\bar{X}_{7_Ueda} &= 2.23655849965836
\end{aligned} \tag{170}$$

for the Ueda system.

The θ _matrix, Θ _matrix, β _column, Ω _column, N _column, Γ _matrix, and d _matrix in equations (166) and (167) for the Duffing and Ueda systems and the moment of momentum of the wheels in Table 6 are used to compute the perturbation torque of the disturbed symmetric gyrostat corresponding to equations (43) – (45) in Section 3.

Example 4 The generalized Lorenz equations

The most well known Lorenz system [1] was first investigated in 1963. It was derived from the Rayleigh-Benard hydrodynamic problem in Earth's atmosphere. It also describes models of lasers and dynamos [19]. The generalized Lorenz system discussed in this example is made up of three nonlinear differential equations that may be expressed in terms of the variables ω_x , ω_y , and ω_z

$$\left. \begin{array}{l} \frac{d\omega_x}{dt} = -\omega_x + \rho\omega_z - \omega_z\omega_y + [-\sigma\omega_z + (\rho+1)\omega_x]m \\ \frac{d\omega_y}{dt} = -\beta''\omega_y + \omega_z\omega_x \\ \frac{d\omega_z}{dt} = -\sigma\omega_z + \mu''\omega_y + \sigma\omega_x + \alpha_0\omega_x\omega_y \end{array} \right\} \quad (171)$$

where the dynamical system (171) is called the Lorenz equations [68] when $\sigma = 10$, $\rho = 28$, $\beta'' = 8/3$, $\mu'' = 0$, $\alpha_0 = 0$, and $m = 0$. Equations (171) are called the generalized Lorenz equations when $\mu'' = 1.0$, $\alpha_0 = 0.25$, and $m = 0$. The generalized Lorenz equations may also be investigated by using the normal form theory of the ordinary differential equations [14]. Chen and Ueta [8] found that this dynamical system described a new attractor when $\sigma = 35$, $\rho = 28$, $\beta'' = 8/3$, $\mu'' = 0$, $\alpha_0 = 0$, and $m = 1$. The phase curves of the generalized Lorenz equations (171) are depicted in Figures 8 and 9 where the initial conditions are given as $\omega_x(0) = 5$, $\omega_y(0) = 7$ and $\omega_z(0) = 5.5$ and the time range is between 0 and 300 seconds. The phase curves of Chen and Ueta equations (171) are depicted in Figure 10 where the initial conditions are given as $\omega_x(0) = 10$, $\omega_y(0) = 0$ and $\omega_z(0) = 37$ and the time range is between 0 and 300 seconds.

Figure 8 Projection ($\omega_x - \omega_y$) of Chaotic trajectory of the Lorenz equations

Figure 9 Projection ($\omega_x - \omega_y$) of Chaotic trajectory of the generalized Lorenz

equations $\mu'' = 1$, $\alpha_0 = 0.25$, and $m = 0$

Figure 10 Projection ($\omega_x - \omega_y$) of Chaotic trajectory of the generalized Lorenz

equations when $\sigma = 35$, $\rho = 28$, $\beta'' = 8/3$, $\mu'' = 0$, $\alpha_0 = 0$, and $m = 1$

Comparing the generalized Lorenz dynamical system (171) with the generic dynamical system of equations (41, 42, 147, 148), one obtains the β _column = $[0]_{3 \times 1}$, Ω _column = $[0]_{3 \times 1}$, N _column = $[0]_{3 \times 1}$, Γ _matrix = $[0]_{3 \times 3}$, d _matrix = $[0]_{3 \times 3}$, θ _matrix and Θ _matrix for the generalized Lorenz equations, respectively

$$\theta \text{matrix} = \begin{bmatrix} m(\rho+1)-1 & 0 & \rho-m\sigma \\ 0 & -\beta'' & 0 \\ \sigma & \mu'' & -\sigma \end{bmatrix}, \quad \Theta \text{matrix} = \begin{bmatrix} 0 & -1 & 0 \\ 0 & 0 & 1 \\ \alpha_0 & 0 & 0 \end{bmatrix} \quad (172)$$

Taking $I_{xx} = I_{yy} = 18 \text{ kg.m}^2$, $I_{zz} = 16 \text{ kg.m}^2$, $\Omega_{z1} = 8$, $\Omega_{z2} = 6$, $\Omega_{z3} = 6$, $\Omega_{z4} = -5$, in *Algorithm 5.1*, one obtains the moments of momentum of the wheels of the torque-free gyrostat models corresponding to the Lorenz, generalized Lorenz and Chen and Ueta system as tabulated in Table 7.

Table 7

	h_x (Nms)	h_y (Nms)	h_z (Nms)
GM-1 of Lorenz	-4.07503227367533	-2.43463453147239	7.500000000000000
GM-2 of Lorenz	-4.07889551196554	2.42815665388391	7.500000000000000
GM-3 of Lorenz	2.96777261690464	3.70481565367082	7.500000000000000
GM-4 of Lorenz	2.96492085916681	-3.70709827657845	7.500000000000000
GM-1 of G. Lorenz	-4.01062457580201	-2.53933531564980	7.500000000000000
GM-2 of G. Lorenz	-4.13571599792087	2.33006148371127	7.500000000000000
GM-3 of G. Lorenz	3.05745173179609	3.63115990298836	7.500000000000000
GM-4 of G. Lorenz	2.87007351687289	-3.78100665710578	7.500000000000000

GM-1 of Chen	-3.19771453415908	-3.50826952946337	7.500000000000000
GM-2 of Chen	-3.19789718927789	3.50810303442500	7.500000000000000
GM-3 of Chen	3.57072181167417	3.12782337688170	7.500000000000000
GM-4 of Chen	3.57051211163381	-3.12806275416744	7.500000000000000

where “GM” stands for “Gyrostat Model” and “G.” for “Generalized”.

The torque-free gyrostat model- k of the Lorenz, generalized Lorenz, Chen and Ueta system corresponds to the k th real root \bar{X}_{k_Lorenz} , $\bar{X}_{k_G_Lorenz}$ and \bar{X}_{k_Chen} of the Melnikov integral equation (144) associated with equations (90) and (145) for $k = 1, 2, 3, 4$. The real roots are given by

$$\begin{aligned}\bar{X}_{1_Lorenz} &= -2.10933989293170; & \bar{X}_{2_Lorenz} &= -1.03384165778741 \\ \bar{X}_{3_Lorenz} &= 0.67538579691389; & \bar{X}_{4_Lorenz} &= 2.46697636307437\end{aligned}\quad (173)$$

for the Lorenz system and

$$\begin{aligned}\bar{X}_{1_G_Lorenz} &= -2.13523635002877; & \bar{X}_{2_G_Lorenz} &= -1.05772361681741 \\ \bar{X}_{3_G_Lorenz} &= 0.69983371045546; & \bar{X}_{4_G_Lorenz} &= 2.49230781108644\end{aligned}\quad (174)$$

for the generalized Lorenz system. And

$$\begin{aligned}\bar{X}_{1_Chen} &= -2.40247155695372; & \bar{X}_{2_Chen} &= -0.73917316203513 \\ \bar{X}_{3_Chen} &= 0.85142066651207; & \bar{X}_{4_Chen} &= 2.29023902795280\end{aligned}\quad (175)$$

for the Chen and Ueta system.

The θ _matrix, Θ _matrix, β _column, Ω _column, N _column, Γ _matrix, and d _matrix in equations (172) for the Lorenz, generalized Lorenz, and Chen and Ueta systems and the moment of momentum of the wheels tabulated in Table 7 may be used to compute the perturbation torque of the disturbed gyrostat corresponding to the respective system of equations by means of equations (43) – (45) in Section 3.

Example 5 The Rossler equations

The Rossler equations are derived from chemical kinetics by Rossler [9]. The system may be described by three coupled nonlinear differential equations [27] in terms of the variables ω_x, ω_y , and ω_z as shown in Figure 11

$$\frac{d\omega_x}{dt} = -\omega_y - \omega_z, \quad \frac{d\omega_y}{dt} = \omega_x + a\omega_y, \quad \frac{d\omega_z}{dt} = b + \omega_z(\omega_x - c) \quad (176)$$

where $a = 0.398$, $b = 2$, $c = 4$. The phase curves of Rossler equations (176) are depicted in Figure 11 where the initial conditions are given as $\omega_x(0) = 0.5$, $\omega_y(0) = 1$ and $\omega_z(0) = 0.25$ and the time range is between 0 and 500 seconds.

Figure 11 Projection ($\omega_x - \omega_y$) of Chaotic trajectory of the Rossler equations

Comparing the Rossler system (176) with the generic dynamical system of equations (41, 42, 147, 148), one obtains the $\beta_{\text{column}} = [0]_{3 \times 1}$, $\Omega_{\text{column}} = [0]_{3 \times 1}$, $N_{\text{column}} = [0]_{3 \times 1}$, $\Gamma_{\text{matrix}} = [0]_{3 \times 3}$, $d_{\text{matrix}} = [0]_{3 \times 3}$, θ_{matrix} and Θ_{matrix} , respectively, as follows

$$\theta_{\text{matrix}} = \begin{bmatrix} 0 & -1 & -1 \\ 1 & a & 0 \\ 0 & 0 & -c \end{bmatrix}, \quad \Theta_{\text{matrix}} = \begin{bmatrix} 0 & 0 & 0 \\ 0 & 0 & 0 \\ 0 & 0 & 1 \end{bmatrix} \quad (177)$$

Taking $I_{xx} = I_{yy} = 18 \text{ kg.m}^2$, $I_{zz} = 16 \text{ kg.m}^2$, $\Omega_{z1} = 8$, $\Omega_{z2} = 6$, $\Omega_{z3} = 6$, and $\Omega_{z4} = -5$ in *Algorithm 5.1*, one obtains the moments of momentum of the wheels of the

torque-free gyrostat models corresponding to the Rossler equations (176) as tabulated in Table 8.

Table 8

	h_x (Nms)	h_y (Nms)	h_z (Nms)
GM-1 of Rossler	-3.37486998635374	-3.33820099882287	7.500000000000000
GM-2 of Rossler	-3.37325086995376	3.33983710705920	7.500000000000000
GM-3 of Rossler	2.94412680234045	3.72363407239137	7.500000000000000
GM-4 of Rossler	2.94544324279953	-3.72259283789940	7.500000000000000

where "GM" stands for "Gyrostat Model".

The torque-free gyrostat model- k of the Rossler equations corresponds to the k th real root, $\bar{X}_{k_Rossler}$, of the Melnikov integral equation (144) associated with equations (90) and (145), where $k = 1,2,3,4$ and the real root of the Melnikov integral equation (144) are presented as follows

$$\begin{aligned}\bar{X}_{1_Rossler} &= -2.35073221772112; & \bar{X}_{2_Rossler} &= -0.79037552807312 \\ \bar{X}_{3_Rossler} &= 0.66901953327242; & \bar{X}_{4_Rossler} &= 2.47221953441105\end{aligned}\quad (178)$$

The θ _matrix, Θ _matrix, β _column, Ω _column, N _column, Γ _matrix, and d _matrix in equations (177) of the Rossler equations and the moment of momentum of the wheels tabulated in Table 8 may be used to compute the perturbation torque of the disturbed gyrostat corresponding to the Rossler equations from equations (43) – (45) established in Section 3.

Example 6 The modified Rossler model of turbulence

In 1979, Rossler [10] proposed a set of six-variable non-linear differential equations arisen from chaos and turbulence of relaxation oscillators. Here, the modified Rossler model of turbulence will be discussed. The modified system in terms of the variables $\omega_x, \omega_y, \omega_z, u_x, u_y$, and u_z are given by equations (121) and (122), with reference to Figure 12 where the initial conditions are given as $\omega_x(0) = 0.1$, $\omega_y(0) = 1$ and $\omega_z(0) = 3$, $u_x(0) = 0$, $u_y(0) = 0$, $u_z(0) = 0$ and the time range is between 0 and 500 seconds.

By a series of transformation, we obtain that the modified Rossler model of turbulence may be described by a three dimensional system (125). Thus, the Θ _matrix, Ω _column, Γ _matrix, and d _matrix are all zero. The θ _matrix, β _column, and N _column for the modified Rossler dynamical system of turbulence are described in equations (126) (see subsection 4.9 for more details).

Figure 12 Projection $(\omega_x - \omega_y)$ of Chaotic trajectory of the modified Rossler model of turbulence

The application of **Procedure B** to deal with the modified Rossler turbulence model described in equations (121) and (122) is exemplified here. The related steps of how to construct the algorithms are rather complicated. The moments of momentum of the wheels of the torque-free symmetric gyrostat according to the required hyperbolic fixed point equivalent to the modified Rossler model of turbulence in equations (125) will be determined. The basic idea of the algorithms described in subsection 4.9 is originated from the convergence issue of the Melnikov integral. It is noted that the

N_column of the modified Rossler model of turbulence is an explicit function of time t_0

as shown in equation (127). When we choose the fixed point $\omega_{xp}, \omega_{yp}, \omega_{zp}$ in equations (139), then the $I_{N_m_Rossler}(t_0)$ in equation (127) due to the N_column will be numerically integrated using equation (136).

Taking $I_{xx} = I_{yy} = 8 \text{ kg.m}^2$, $\Omega_{z2} = 10$, $\Omega_{z3} = 10$, $\Omega_{z4} = 3$, for given $\Omega_{z1} = 10.10667$, $t_0 = 0.155$, one obtains the principal moment of inertia of the gyrostat, $I_{zz} = 72.2989938 \text{ kg.m}^2$ computed from the Algorithm 5.2. From equation (140), the moments of momentum of the wheels of the torque-free gyrostat models corresponding to the modified Rossler model of turbulence in the integral-differential equations (125) are given by

$$h_x = h_y = 110.8078325318233 \text{ (Nms)}, \quad h_z = -532.1790214488551 \text{ (Nms)} \quad (179)$$

The torque-free gyrostat model of the modified Rossler model of turbulence corresponds to the real root $\bar{X}_{Rossler_Turbulence}$ of the Melnikov integral equation (144) associated with equations (90) and (145), where the real root of the Melnikov integral equation (144) is given by

$$\bar{X}_{Rossler_Turbulence} = 10.10667 \quad (180)$$

The θ_matrix , Θ_matrix , β_column , Ω_column , N_column , Γ_matrix , and d_matrix in equations (126) for the modified Rossler model of turbulence system (125) according to results of the moments of momentum of the wheel in equation (179) may be used to compute the perturbation torques of the disturbed gyrostat corresponding to the model of the modified Rossler model of turbulence from equations (43) to (45) established in Section 3.

Example 7 The modified Brockett equations

The modified Brockett system of Brockett [3] and Aziz-Alaoui [4] in Figure 13 is governed by

$$\frac{d\omega_x}{dt} = \omega_y, \quad \frac{d\omega_y}{dt} = \omega_z, \quad \frac{d\omega_z}{dt} = -\beta''\omega_y - \gamma''\omega_z + f(\omega_x) \quad (181)$$

where $f(\omega_x)$ is the Chua function in equation (105). The parameters are given as $\beta''=1.25$, $\gamma''=1.0$ and the coefficients in the Chua function (105) are defined by $m_0=1.8$, $m_1=-2.5m_0$. The phase curves of the modified Brockett system (181) are depicted in Figure 13 where the initial conditions are $\omega_x(0)=0.05$, $\omega_y(0)=0.07$, $\omega_z(0)=0.5$ and the time range is between 0 and 1000 seconds.

Figure 13 Projection $(\omega_x - \omega_y)$ of Chaotic trajectory of the modified Brockett system

Comparing the modified Brockett system in equations (181) with the generic dynamical system of equations (41, 42, 147, 148), one obtains the Θ _matrix = $[0]_{3 \times 3}$, β _column = $[0]_{3 \times 1}$, Ω _column = $[0]_{3 \times 1}$, Γ _matrix = $[0]_{3 \times 3}$, d _matrix = $[0]_{3 \times 3}$, θ _matrix and N _column below, respectively

$$\theta \text{matrix} = \begin{bmatrix} 0 & 1 & 0 \\ 0 & 0 & 1 \\ 0 & -\beta'' & -\gamma'' \end{bmatrix}, \quad N \text{column} = \begin{bmatrix} 0 \\ 0 \\ f(\omega_x) \end{bmatrix} \quad (182)$$

The contribution of the term N column in the second of equations (182) to the Melnikov integral is computed from equation (52) as follows

$$I_{N-\text{Brockett}} = \int_{-\infty}^{+\infty} [I_{zz} f(\bar{\omega}_x(t) \bar{W}_z(t))] dt \quad (183)$$

The integral (183) can be computed analytically in the same way as equation (107) for the Chua double scroll system in subsection 4.8. The detailed procedures are omitted here.

Taking $I_{xx} = I_{yy} = 18 \text{ kg.m}^2$, $I_{zz} = 16 \text{ kg.m}^2$, $\Omega_{z1} = 8$, $\Omega_{z2} = 6$, $\Omega_{z3} = 6$, and $\Omega_{z4} = -5$ in *Algorithm 5.1*, one obtains the moments of momentum of the wheels of the torque-free gyrostat model corresponding to the modified Brockett equations in equations (181) as tabulated in Table 9.

Table 9

	h_x (Nms)	h_y (Nms)	h_z (Nms)
GM-1of M. Brockett	-4.74690572066275	-0.01481257818833	7.500000000000000
GM-2of M. Brockett	-0.25347870663268	4.74015631373240	7.500000000000000
GM-3of M. Brockett	4.74691034158596	0.01324923686830	7.500000000000000

where “GM” stands for “Gyrostat Model” and “M.” means “modified”.

The torque-free gyrostat model- k of the modified Brockett systems corresponds to the k th real root $\bar{X}_{k-\text{Brockett}}$ of the Melnikov integral equation (144) associated with equations (90) and (145) for $k = 1, 2$, and 3 given by

$$\begin{aligned}\bar{X}_{1\text{-Brockett}} &= -1.57391678693924; & \bar{X}_{2\text{-Brockett}} &= 1.56800520551612 \\ \bar{X}_{3\text{-Brockett}} &= -0.05342387295277\end{aligned}\quad (184)$$

The θ _matrix, Θ _matrix, β _column, Ω _column, N _column, Γ _matrix and d _matrix in equations (182) for the modified Brockett system and results of the moments of momentum of the wheels in Table 9 may be used to compute the perturbation torques of the disturbed symmetric gyrostat corresponding to the modified Brockett system from equations (43) to (45) established in Section 3.

Example 8 The modified Kapitaniak equations

The modified Kapitaniak system [7] with reference to Figure 14, is defined by

$$\left. \begin{aligned}\frac{d\omega_x}{dt} &= \omega_y - f(\omega_x) \\ \frac{d\omega_y}{dt} &= -\theta''[\omega_x + (v+1)\omega_y] + A\sin(\Omega_x t) + A\sin(\Omega_y t) + A\sin(\Omega_z t) \\ \frac{d\omega_z}{dt} &= 0\end{aligned}\right\} \quad (185)$$

with $f(\omega_x)$ is the Chua function defined in equation (105). The parameters are given by

$\theta''=1$, $v=0.015$, $A=2.5$, $\Omega_x=\sqrt{2}$, $\Omega_y=\sqrt{3}$, $\Omega_z=\sqrt{5}$. The coefficients of the Chua function $f(\omega_x)$ in equation (105) are defined by $m_0=-1.02$, $m_1=0.55$. The original Kapitaniak system may be found in Aziz-Alaoui [4] and Kapitaniak [7]. The phase curves of the modified Kapitaniak system (185) are depicted in Figure 14 where the initial conditions are $\omega_x(0)=1.1$, $\omega_y(0)=2.0$ and the time range is between 0 and 500 seconds.

Figure 14 Projection ($\omega_x - \omega_y$) of Chaotic trajectory of the modified Kapitaniak system

Comparing the modified Kapitaniak system equations (185) with the generic dynamical system of equations (41) and (42) as well as equations (147) and (148), one obtains the Θ _matrix = $[0]_{3 \times 3}$, β _column = $[0]_{3 \times 1}$, Γ _matrix = $[0]_{3 \times 3}$, and θ _matrix, Ω _column, d _matrix and N _column below, respectively

$$\theta\text{matrix} = \begin{bmatrix} 0 & 1 & 0 \\ -\theta'' & -\theta''(v+1) & 0 \\ 0 & 0 & 0 \end{bmatrix}, \quad \Omega\text{column} = \begin{bmatrix} \sqrt{2} \\ \sqrt{3} \\ \sqrt{5} \end{bmatrix} \quad (186)$$

$$N\text{column} = \begin{bmatrix} -f(\omega_x) \\ 0 \\ 0 \end{bmatrix}, \quad d\text{matrix} = \begin{bmatrix} 0 & 0 & 0 \\ A & A & A \\ 0 & 0 & 0 \end{bmatrix} \quad (187)$$

The contribution of the term $N_x(\omega_x, \omega_y, \omega_z, t)$ in equations (187) to the Melnikov integral is computed from equation (52) as follows

$$I_{N\text{-Kapitaniak}} = \int_{-\infty}^{+\infty} [-I_{xx} f(\bar{\omega}_x(t) \bar{W}_x(t))] dt \quad (188)$$

The integral of equation (188) can be computed in the same way as equation (107) for the Chua double scroll system in subsection 4.8. The detailed procedures are omitted here.

Because the Melnikov integral is t_0 -dependent, one may assume that the equation (83), i.e., $I_{\text{forced}}(t_0) = 0$, holds at first. Taking $I_{xx} = I_{yy} = 18 \text{ kg.m}^2$, $I_{zz} = 16 \text{ kg.m}^2$, $\Omega_{z1} = 8$, $\Omega_{z2} = 6$, $\Omega_{z3} = 6$, and $\Omega_{z4} = -5$ in *Algorithm 5.1*, one obtains the moments of

momentum of the wheels of the torque-free gyrostat models corresponding to the modified Kapitaniak system in equations (185) as tabulated in Table 10.

Table 10

	h_x (Nms)	h_y (Nms)	h_z (Nms)
GM-1 of M. Kapitaniak	-3.35705709062978	-3.35611397654872	7.50000000000000
GM-2 of M. Kapitaniak	-3.35765103251422	3.35551976259857	7.50000000000000
GM-3 of M. Kapitaniak	3.35765103251422	3.35551976259857	7.50000000000000
GM-4 of M. Kapitaniak	3.35705709062978	-3.35611397654872	7.50000000000000

where "M-K" stands for "modified-Kapitaniak".

Table 11

	S_x (Nms)	S_y (Nms)	S_z (Nms)
GM-1 of M. Kapitaniak	23.84464204593550	10.59740322766257	2.78802113384110
GM-2 of M. Kapitaniak	-23.8404202528023	-10.5955269133069	-2.78752750309356
GM-3 of M. Kapitaniak	-23.8404202528023	-10.5955269133069	-2.78752750309356
GM-4 of M. Kapitaniak	23.84464204593550	10.59740322766257	2.78802113384110

Table 12

	B_x (Nms)	B_y (Nms)	B_z (Nms)
GM-1 of M. Kapitaniak	9.39053572091581	4.30246536925664	1.16812120859438
GM-2 of M. Kapitaniak	9.39219712622750	4.30322657596841	1.16832787654585

GM-3 of M. Kapitaniak	-9.39219712622750	-4.30322657596841	-1.16832787654585
GM-4 of M. Kapitaniak	-9.39053572091581	-4.30246536925664	-1.16812120859438

where “GM” stands for “Gyrostat Model” and “M.” for “Modified”.

The torque-free gyrostat model- k of the Kapitaniak system corresponds to the k th real root $\bar{X}_{k_Kapitaniak}$ of the Melnikov integral equation (144) associated with equations (90) and (145) for $k = 1, 2, 3$, and 4 given by

$$\begin{aligned}\bar{X}_{1_Kapitaniak} &= -2.35605400307152; & \bar{X}_{2_Kapitaniak} &= -0.78571563928315 \\ \bar{X}_{3_Kapitaniak} &= 0.78571563928315; & \bar{X}_{4_Kapitaniak} &= 2.35605400307152\end{aligned}\quad (189)$$

The θ _matrix, Θ _matrix, β _column, Ω _column, N _column, Γ _matrix, and d _matrix in equations (186) and (187) for the modified Kapitaniak system and results of the moments of momentum of the wheels in Table 10 may be used to compute the perturbation torque of the disturbed symmetric gyrostat corresponding to the modified Kapitaniak system from equations (43) to (45) established in Section 3. Obviously, there exist many zeros t_0 satisfying the assumed constraint equation $I_{\text{forced}}(t_0) = 0$ associated with the equation (83). The coefficients of the equation $I_{\text{forced}}(t_0) = 0$ for the modified Kapitaniak system are tabulated in Tables 11 and 12.

Example 9 The YSVO 2×2-grid scroll system

In 2002, Yalcin, Suykens, Vandewalle and Ozoguz [4], abbr. YSVO, constructed a new family of the scroll grid system that generalized the Chua double scroll system. The 2×2 grid scroll system is governed by

$$\frac{d\omega_x}{dt} = \omega_y - f_x(\omega_y), \quad \frac{d\omega_y}{dt} = \omega_z, \quad \frac{d\omega_z}{dt} = -a\omega_x - a\omega_y - a\omega_z + af_z(\omega_x) \quad (190)$$

where $a = 0.8$, and

$$f_x(\omega_y) = \begin{cases} 1 & \text{if } \omega_y \geq 0.5 \\ 0 & \text{if } \omega_y < 0.5 \end{cases}, \quad f_z(\omega_x) = \begin{cases} 2 & \text{if } \omega_x \geq 0.5 \\ 0 & \text{if } \omega_x < 0.5 \end{cases} \quad (191)$$

The phase curves of the YSVO system (190) are depicted in Figure 15 where the initial conditions are $\omega_x(0) = 0.05$, $\omega_y(0) = 0$, $\omega_z(0) = 0.04$ and the time range is between 0 and 3000 seconds.

Figure 15 Projection $(\omega_x - \omega_y)$ of Chaotic trajectory of the YSVO 2×2 scroll
system

Comparing the YSVO system (190) with the generic dynamical system of equations (41) and (42) as well as equations (147) and (148), one obtains the Θ _matrix = $[0]_{3 \times 3}$, Ω _column = $[0]_{3 \times 1}$, β _column = $[0]_{3 \times 1}$, Γ _matrix = $[0]_{3 \times 3}$, d _matrix = $[0]_{3 \times 3}$, and θ _matrix and N _column of the YSVO 2×2 scroll systems below, respectively

$$\theta \text{matrix} = \begin{bmatrix} 0 & 1 & 0 \\ 0 & 0 & 1 \\ -a & -a & -a \end{bmatrix}, \quad N \text{column} = \begin{bmatrix} -f_x(\omega_y) \\ 0 \\ af_z(\omega_x) \end{bmatrix} \quad (192)$$

The contribution of N _column in the second of equations (192) of the YSVO system (190) to the Melnikov integral equation is computed from equation (52) and the second of equations (192) as follows

$$I_{N-YSVO} = \int_{-\infty}^{+\infty} \left[-I_{xx} f_x(\bar{\omega}_y(t) \bar{W}_x(t) + a I_{zz} f_z(\bar{\omega}_x(t) \bar{W}_z(t)) \right] dt \quad (193)$$

Substituting equations (191) into equation (193), one obtains

$$I_{N-YSVO} = - \int_{t_y}^{+\infty} I_{xx} \bar{W}_x(t) dt + \int_{t_x}^{+\infty} 2a I_{zz} \bar{W}_z(t) dt \quad (194)$$

where t_y and t_x satisfy the following equations

$$\left. \begin{aligned} \frac{\omega_{y0} + \omega_{y1} \tanh(\beta t_y) + \omega_{y2} \tanh^2(\beta t_y) + \omega_{y3} \tanh^3(\beta t_y) + \omega_{y4} \tanh^4(\beta t_y)}{(D_3 + D_4 \tanh^2(\beta t_y))^2} &= \frac{1}{2} \\ \frac{\omega_{x0} + \omega_{x1} \tanh(\beta t_x) + \omega_{x2} \tanh^2(\beta t_x) + \omega_{x3} \tanh^3(\beta t_x) + \omega_{x4} \tanh^4(\beta t_x)}{(D_3 + D_4 \tanh^2(\beta t_x))^2} &= \frac{1}{2} \end{aligned} \right\} \quad (195)$$

Introducing the transformation $x = \tanh[\beta(t - t_a)]$, one gets from equation (194)

$$I_{N-YSVO} = -I_{xx} \int_{\tanh(\beta t_y)}^{+1} \frac{(R_{x0} + R_{x1}x + R_{x2}x^2)}{\beta(D_3 + D_4x^2)^2} dx + 2a I_{zz} \int_{\tanh(\beta t_x)}^{+1} \frac{(R_{z0} + R_{z1}x + R_{z2}x^2)}{\beta(D_3 + D_4x^2)^2} dx \quad (196)$$

where $R_{k0} = W_{k0}$, $R_{k1} = W_{k1}$, $R_{k2} = W_{k2} + W_{k0}$ for $k = x$ or z .

The integral (196) can be analytically integrated in the same way as the integral (115) of the Chua double scroll systems. The detailed procedures are omitted here.

Taking $I_{xx} = I_{yy} = 18 \text{ kg.m}^2$, $I_{zz} = 16 \text{ kg.m}^2$, $\Omega_{z1} = 8$, $\Omega_{z2} = 6$, $\Omega_{z3} = 6$, and $\Omega_{z4} = -5$ in *Algorithm 5.1*, one obtains the moments of momentum of the wheels of the torque-free gyrostat models corresponding to the YSVO system as tabulated in Table 13.

Table 13

	$h_x(\text{Nms})$	$h_y(\text{Nms})$	$h_z(\text{Nms})$
GM-1 of YSVO	-4.73865308160971	-0.28017905968164	7.500000000000000

GM-2 of YSVO	-0.36306756062444	4.73302390441413	7.500000000000000
GM-3 of YSVO	4.74291493840414	-0.19516972202731	7.500000000000000

where “GM” means “Gyrostat Model”.

The torque-free gyrostat model- k of the YSVO system corresponds to the k th real root \bar{X}_{k_ysvo} of the Melnikov integral equation (144) associated with equations (90) and (145) for $k = 1, 2$, and 3 which is given by

$$\begin{aligned}\bar{X}_{1_ysvo} &= -1.62985387826499; & \bar{X}_{2_ysvo} &= -0.07655949652173 \\ \bar{X}_{3_ysvo} &= 1.61192286521515\end{aligned}\tag{197}$$

The obtained θ _matrix, Θ _matrix, β _column, Ω _column, N _column, Γ _matrix, and d _matrix in equations (192) for the YSVO system and the results of the moment of momentum of the wheels tabulated in Table 13 may be used to compute the perturbation torque of the disturbed gyrostat corresponding to the YSVO system in equations (43) – (45) established in Section 3.

Therefore, when given the set of principal moments of inertia of the gyrostat I_{xx}, I_{yy}, I_{zz} and the four real roots $\Omega_{z1} > \Omega_{z2} = \Omega_{z3} > \Omega_{z4}$ of the polynomial equation (13), through searching for the real roots of the Melnikov integral equation (144) constrained by equation (145) in **Procedure A**, the particular sets of numerical results of the moments of momentum of the wheels for the symmetric gyrostats corresponding to the dynamical systems of the modified Brockett, Chua, Duffing, Ueda, modified Kapitaniak, generalized Lorenz, forced Lorenz, Rossler, and YSVO are found in Examples (1 - 5, 7 - 9). The developed algorithms in **Procedure B** are applied to the modified Rossler model of turbulence by assuming the required hyperbolic fixed point of

the symmetric gyrostat equivalent to the modified Rossler model of turbulence in equations (121) and (122). Thus, the Melnikov integral can be thought of as the function of the parameter Ω_{z1} , i.e., $M(t_0) \equiv M(\Omega_{z1}, t_0)$. When the initial parameter t_0 , the set of principal moments of inertia of the gyrostat I_{xx}, I_{yy}, I_{zz} where $I_{zz} = I_{zz}(\Omega_{z1})$ is determined from equation (140), and the four real roots $\Omega_{z2} = \Omega_{z3} > \Omega_{z4}$ of the polynomial equation (13) are given, through searching for the real roots with respect to the variable Ω_{z1} of the Melnikov integral equation (90) in **Procedure B**, one can find the expected moments of momentum of the wheels h_x, h_y, h_z .

The paper has shown that one could decide whether a given dynamical system is chaotic according to the real zeros of the Melnikov integral if the real zeros exist in the equation of the Melnikov integral which uses the coefficients of a dynamical system as input parameters if the dynamics is chaotic. The Melnikov integral theory discussed in this paper deals with a necessary condition for the existence of chaos in a given dynamical system by detecting transversal intersections of stable and unstable manifolds of the equivalent symmetric gyrostat.

Section 7. Conclusions

A connection of the Melnikov integral equation to certain 3D oscillators is established by means of the homoclinic orbits associated with the torque-free symmetric gyrostats. Based on the version of the Melnikov integral [39] for the rotational motions of the gyrostats subjected to small perturbation torques, the dynamical systems of a class of 3D oscillators including the modified Brockett, Chua, Duffing, Ueda, generalized Lorenz,

forced Lorenz, Rossler, modified Rossler model of turbulence and YSVO 2-D grid scroll systems can be derived from the system of the rotational motions of the equivalent forced symmetric gyrostats. The possible chaos in the investigated dynamical systems is attributed to the homoclinic bifurcations and the transversal intersections between the stable and unstable manifolds of the dynamical systems mentioned above. The algorithms to determine numerically the moments of momentum of the wheels as well as the principal moments of inertia of the equivalent symmetric gyrostat corresponding to the dynamical systems are given in Procedures A and B, through searching for the real zeros with respect to the specific variables of the Melnikov integral equation under the appropriate constraint equations. The Melnikov integral for the perturbed attitude motion of the equivalent symmetric gyrostat is the effective means to investigate the necessary conditions for chaos in the dynamical systems listed in Examples (1 - 9).

Acknowledgement

The research is supported partially by the Hong Kong Research Grant Council #CityU 1026/01E.

Appendix: The Forced Attitude Motions of a Gyrostat

The rotational motions of a gyrostat subject to small external torques may be made equivalent to a slowly varying oscillator by means of the Deprit variables by Kuang *et al* [39]

$$\left. \begin{aligned} \frac{dl}{dt} &= \frac{\partial}{\partial L} H_a(l, L, G) + \varepsilon f_l(l, L, G, t; \mu) \\ \frac{dL}{dt} &= -\frac{\partial}{\partial l} H_a(l, L, G) + \varepsilon f_L(l, L, G, t; \mu) \\ \frac{dG}{dt} &= \varepsilon f_G(l, L, G, t; \mu) \end{aligned} \right\} \quad (198)$$

where ε is a small parameter, $H_a(l, L, G)$ is a scalar-valued function of a one-parameter family of Hamiltonians when $\varepsilon = 0$, and μ is a vector of system parameters. Functions $f_l(l, L, G, t; \mu)$, $f_L(l, L, G, t; \mu)$ and $f_G(l, L, G, t; \mu)$ are periodic in time t with fixed period. The expressions of $H_a(l, L, G)$, $f_l(l, L, G, t; \mu)$, $f_L(l, L, G, t; \mu)$ and $f_G(l, L, G, t; \mu)$ for the rotational motions of the gyrostat can be found in Kuang *et al* [39].

The Melnikov integral corresponding to the first order measure in the perturbation parameter ε of the separation of the stable and unstable manifolds of the disturbed gyrostat can be obtained [39] as proposed by Wiggins and Shaw [13],

$$\begin{aligned} M(t_0) &= \int_{-\infty}^{+\infty} \frac{\partial}{\partial L} H_a(\bar{l}(t), \bar{L}(t), G_p) f_L(\bar{l}(t), \bar{L}(t), G_p, t + t_0; \mu) dt \\ &+ \int_{-\infty}^{+\infty} \frac{\partial}{\partial l} H_a(\bar{l}(t), \bar{L}(t), G_p) f_l(\bar{l}(t), \bar{L}(t), G_p, t + t_0; \mu) dt \\ &+ \int_{-\infty}^{+\infty} \frac{\partial}{\partial G} H_a(\bar{l}(t), \bar{L}(t), G_p) f_G(\bar{l}(t), \bar{L}(t), G_p, t + t_0; \mu) dt \\ &- \frac{\partial}{\partial G} H_a(l_p, L_p, G_p) \int_{-\infty}^{+\infty} f_G(\bar{l}(t), \bar{L}(t), G_p, t + t_0; \mu) dt \end{aligned} \quad (199)$$

where $\bar{L}(t)$ and $\bar{l}(t)$ are the homoclinic orbits of the torque-free symmetric gyrostat in terms of Deprit variables which can be related to the homoclinic orbits with respect to the angular velocities $\bar{\omega}_x(t)$, $\bar{\omega}_y(t)$, and $\bar{\omega}_z(t)$ in equations (5). The parameters l_p, L_p relate

to a hyperbolic fixed point ω_{xp}, ω_{yp} , and ω_{zp} defined in equations (32) and (33). The definition of G_p can be found in the second of equations (4). More details can be found in Kuang *et al* [39].

Simplifying the Melnikov integral (199) to the rotational motions of disturbed gyrostat yields [39] the particular Melnikov integral in equation (22). For periodic disturbances, one has the following Corollaries.

Corollary 1. Suppose that there exists a point \bar{t}_0 such that

$$M(\bar{t}_0) = 0 \quad \text{and} \quad \frac{\partial}{\partial t_0} M(\bar{t}_0) \neq 0 \quad (200)$$

Then, for ε sufficiently small near \bar{t}_0 , the stable and unstable manifolds of the symmetric gyrostat represented by equations (198) or (1) intersect transversely.

Corollary 1 is applicable to the dynamical systems of Duffing, Ueda, periodically forced Lorenz, modified Rossler turbulence model and modified Kapitaniak dynamical systems with forced excitations which may be regarded as the functions of time t and the state variables ω_x, ω_y , and ω_z . Corollary 1 is derived from Theorem 2.4 in Wiggins and Shaw [13] who discussed the chaos and three-dimensional horse-shoe in slowly varying oscillators or Theorem 2 due to Tong and Tabarrok [55]. However, the system referred to in this paper is the rotational motions of the forced gyrostat.

When the disturbance torque that does not depend upon time explicitly, the Melnikov integral (22) is t_0 -independent so that transversal intersections of homoclinic orbits do not occur. However, if the perturbation torque depends upon a parameter of the system, one has the following Corollary 2.

Corollary 2. Suppose the homoclinic orbit of equations (198) for the rotational motions of the gyrostat depends on a real parameter $\bar{\mu}$ and there exists a point $\bar{\mu}_0$ such that

$$M(\bar{\mu}_0) = 0 \quad \text{and} \quad \frac{\partial}{\partial \bar{\mu}} M(\bar{\mu}_0) \neq 0 \quad (201)$$

then for ε sufficiently small near $\bar{\mu}_0$, there exists a bifurcation value $\bar{\mu}$ at which non-transversal homoclinic orbits of the symmetric gyrostat defined by equations (198) occur.

Corollary 2 is applicable to the dynamical systems of modified Brockett, Chua, generalized Lorenz, Rossler and YSVO with non-periodic forced excitations which may be regarded as the functions of the state variables ω_x, ω_y , and ω_z only.

More details of the application of Corollary 1 and 2 with respect to the generic Hamiltonian systems are found in Wiggins and Shaw [13] or Wiggins and Holmes [69] and Tong and Tabarrok [55]. The applications of the Corollary 1 and 2 to the chaotic attitude dynamics detection are found in the original work based on the different version of Melnikov integral (see Tong *et al* [52, 54, 55]). The Melnikov integral (22) for the forced attitude motions of the gyrostat is derived from the Melnikov integral (199) for a one-and-half degree of freedom Hamiltonian system [39, 41]. The derivation of the Melnikov integral (22) from the Melnikov integral (199) is sophisticated and the Deprit variables play a key role in the formulation of the Hamiltonian equations of the forced attitude motions of the gyrostat. More details of the Hamiltonian equations with respect to the rotational motion of the gyrostat in equations (197) in terms of the Deprit variables and the detailed formulation for the Melnikov integral in equation (22) can be found in Kuang *et al* [38, 39, 41, 56].

References

- [1] E. N. Lorenz, Deterministic nonperiodic flow, *Journal of the Atmospheric Sciences* 20 (1963) 130 -141.
- [2] V. K. Melnikov, On the stability of the centre for time-periodic perturbations, *Transactions Moscow Mathematical Society* 12 (1963) 1 – 57.
- [3] R. W. Brockett, On the conditions leading to chaos in feedback systems, *Proceedings of IEEE International Conference on Decision and Control* (1982) 932 – 936.
- [4] M. A. Aziz-Alaoui, Differential equations with multispiral attractors, *International Journal of Bifurcation and Chaos* 9 (1999) 1009 – 1039.
- [5] T. S. Parker, L. O. Chua, *Practical numerical algorithms for chaotic systems*, Berlin, New York, Springer Verlag, 1989.
- [6] Y. Ueda, Random phenomena resulting from nonlinearity in the system described by Duffing's equation, *International Journal of Non-linear Mechanics* 20 (1985) 481 – 491.
- [7] T. Kapitaniak, Strange nonchaotic trajectory on torus, *International Journal of Bifurcation and Chaos* 7 (1997) 423 – 429.
- [8] G. Chen, T. Ueta, Yet another chaotic attractor, *International Journal of Bifurcation and Chaos* 9 (1999) 1465 – 1466.
- [9] E. Rossler, An equation for continuous chaos, *Physics Letters* 57A (1976) 397 – 398.
- [10] E. Rossler, Chaos and turbulence, in H. Haken (eds), *dynamics of synergetic systems: Proceedings of the International symposium on synergetics*, Bielefeld, Fed. Rep. of Germany, Sept. (24-29), Berlin: Springer-Verlag, 1979, pp. 147 - 153.

[11] M. E. Yalcin, J. A. K. Suykens, J. Vandewalle, S. Ozoguz, Families of scroll grid attractors, *International Journal of Bifurcation and Chaos* 12 (2002) 23 – 41.

[12] P. J. Holmes, J. E. Marsden, Horseshoe and Arnold diffusion for Hamiltonian system on Lie groups, *Indiana University Mathematics Journal* 32 (1983) 273 – 309.

[13] S. Wiggins, S. W. Shaw, Chaos and three-dimensional horseshoe in slowly varying oscillators, *ASME Journal of Applied Mechanics* 55 (1988) 959 – 968.

[14] J. Guckenheimer, P. Holmes, *Non-linear oscillations, dynamical systems, and bifurcations of vector fields*, Springer-Verlag, New York Inc., 1983.

[15] Y. S. Chen, A. Y. T. Leung, *Bifurcation and chaos in engineering*, Springer-Verlag, London, 1998.

[16] S. Smale, Finding a horseshoe on the beaches of Rio, *Mathematical Intelligencer* 20 (1998) 1 – 16.

[17] A.Y.T. Leung, T.C. Fung, Construction of Chaotic Regions, *Journal of Sound & Vibration* 131(1989) 445-455.

[18] M. J. Feigenbaum, Quantitative universality for a class of non-linear transformations, *Journal of Statistical Physics* 19 (1978) 25 – 52.

[19] R. G. Harrison, D. J. Biswas, Chaos in light, *Nature* 321(1986) 394 – 401.

[20] F. C. Moon, *Chaotic and fractal dynamics: an introduction for applied scientists and engineers*, John Wiley & Sons Inc., 1992.

[21] D. K. Campbell, G. Mayer-Kress, Chaos and politics: applications of non-linear dynamics to socio-political issues, in: C., Grebogi, J. A. Yorke (Eds), *The Impact of chaos on science and society*, United Nations University Press, Tokyo, New York, Paris, 1997, pp. 18 - 63.

[22] S. R. Bishop, The impact of chaos on engineering, in: C., Grebogi, J. A. Yorke (Eds), *The Impact of chaos on science and society*, United Nations University Press, Tokyo, New York, Paris, 1997, pp. 255 – 274.

[23] E. Ott, C. Grebogi, J. Yorke, Controlling chaos, *Physical Review Letters* 64 (1990) 1196 – 1199.

[24] T. Shinbrot, C. Grebogi, E. Ott, J. Yorke, Using small perturbations to control chaos, *Nature* 363 (1993) 411 – 417.

[25] A. Wolf, J. B. Swift, H. L. Swinney, J. A. Vastano, Determining Lyapunov exponents from a time series, *Physica D: Nonlinear Phenomenon* 16 (1985) 285 – 317.

[26] R. Festa, A. Mazzino, D. Vincenzi, An analytical approach to chaos in Lorenz-like system: a class of dynamical equations, *Europhysics Letters* 56 (2001) 47 – 53.

[27] J. M. T. Thompson, H. B. Stewart, *Non-linear dynamics and chaos: geometrical methods for engineers and scientists*, Chichester [West Sussex]; New York: Wiley, 1986.

[28] W. Tucker, *The Lorenz attractor exists*, C. R. Acad. Sci. Paris, t. (Série I) 328 (1999) 1197 – 1202.

[29] I. Stewart, The Lorenz attractor exists, *Nature* 406 (2000) 948 – 949.

[30] S. Smale, Mathematical problems for the next century, *Mathematical Intelligencer* 20 (1998) 7 – 15.

[31] P. C. Hughes, *Spacecraft attitude dynamics*, Wiley, New York, 1986.

[32] V. V. Rumyantsev, On the Lyapunov's methods in the study of stability of motions of rigid bodies with fluid-filled cavities, *Advances in Applied Mechanics*, Vol. 8, Academic, New York, 1964, pp. 183 – 232.

[33] J. Wittenburg, Beitrage zur dynamik von gynostaten, *Accademia Nazional dei Lincei, Quaderno N.* 217 (1975) 1 – 187.

[34] A. Wangerin, *Uber die Bewegung miteinander verbundener Korper*, Universitats-Schrift Halle, 1889.

[35] V. Volterra, Sur la theories des variations des latitude, *Acta Mathematica* 22 (1898) 201 – 357.

[36] F. Pfeiffer, Problem of contained rotating fluids with respect to aerospace applications, ESA, Special Publication 129, France, 1977, pp. 55 – 62.

[37] J. L. Kuang, A. Y. T. Leung, H_∞ feedback for the attitude control of liquid-filled spacecraft, *AIAA Journal of Guidance, Dynamics, and Control* 24 (2001) 46 – 53.

[38] J. L. Kuang, S. H. Tan, K. Arichandran, A. Y. T. Leung, Chaotic dynamics of an asymmetrical gyrostat, *International Journal of Non-linear Mechanics* 36 (2001) 1213 – 1233.

[39] J. L. Kuang, S. H. Tan, K. Arichandran, A. Y. T. Leung, Chaotic attitude motions of gyrostat satellites via the Melnikov integral, *International Journal of Bifurcation and Chaos* 11(2001), 1233 – 1260.

[40] A. Deprit, A free rotation of a rigid body studied in the phase plane, *American Journal of Physics* 35 (1967) 424 – 428.

[41] J. L. Kuang, S. H. Tan, A. Y. T. Leung, Chaotic attitude motion of gyrostats under small perturbation torques, *Journal of Sound and Vibration* 235 (2000) 175 – 200.

[42] G. L. Gray, I. Dobson, D. C. Kammer, Chaos in a spacecraft attitude manoeuvre due to time-periodic perturbations, *ASME Journal of Applied Mechanics* 63 (1996) 501 – 508.

[43] G. L. Gray, A. P. Mazzoleni, D. R. Campbell III, Analytical criterion for chaotic dynamics in flexible satellites with nonlinear controller damping, *AIAA Journal of Guidance, Control, and Dynamics* 21 (1998) 558 – 565.

[44] G. L. Gray, D. C. Kammer, I. Dobson, A. J. Miller, Heteroclinic bifurcations in rigid bodies containing internally moving parts and a viscous damper, *ASME Journal of Applied Mechanics* 66 (1999) 720 – 728.

[45] C. Or, Chaotic motions of a dual-spin body, *ASME Journal of Applied Mechanics* 65 (1998) 150 – 156.

[46] S. N. Chow, J. Hale, J. Mallet-Paret, An example of bifurcation to homoclinic orbits, *Journal of Differential Equations* 37 (1980) 351 -373.

[47] J. H. Cooper, R. H. Bishop, Chaos in rigid body attitude dynamics, *AIAA Guidance, Navigation, and Control Conference*, Portland, Oregon, AIAA Paper 99-3970, Aug. 1999.

[48] J. Miller, G. L. Gray, A. P. Mazzoleni, Nonlinear spacecraft dynamics with a flexible appendage, damping, and moving internal submasses, *AIAA Journal of Guidance, Control, and Dynamics* 24 (2001) 605 – 615.

[49] L. Q. Chen and Y. Z. Liu, Chaotic attitude motion of a magnetic spacecraft and its control, *International Journal of Nonlinear Mechanics* 37 (2002) 493 – 504.

[50] P. J. Holmes, J. E. Marsden, Horseshoes in perturbations of Hamiltonian systems with two degrees of freedom, *Communications in Mathematical Physics* 82 (1982) , 523 – 544.

[51] P. J. Holmes and J. E. Marsden, Melnikov's method and Arnold diffusion for perturbations of integrable Hamiltonian systems, *Journal of Mathematical Physics* 23 (1982) 669 – 675.

[52] X. Tong, B. Tabarrok, F. P. J. Rimrott, Chaotic motion of an asymmetric gyrostat in the gravitational field, *International Journal of Non-linear Mechanics* 30 (1995) 191 – 203.

[53] J. L. Kuang, S. H. Tan, A. Y. T. Leung, Chaotic attitude tumbling of an asymmetric gyrostat in a gravitational field, *AIAA Journal of Guidance, Dynamics, and Control* 25 (2002) 804 – 814.

[54] X. Tong, B. Tabarrok, Melnikov's method for rigid bodies subject to small perturbation torques, *Archive of Applied Mechanics* 66 (1996) 215 – 230.

[55] X. Tong, B. Tabarrok, Bifurcation of self-excited rigid bodies subjected to small perturbation torques, *AIAA Journal of Guidance, Control, and Dynamics* 20 (1997) 123 – 128.

[56] J. L. Kuang, S. H. Tan, A. Y. T. Leung, On the Melnikov's method in the study of chaotic motions of a gyrostat, *International Journal of Control* 75 (2002) 328 – 351.

[57] P. A. Meehan, S. F. Asokanthan, Chaotic motion in a spinning spacecraft with internal energy dissipation, *Fields Institute communications*, edited by W. H. Kliemann, W. F. Langford, N. S. Namachchivaya, Vol. 9, American Mathematical society, Providence, RI, 1996, pp. 175 – 202.

[58] P. A. Meehan, S. F. Asokanthan, Non-linear instabilities in a dual-spin spacecraft with an axial nutational damper, *Advances in the Astronautical Sciences* 93 (1996) 905 – 923.

[59] P. A. Meehan, S. F. Asokanthan, Control of chaotic motion in a spinning spacecraft with a circumferential nutational damper, *Nonlinear Dynamics* 17 (1998) 269 – 284.

[60] P. A. Meehan and S. F. Asokanthan, Control of chaotic motion in a dual-spin spacecraft with nutational damping, *Journal of Guidance, Control, and Dynamics* 25 (2002) 209 – 214.

[61] P. A. Meehan, S. F. Asokanthan, Control of chaotic instabilities in a spinning spacecraft with dissipation using Lyapunov's method, *Chaos, Solitons and Fractals* 13 (2002) 1857 – 1869.

[62] V. V. Beletskii, M. L. Pivovarov, E. L. Starostin, Regular and chaotic motions in applied dynamics of a rigid body, *Chaos: An Interdisciplinary Journal of Non-linear Sciences* 6 (1996) 155 – 166.

[63] V. V. Beletskii, R. V. F. Lopes, M. L. Pivovarov, Chaos in spacecraft attitude motion in Earth's magnetic field, *Chaos: An Interdisciplinary Journal of Non-linear Sciences* 9 (1999) 493 – 498.

[64] S. A. Dovbysh, Some new dynamical effects in the perturbed Euler-Poinsot problem due to splitting of separatrices, *Journal of Applied Mathematics and Mechanics* 53 (1989) 165 – 173.

[65] J. Koiller, A mechanical system with a 'Wild' horseshoe, *Journal of Mathematical Physics* 25 (1984) 1599 – 604.

[66] V. N. Rubanovskii, On the relative equilibria of a satellite-gyrostat, their branchings and stability, *Journal of Applied Mathematics and Mechanics* 52 (1988) 710 – 714.

[67] W. H. Press, S. A. Teukolsky, W. T. Vetterling, B. P. Flannery, *Numerical Recipes in C++: the Art of Scientific Computing*, 2nd, (Hardcover) Cambridge University Press, 2002.

[68] D. Ruelle, Strange Attractors, *La Recherche* No. 108 (1980), 126 – 137. Also in T. Kapitaniak (Eds) *Chaotic oscillators: theory and applications*, World Scientific: Singapore, New Jersey, London, Hong Kong, 1991, pp. 40 – 51.

[69] S. Wiggins, P. J. Holmes, Homoclinic orbits in slowly varying oscillators, *SIAM Journal on Mathematical Analysis* 18 (1987) 612 – 629.

Captions of Figures

Figure 1 The configuration of a gyrostat rotating about a fixed point O.

Figure 2. Projection $(\omega_x - \omega_y)$ of the chaotic phase portrait of the forced Lorenz equations.

Figure 3. Projection $(\omega_x - \omega_z)$ of the chaotic phase portrait of the forced Lorenz equations.

Figure 4. Projection $(\omega_y - \omega_z)$ of the chaotic phase portrait of the forced Lorenz equations.

Figure 5 Projection of the chaotic trajectory of the Chua double scroll system.

Figure 6 Projection of the chaotic trajectory of the Duffing system.

Figure 7 Projection of the chaotic trajectory of the Ueda system.

Figure 8 Projection of the chaotic trajectory of the Lorenz system.

Figure 9 Projection of the chaotic trajectory of the generalized Lorenz system.

Figure 10 Projection of the chaotic trajectory of the Chen and Ueta system.

Figure 11 Projection of the chaotic trajectory of the Rossler system.

Figure 12 Projection of the chaotic trajectory of the modified Rossler turbulence.

Figure 13 Projection of the chaotic trajectory of the modified Brockett system.

Figure 14 Projection of the chaotic trajectory of the modified Kapitaniak system.

Figure 15 Projection of the chaotic trajectory of the YSVO system.

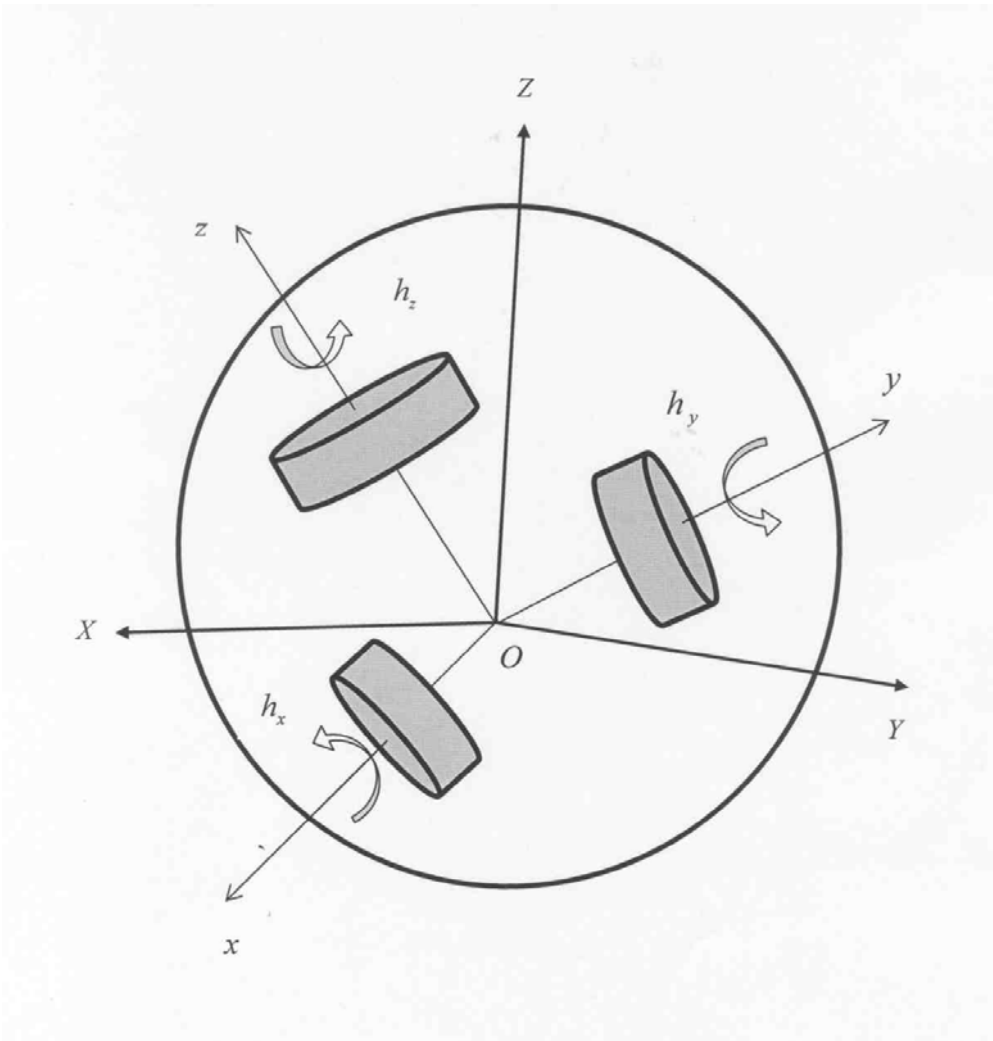


Figure 1 The configuration of a gyrostat rotating about a fixed point O .

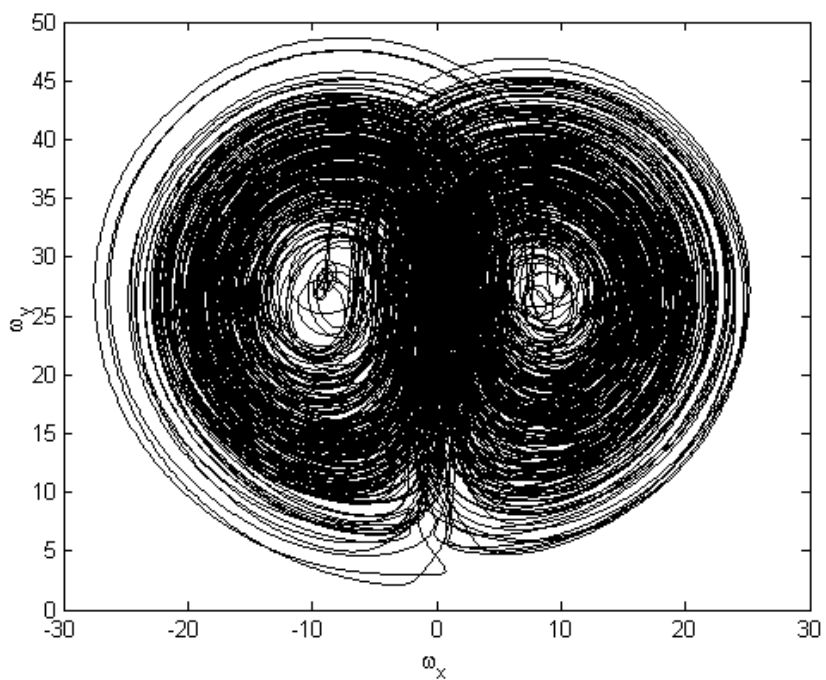


Figure 2. Projection $(\omega_x - \omega_y)$ of the chaotic phase portrait of the forced Lorenz equations.

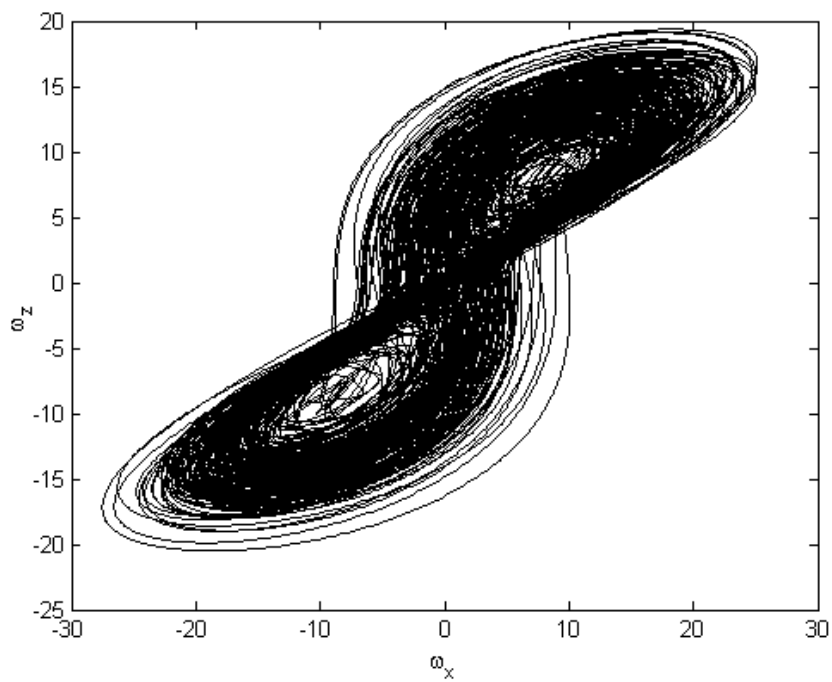


Figure 3. Projection $(\omega_x - \omega_z)$ of the chaotic phase portrait of the forced Lorenz equations.

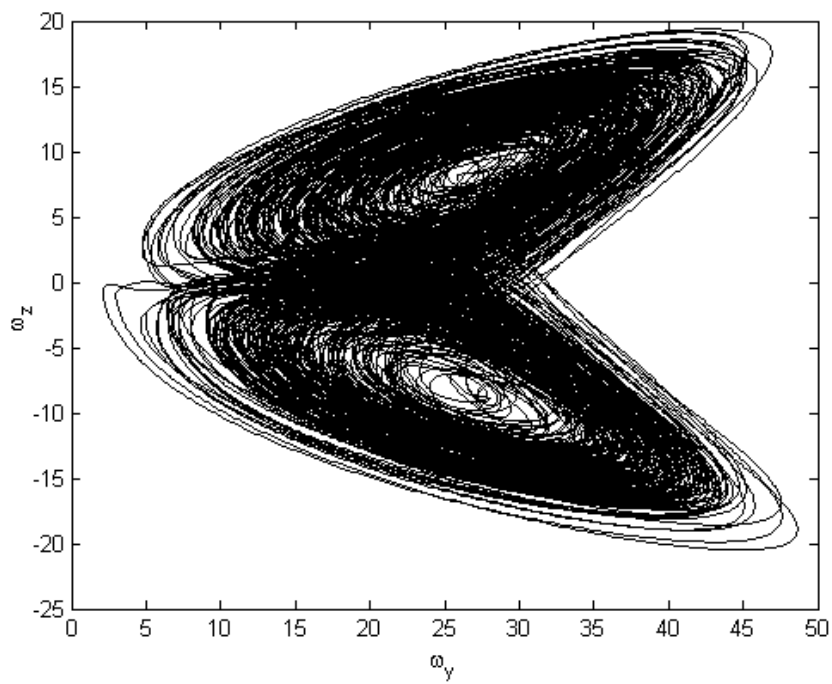


Figure 4. Projection $(\omega_y - \omega_z)$ of the chaotic phase portrait of the forced Lorenz equations.

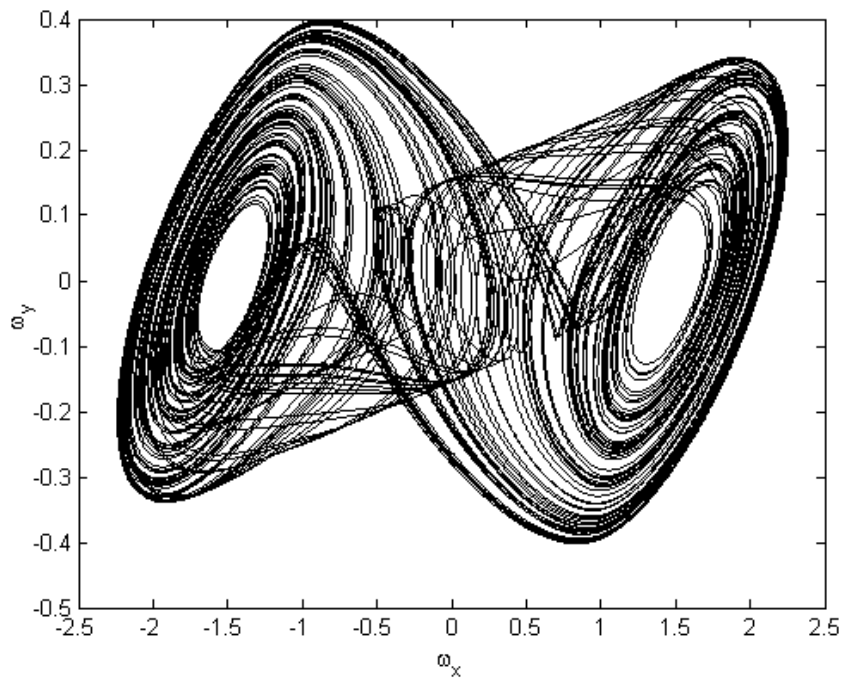


Figure 5 Projection of the chaotic trajectory of the Chua double scroll equations

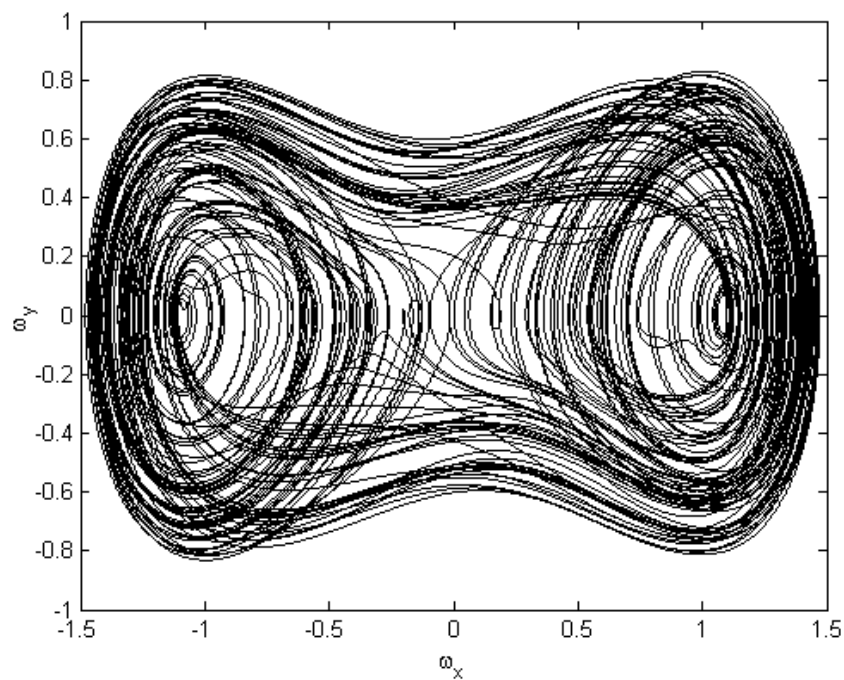


Figure 6 Projection of the chaotic trajectory of the Duffing equations

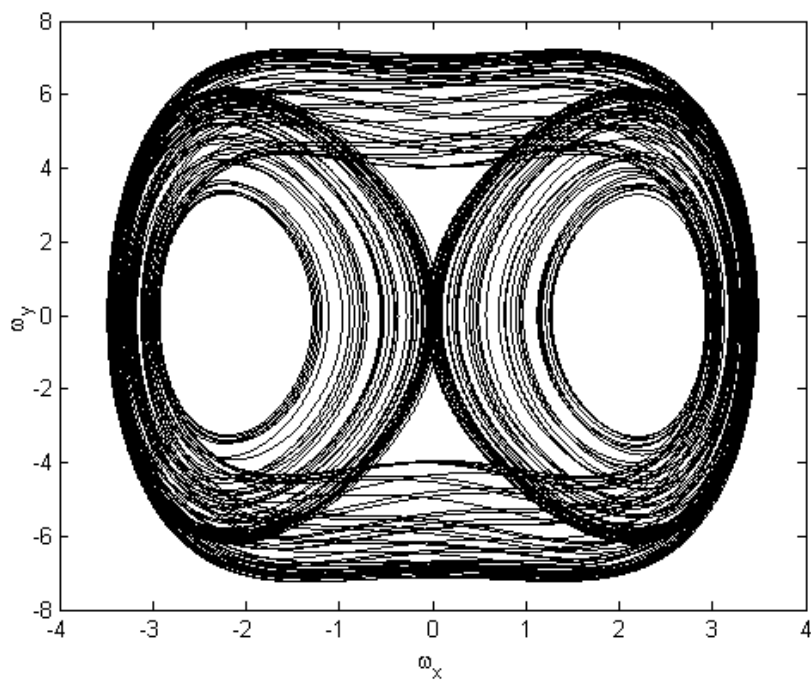


Figure 7 Projection of the chaotic trajectory of the Ueda equations

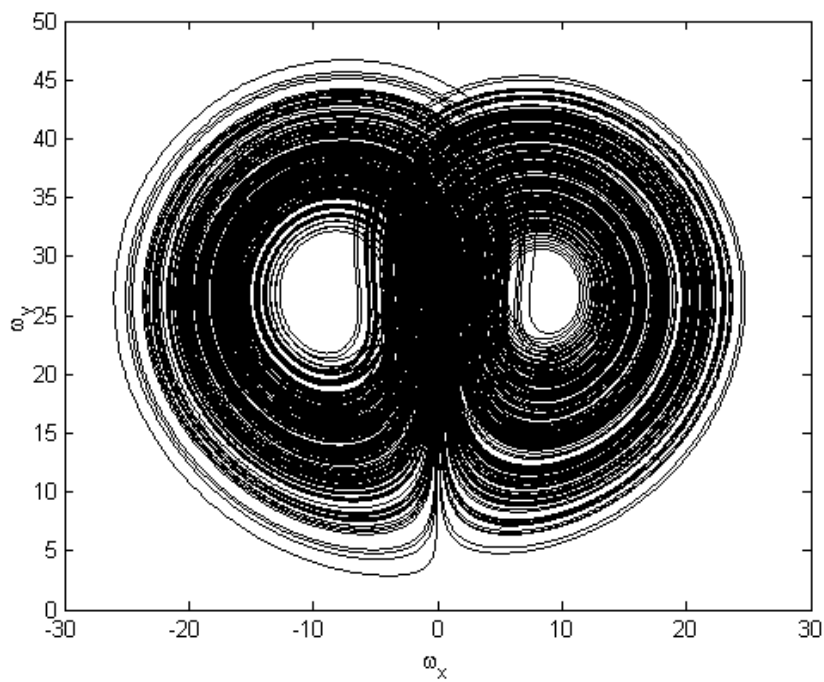


Figure 9 Projection of the chaotic trajectory of the Lorenz equations.

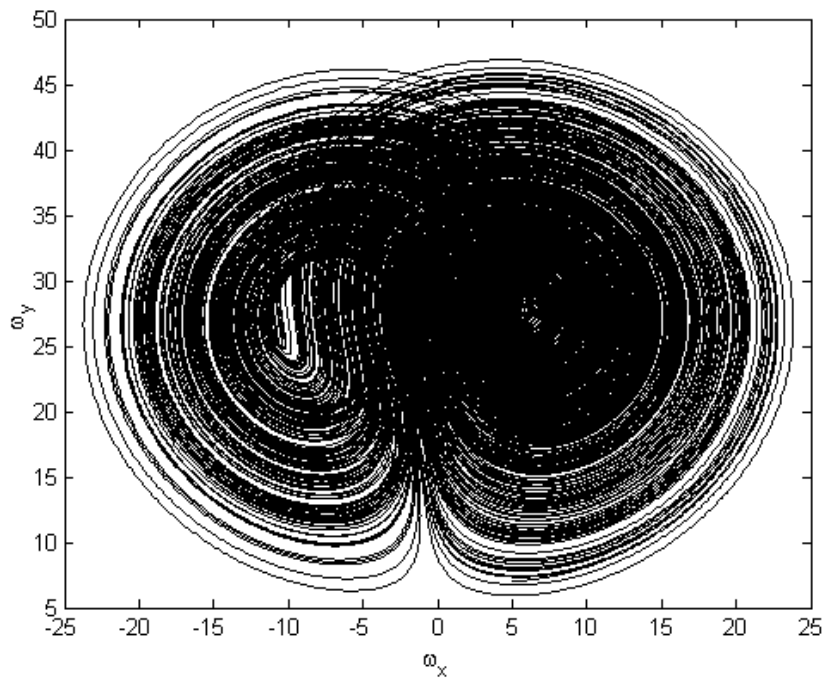


Figure 9 Projection of the chaotic trajectory of the generalized Lorenz equations

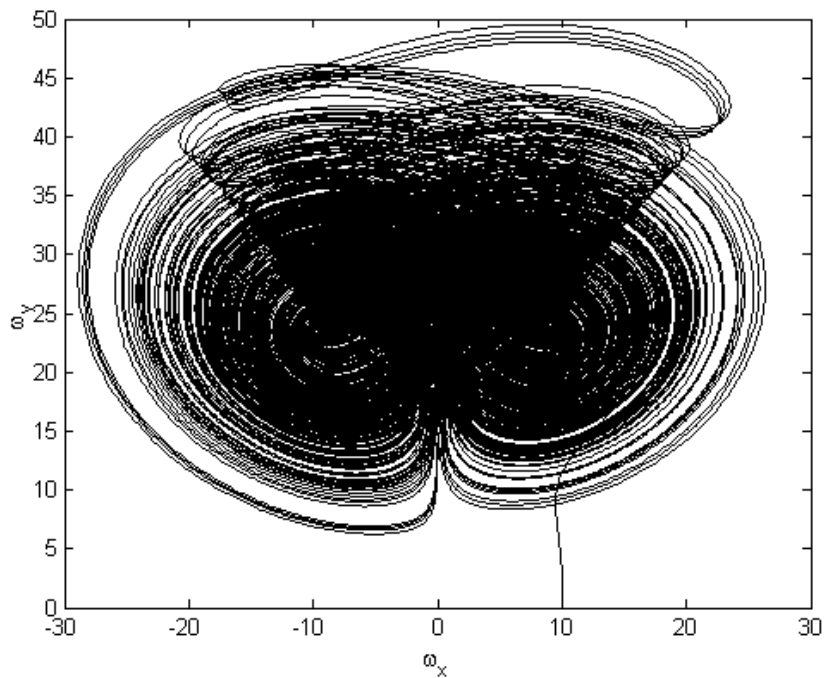


Figure 10 Projection of the chaotic trajectory of the Chen equations

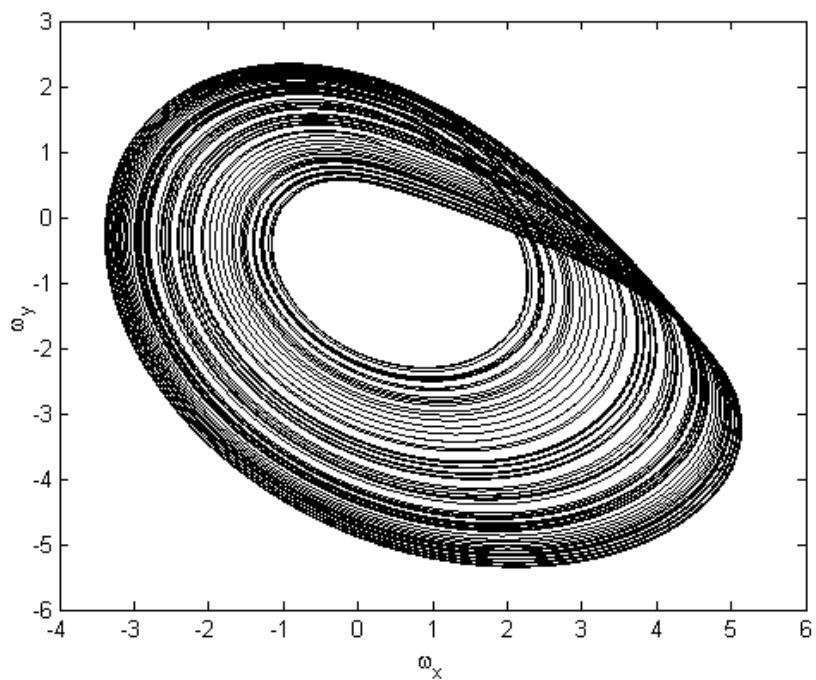


Figure 11 Projection of the chaotic trajectory of the Rossler equations

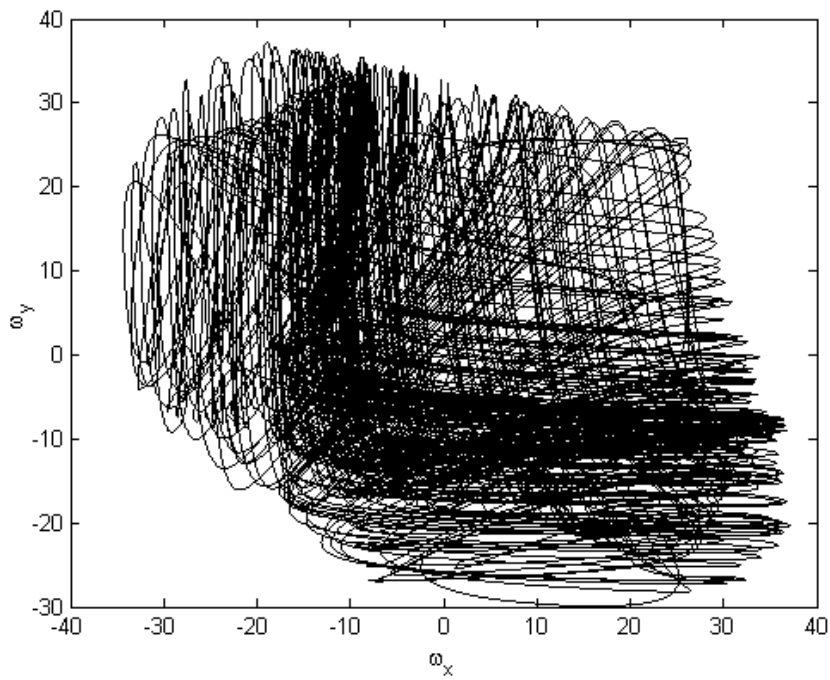


Figure 12 Projection of the chaotic trajectory of the modified Rossler turbulence.

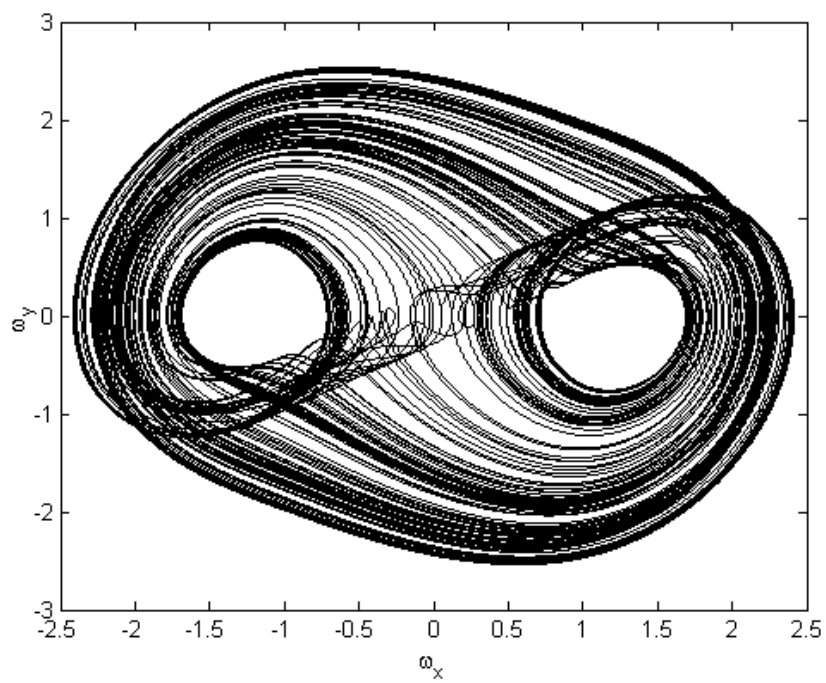


Figure 13 Projection of the chaotic trajectory of the modified Brockett equations.

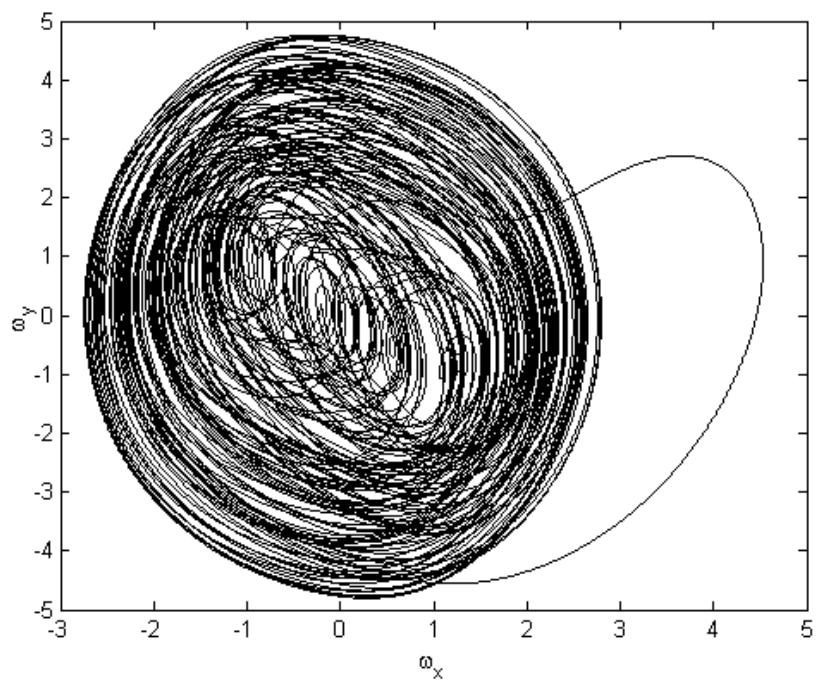


Figure 14 Projection of the chaotic trajectory of the modified Kapitaniak equations.

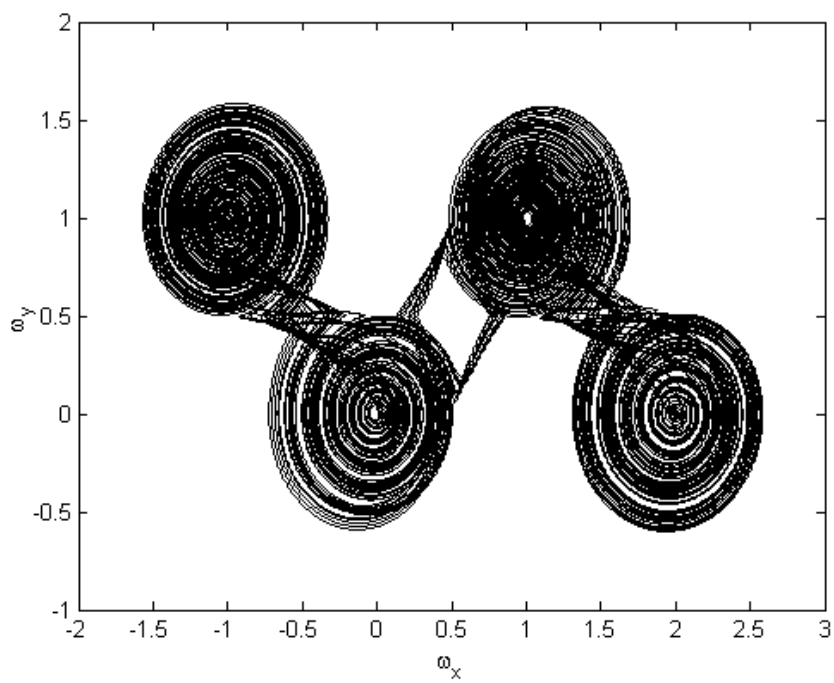


Figure 15 Projection of the chaotic trajectory of the YSVO system